

Development and Application of Quinone-Catalyzed C–C Bond Cleavage Reactions

By

Benjamin John Haugeberg

Submitted to the graduate degree program in the Department of Chemistry and the Graduate Faculty of the University of Kansas in partial fulfillment of the requirements for the degree of
Master of Sciences.

Chairperson Michael D. Clift

Paul R. Hanson

Michael Rubin

Date Defended: July 25, 2016

The Thesis Committee for Benjamin J. Haugeberg certifies that this is the approved version of
the following thesis:

**Development and Application of Quinone-Catalyzed C–C Bond Cleavage
Reactions**

Chairperson Michael D. Clift

Date Approved: July 28, 2016

Abstract

Development and Application of Quinone Cofactor Mimic Catalysis

Benjamin John Haugeberg

Organocatalysis is a synthetic field of ever increasing development and utility. Of the reactions and small molecule catalysts developed over the last 20 years, a considerable portion have been inspired by cofactors that are important to biological systems. Research in the Clift group focuses on developing modes for catalysis through applications of quinone cofactor mimics.

Our studies were motivated by developing a new synthesis of β -amino acids through quinone-catalyzed oxidative-decarboxylation. In this process, we developed a protocol for quinone-catalyzed oxidative-decarboxylation of α -aryl amino acids in which homologation products were isolated following Mukaiyama–Mannich addition. In all, isolated 20 homologated products (15-95% yields) in first demonstration of quinone-catalyzed oxidative-decarboxylation of α -aryl amino acids.

Following the development of quinone-catalyzed oxidative-decarboxylation, we sought to explore the potential of quinone catalysts in related oxidative C–C bond cleavage reactions. Initial studies on the development of a protocol for the deformylation of amino alcohols is shown as well.

Acknowledgements

Of the many people who deserve credit, I would like to thank my research advisor Michael D. Clift most. You have shown me what it takes to understand chemistry and synthesis on a fundamental level, have molded my presentation style, and provided many opportunities for self-improvement. Thank you for everything you have done for me.

This thank you goes to the steering committee of the Graduate Training Program in Dynamic Aspects of Chemical Biology program. They provided me with opportunity and encouragement to expand my knowledge base in a unique way. The funding they provided also left an impression and is greatly appreciated.

To the past and present members of the Clift group, thank you. You've provided guidance, support, motivation, and laughter. It has been an honor serving with you.

Lastly, I would like to thank my family. You have all been supportive throughout this process, offering encouragement along each step. A special thanks is reserved for my fiancé, Amy. She's spent many lonely nights waiting for me to finish my schooling. Thank you for your patience and support.

Abbreviations

DMF	dimethylformamide
PLP	pyridoxal 5'-phosphate
NADH	nicotinamide adenine dinucleotide
NHC	N-heterocyclic carbene
TPP	thiamine pyrophosphate
ee	enantiomeric excess
Lys	lysine
Tyr	tyrosine
tBuOH	tert-butanol
ADP	adenosine diphosphate
TPQ	topaquinone
BSAO	bovine serum amine oxidase
MeCN	acetonitrile
rt	room temperature
MeOH	methanol
LiTMP	lithium tetramethylpiperidide
nBuLi	n-butyllithium
EtOH	ethanol
AcCl	acetyl chloride
DMSO	dimethyl sulfoxide
THF	tetrahydrofuran

iPrOH	isopropanol
cat.	catalyst
Et ₃ N	triethylamine
SKA	silyl ketene acetal
CAN	ceric ammonium nitrate
RDS	rate determining step

Table of Contents

Chapter 1: An Introduction to Cofactor-Inspired Organocatalysis	1
1.1: The Development of Organocatalysis	2
1.2: Thiamine: Nature's N-Heterocyclic Carbene Catalyst	5
1.3 Pyridoxal 5'-Phosphate (Vitamin B6): A Versatile Cofactor	8
1.4 NADH as Nature's Hydride Source	12
1.5 Summary for Chapter 1	15
 Chapter 2: Development of Quinone-Catalyzed Oxidative C–C Bond Cleavage and its Application to Amino Acid Homologation	 16
2.1 Introduction to Quinone Cofactors and Their Applications in Organocatalytic Reactions	16
2.2 β -Amino Acid Synthesis via Oxidative-Decarboxylation/Mukaiyama–Mannich Addition	20
2.2.1 Classical Methods for β -Amino Acid Synthesis	21
2.3 Development of Oxidative-Decarboxylation: Substrate Scope and Reaction Conditions	24
2.3.1 Scope of Oxidative-Decarboxylation in Acetonitrile:Water	26
2.3.2 Scope of Oxidative-Decarboxylation in EtOH	28
2.3.3 Study of Amine Reaction Partners Other Than Anisidine	29
2.4 Development of Conditions for β -amino ester synthesis	31

2.4.1 β -Amino Ester Synthesis Using gem-Dimethyl Silyl Ketene Acetal Nucleophile	33
2.4.2 β -Amino Ester Synthesis Using Silyl Ketene (Thio)Acetal Nucleophile	34
2.4.3 Deprotection of Homologation Products	36
2.5 Mechanistic Studies for Quinone-Catalyzed Oxidative-Decarboxylation	36
2.5.1 Hammett Analysis on Quinone-Catalyzed Oxidative-Decarboxylation	37
2.5.2 Hammett Analysis on Stoichiometric Quinone-Promoted Oxidative-Decarboxylation	39
2.6 Quinone-Catalyzed Amino Alcohol Deformylation	41
2.6.1 Development of Quinone-Catalyzed Amino Alcohol Deformylation	41
2.6.2 Optimization of Quinone-Catalyzed Amino Alcohol Deformylation	42
2.6.3 Preliminary Scope Studies for Quinone-Catalyzed Deformylation	44
2.7 Summary for Chapter 2	45
2.8 General Experimental Section	45
2.9 General Experimental Procedures for Sequential Oxidative–Decarboxylation/Mannich Addition	46
2.9.1 Characterization Data for II-39-51 , II-71-80 , and II-82-91	49
2.9.2 Experimental Section for Hammett Experiments	65
2.10 Chapter 1 and 2 References	81
NMR Spectra for All Compounds	89

List of Figures

1.1: Number of Publications of Organocatalytic Reactions	2
1.2: Thiamine and Thiamine Diphosphate (TPP)	5
1.3: Pyridoxal 5'-Phosphate (Vitamin B6)	8
1.4: Early Examples of NAD ⁺ Variants	13
1.5: Hantzsch Ester	14
2.1: Selected β -Amino Acid-Derived Pharmaceuticals	21
2.2: Proposed Mechanism for Quinone-Catalyzed Amino Acid Functionalization	23
2.3 Proposed Mechanism and Interpretation of the Hammett Analysis	37
2.4: Reaction Rates for Quinone-Catalyzed Oxidative-Decarboxylation	38
2.5: Hammett Plot for Quinone-Catalyzed Oxidative-Decarboxylation	39
2.6: Reaction Rates for Stoichiometric Quinone-Promoted Oxidative-Decarboxylation	40
2.7: Hammett Plot for Stoichiometric Quinone-Promoted Oxidative-Decarboxylation	41
2.8: Proposed Mechanism for Quinone-Catalyzed Amino Alcohol Deformylation	42

List of Schemes

1.1: Hajos–Parrish Reaction	3
1.2: Lysine Catalyzed Aldol by Fructose Bisphosphate Aldolase	4
1.3: Thiamine Catalyzed Benzoin Condensation	6
1.4: Proposed Mechanism for NHC-Catalyzed Benzoin Condensation	7

1.5: NHC Catalyzed Asymmetric Stetter Reaction	8
1.6: PLP Promoted Transamination of Tyrosine Aminotransferase	9
1.7: PLP Catalyzed Racemization	10
1.8: PLP Mimic Catalyzed Oxidation	10
1.9: PLP Mimic Catalyzed Racemization of Phenylglycine	11
1.10: PLP Mimic-Catalyzed Dynamic Kinetic Resolution	11
1.11: Mechanism for NAHD Hydride Transfer	12
1.12: Enzymatic Dihydrofolate Reductase by NAD ⁺ and NADH	13
1.13: Reduction of Imine via Enantioselective Transfer Hydrogenation Using Hantzsch Ester	14
2.1: Discovery of TPQ as Cofactor in Active Site of BSAO	17
2.2: Mechanism of Topa-quinone Oxidation of Amino Acid	18
2.3: Mure and Klinman's Quinone-Catalyzed Amine Oxidation	19
2.4: Stahl's Quinone-Catalyzed Amine Oxidation	19
2.5: Formal Quinone-Catalyzed Amine Functionalization	20
2.6: Arndt-Eistert Homologation	21
2.7: Kowalski Ester Homologation	22
2.9: Deprotection of Homologation Products	36

List of Tables

2.1: Reaction Discovery and Optimization	25
2.2: Isolated Yields for Oxidative-Decarboxylation with Acetonitrile:Water Solvent	27
2.3: NMR Yields for Oxidative-Decarboxylation with EtOH Solvent	29
2.4: Substrate Scope for Primary Amine Coupling Partners	30
2.5: Optimization of Two-Step, 1-Pot β -Amino Ester Synthesis	32
2.6: Scope Studies Using gem-Dimethyl Silyl Ketene Acetal Nucleophile	33
2.7: Scope Studies using Silyl Ketene (Thio)acetal Nucleophile	35
2.8: Optimization of Amino Alcohol Deformylation	43
2.9: Preliminary Scope Studies for Deformylation	44

Chapter 1

An Introduction to Cofactor-Inspired Organocatalysis

Chapter 1

1.1: The Development of Organocatalysis

Organocatalysis is the use of small molecules to catalyze organic transformations. The merger of organocatalysis into a single field is relatively new. Over that last century, sporadic examples of reactions utilizing small organic molecules as catalysts have been developed, but have been considered isolated occurrences. Beginning in the late 1990s, the number of publications describing emerging organocatalytic processes began increasing significantly. In a review, MacMillan noted that between 1998 and 2008, over 1500 publications describing organocatalysis in more than 130 discrete reaction types had been described.¹ Today, organocatalysis is now considered a standard means for reaction development.

Figure 1.1: Number of Publications of Organocatalytic Reactions

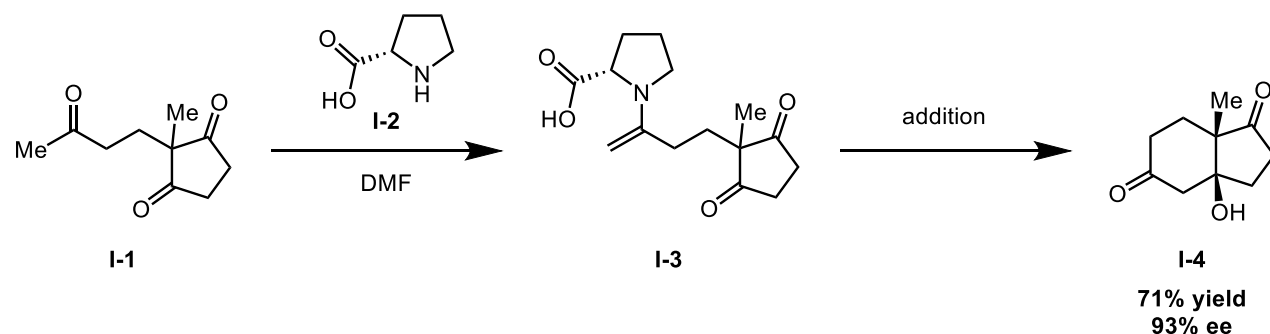


In the same review, MacMillan credits the rapid growth of organocatalysis to, “first, the conceptualization of the field; second, the advantages of organocatalytic research; and, third the advent of generic modes of catalyst activation, induction and reactivity.”¹ If conceptualization

organocatalysis as a serious branch of synthetic chemistry drove initial reaction development, the advantages of organocatalysis motivated researchers to develop generic modes of activation, induction, and reactivity. Organocatalysis has many advantages: the relative cost to make and use them is low when compared to other modes of catalysis, a large pool of chiral molecules exists to enable synthesis of new catalysts, and the catalysts are generally non-toxic and insensitive to exposure to moisture and air and they are relatively simple to use. These qualities have made organocatalysis an expanding field that continues to grow.²

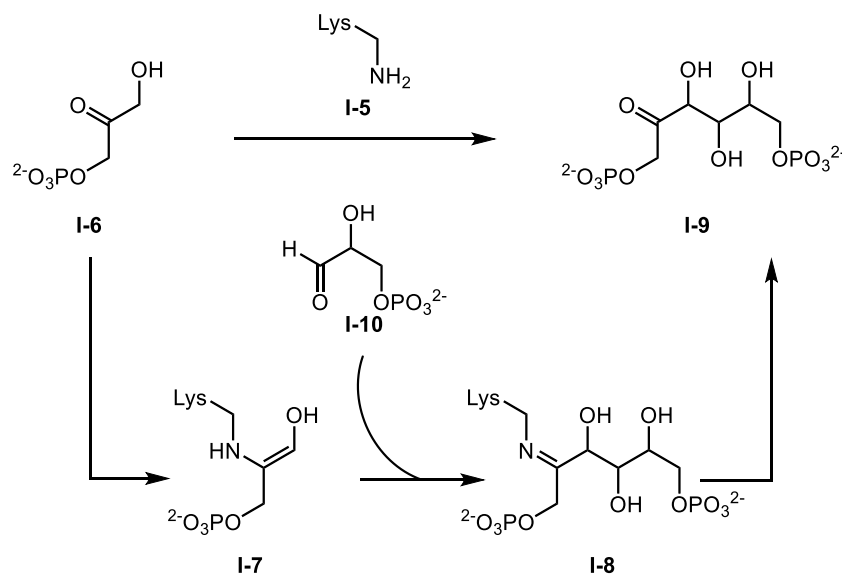
The origin of organocatalysis is often traced back to the Hajos–Parrish reaction. (Scheme 1.1). This is one of the first accounts of a small molecule catalyzed an asymmetric transformation.³ The chemistry was developed for the synthesis of new intermediates and natural products, such as steroids, in asymmetric fashion. In their report, Hajos and Parrish use 3 mol % of a L-proline catalyst (**I-2**) to promote an intramolecular enantioselective aldol cyclization of triketone **I-1** to form optically enriched bicyclic diketone **I-4** in 71% yield. This is the first example of an asymmetric reaction carried out using a chiral organic molecule.

Scheme 1.1: Hajos–Parrish Reaction



The Hajos–Parrish reaction later inspired many new enamine catalysts and subsequent reactions many years after the initial discovery. Some examples of these developments includes List’s proline catalyzed aldols,⁴ Jørgensen’s prolinol catalyst,⁵ MacMillan’s iminium Diels–Alder,⁶ and many more.⁷ While the conceptualization of the Hajos–Parrish reaction was undoubtedly influenced by previous reactions,⁷⁴ an equally important and influential discovery was made in the 1960s describing a biological variant of asymmetric enamine catalysis. In nature, aldolase enzymes catalyze intermolecular aldol reactions (Scheme 1.2). This enzymatic reaction differs fundamentally from proline-based enamine catalysis in that a primary amine in a lysine residue is used.⁸ This process did not directly influence the work of Hajos and Parrish, but there is a clear parallel between the Hajos–Parrish reaction and enzymatic aldol reactions.

Scheme 1.2: Lysine Catalyzed Aldol by Fructose Bisphosphate Aldolase



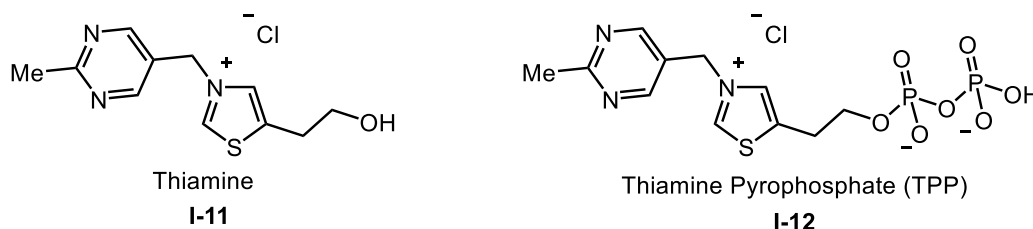
In studying enzymes and other biological processes over the past century, a number of small, non-protein molecules have been identified that are vital in assisting efficient and selective

chemical transformations in enzymatic systems. These molecules are commonly referred to as cofactors. Under the circumstances described by MacMillan, researchers realized that cofactors found in nature could be used as a platform to develop many important synthetic transformations. Since then, the field of organocatalysis has seen a surge in the development of many biologically-inspired organocatalysts and many new reactions have emerged as a result. Some of the most influential cofactors include: thiamine, pyridoxal 5'-phosphate (PLP), and nicotinamide adenine dinucleotide (NADH).

1.2: Thiamine: Nature's N-Heterocyclic Carbene Catalyst

Thiamine, commonly known as vitamin B₁, is a natural thiazolium salt involved as an N-heterocyclic carbene (NHC) in many enzymatic processes.⁹ This coenzyme was first isolated by Dutch chemists Petrus and Donath in the 1920s and the structure was determined by Williams in 1936 (**I-11**) without knowledge of its function.^{10,11} Later it was discovered this thiazolium salt exists more commonly as thiamine pyrophosphate (TPP, **I-12**) in biological environments (Figure 1.2).¹²

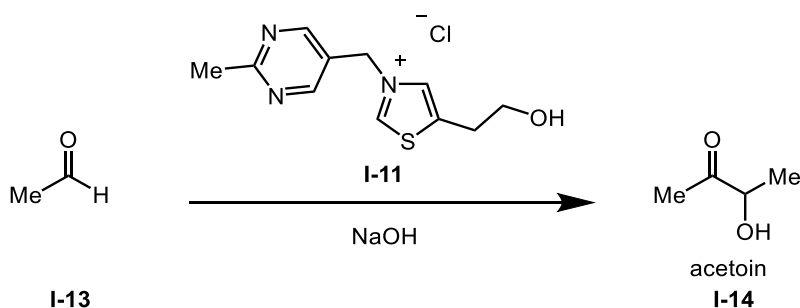
Figure 1.2: Thiamine and Thiamine Diphosphate (TPP)



In the 1950s, Mizuhara and co-workers determined the catalytic role of thiamine in enzymatic active sites as a nucleophilic carbene (Scheme 1.3). Their studies showed high

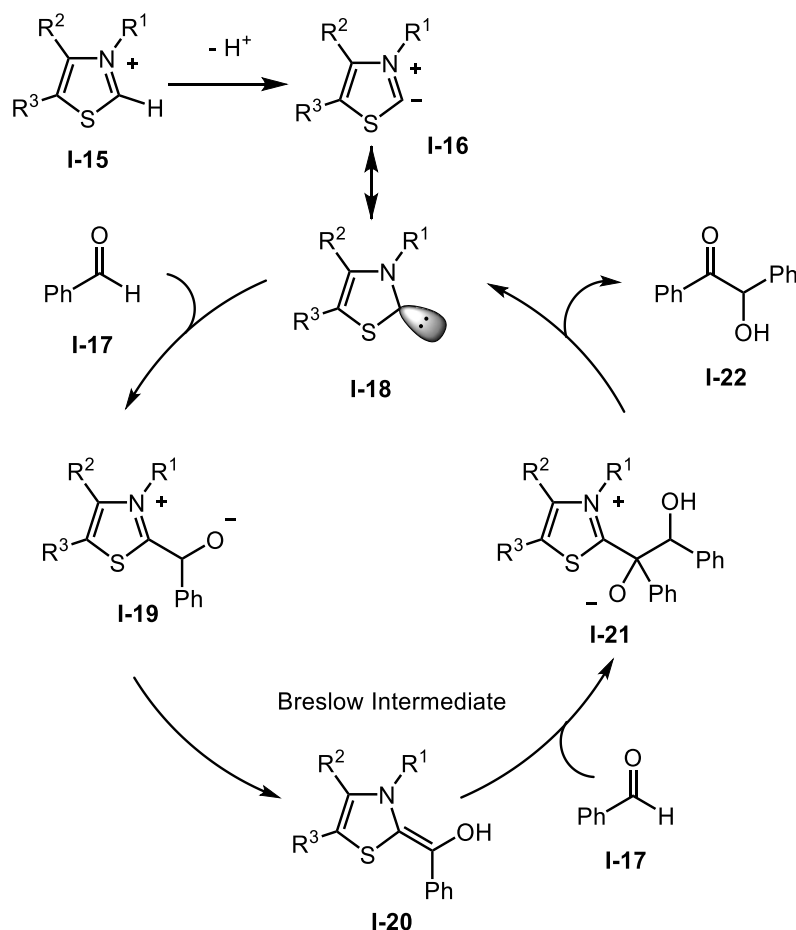
concentrations of thiamine hydrochloride (**I-11**) in alkaline solution catalyzed a benzoin condensation and subsequent formation of acetoin (**I-14**) from acetaldehyde (**I-13**).¹³ From their seminal discoveries, thiamine and TPP have been shown to carry out a number of carbene catalyzed reactions in biological systems.^{9,12}

Scheme 1.3: Thiamine-Catalyzed Benzoin Condensation



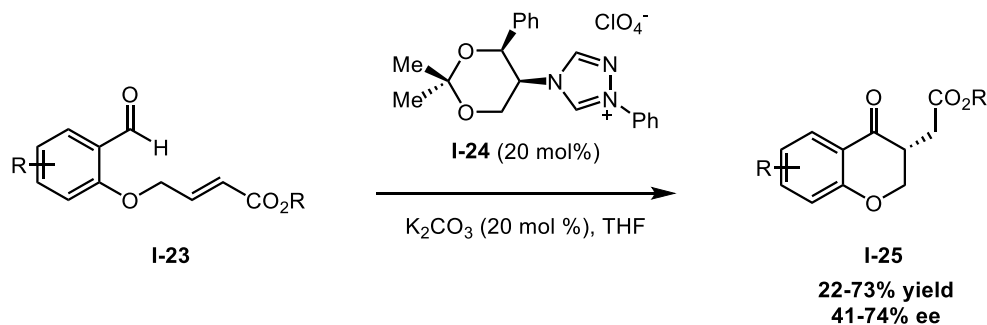
By the time the function of thiamine had been discovered in the 1950s, carbene chemistry had been relatively well established.^{14,15} The discovery of the biological role of thiamine prompted the development of NHC chemistry. The development of the field was accelerated when Breslow proposed a mechanism for the NHC-catalyzed benzoin condensation.¹⁶ In the proposed mechanism, he describes generation of a carbene through a deprotonation of **I-15**, to give thiazol **I-16**, which can be drawn as carbene **I-18** (Scheme 1.4). NHC **I-18** then adds to aldehyde **I-17** to form **I-19**, which goes on to form the so-called Breslow intermediate (**I-20**). This species acts as a nucleophile and will add to another molecule of benzaldehyde to give intermediate **I-21**. The NHC is then eliminated to give the benzoin product **I-22**, thereby completing the catalytic cycle. It should be noted that this mechanism is accepted, but has been disputed.¹⁷

Scheme 1.4: Proposed Mechanism for the NHC-Catalyzed Benzoin Condensation



Since the discovery of thiamine and the studies carried out by Breslow, NHC catalysis has been used to develop many stable carbene reagents and many organocatalytic reactions. One particular process that was developed based on thiamine derivatives is the Stetter reaction.¹⁸ Enders and co-workers developed a chiral thiazolium salt **I-24** in investigations for the development of asymmetric variants of the Stetter reaction (Scheme 1.5).¹⁹ The intramolecular reaction shows the conversion of **I-23** to bicyclic **I-25** in modest yields and ee, but provides an initial example for NHC-catalyzed asymmetric transformations.

Scheme 1.5: NHC Catalyzed Asymmetric Stetter Reaction

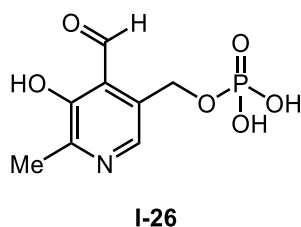


From these early examples, many selective and high yielding NHC-catalyzed processes have been developed.

1.3 Pyridoxal 5'-Phosphate (Vitamin B₆): A Versatile Cofactor

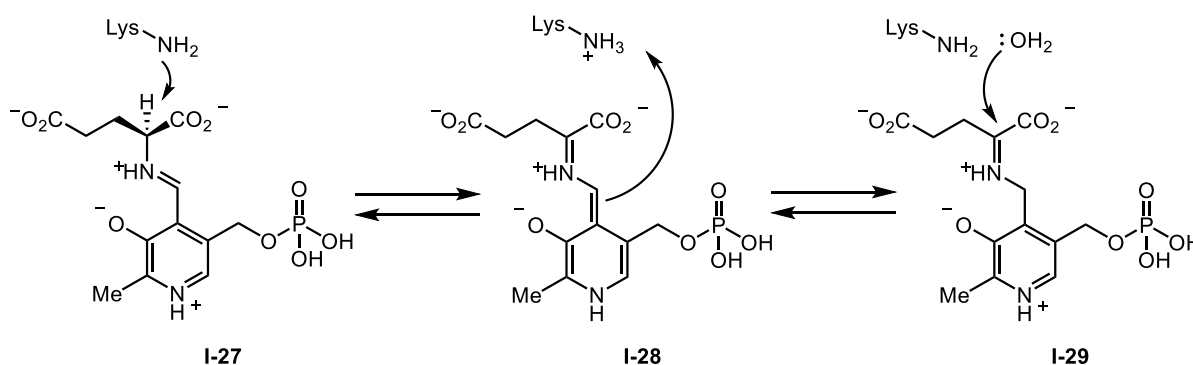
Another important cofactor found in nature is pyridoxal 5'-phosphate (PLP, Figure 1.3). It was first discovered by Grygory in 1934 and termed vitamin B₆.²⁰ Since the discovery, pyridoxal 5'-phosphate (**I-26**) has been studied extensively owing to its versatile catalytic utility. In nature, PLP cofactors are responsible for promoting transamination, deamination, decarboxylation, elimination, and racemization reactions of amino acids.²¹ Given its biological prevalence and fundamental importance, mechanisms of PLP-catalyzed reactions are now routinely covered in biology textbooks.^{9, 22-24}

Figure 1.3: Pyridoxal 5'-Phosphate (Vitamin B₆)



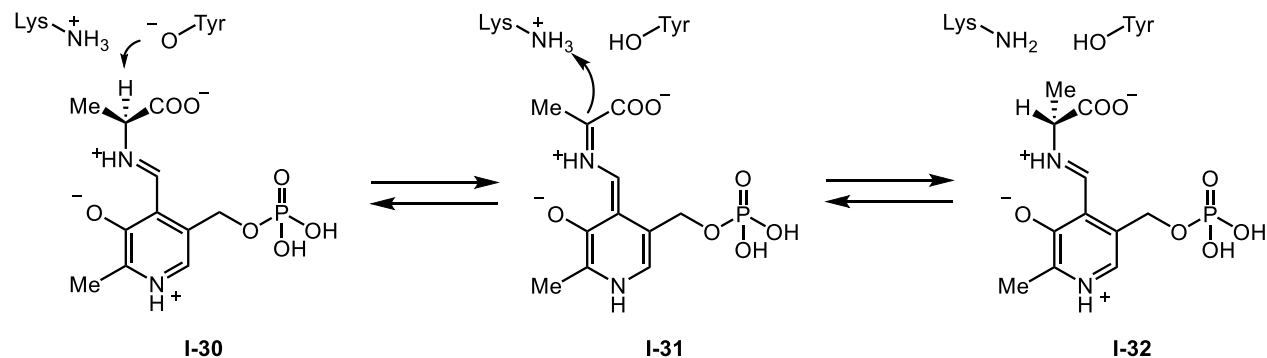
Aminotransferases utilize PLP in transamination processes. Scheme 1.6 shows the first half-reaction where a lysine residue initiates proton abstraction from the glutamate condensed to PLP (**I-26**), yielding the quinonoid intermediate **I-28**. Reprotonation of the cofactor by that lysine lends intermediate **I-29**, which is subsequently hydrolyzed to release α -ketoglutarate (not shown).¹⁹ In a comprehensive catalytic cycle, a subsequent reaction with a different α -ketoacid would generate the corresponding amino acid and return the PLP cofactor.

Scheme 1.6: PLP-Promoted Transamination of Aminotransferases



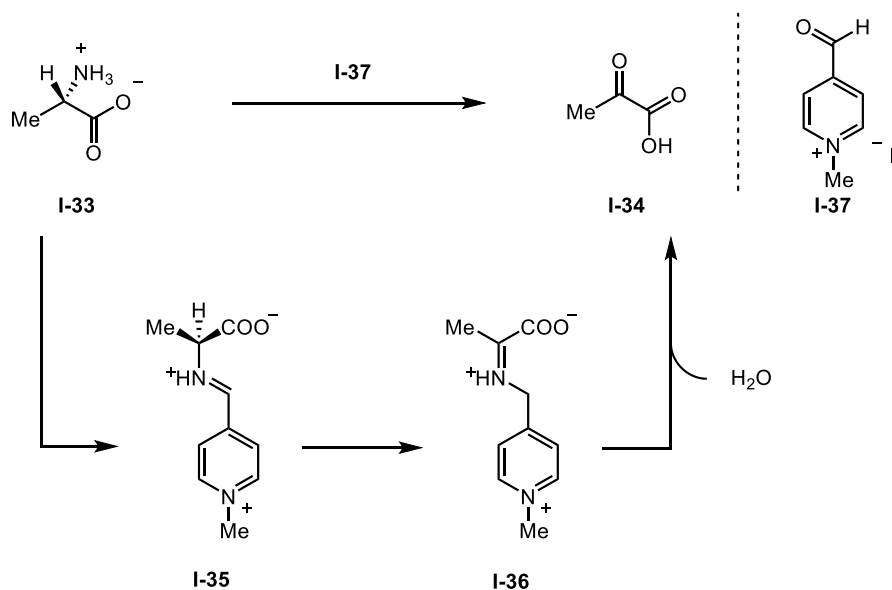
PLP is also responsible for amino acid racemization in biological systems. Bacterial alanine racemase promotes the stereoconversion of L-alanine using a PLP cofactor. (Scheme 1.7).¹⁹ In this process, alanine condenses to a PLP cofactor to lend imine **I-30**, which then undergoes a tyrosine promoted deprotonation to give intermediate **I-31**. A nearby enzyme bound lysine moiety promotes selective protonation to **I-32**, which upon hydrolysis yields D-alanine.

Scheme 1.7: PLP-Catalyzed Racemization



Given PLP's importance and versatility in biological systems, interest in PLP mimics and their reaction capabilities has been pursued. In an early example, Maley and Bruice showed that a PLP mimic 1-methyl-4-formyl-pyridinium iodide (**I-37**) promoted the conversion of L-alanine (**I-33**) to keto-acid **I-34** through Schiff base intermediates **I-35** and **I-36** (Scheme 1.8).²⁵

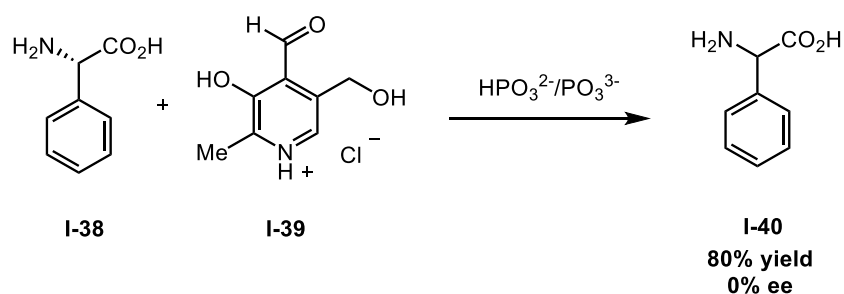
Scheme 1.8: PLP Mimic Catalyzed Oxidation



These experiments focused on understanding the role of PLP in transamination.⁷¹ In their studies, they showed a number of PLP mimics could act as competent reaction partners to perform the biomimetic synthesis of keto-acid **I-34** in a half-transamination.

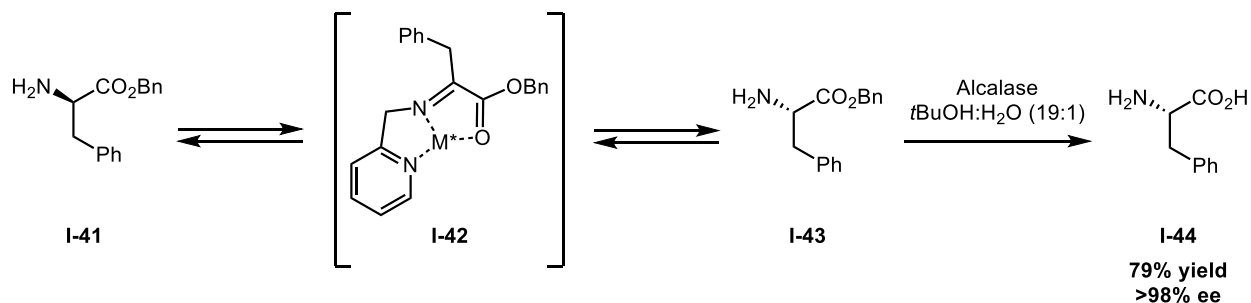
Kudra and co-workers have studied the ability of PLP mimics to catalyze racemization of amino acids.²⁶ Their experiments started with an enantioenriched isomer of phenylglycine (Scheme 1.9). After submitting **I-38** to phosphate buffer conditions in the presence of an achiral PLP mimic **I-39**, they were able to isolate a completely racemic product **I-40** in good yields.

Scheme 1.9: PLP Mimic Catalyzed Racemization of Phenylglycine



Building from Kudra's example PLP-mediated racemization, recently Aron and co-workers have demonstrated the ability to control racemization to give exclusively one enantiomer from a racemic mixture of phenylalanine (Scheme 1.10).

Scheme 1.10: PLP Mimic-Catalyzed Dynamic Kinetic Resolution

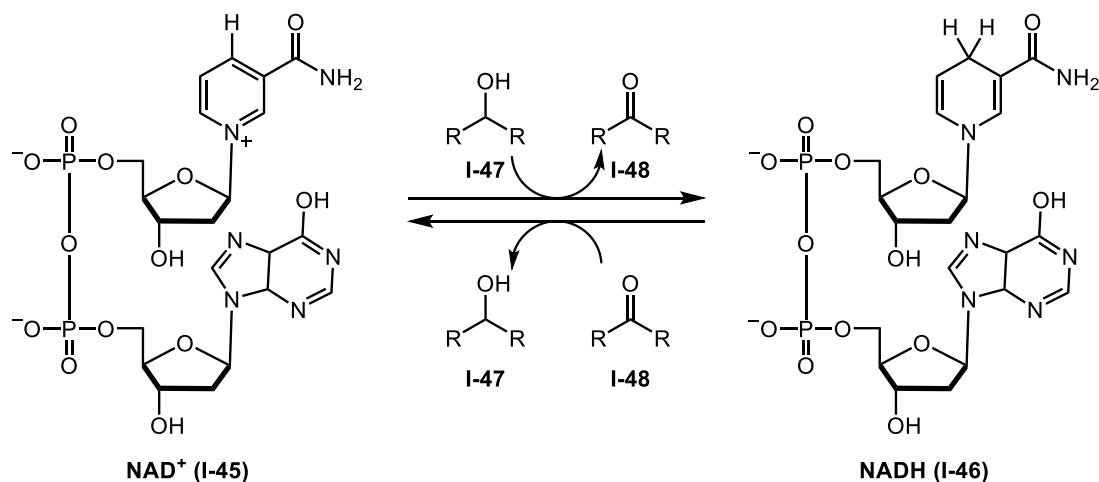


In their dynamic kinetic resolution, they identified zinc complexes of **I-42** that, when introduced to an esterase called alcalase, provided a single enantiomer of amino acid product **I-44**.²⁷ This is one of many examples of how utilizing PLP mimic catalysis can deliver good yielding products with high enantioselectivities.²⁸

1.4 NADH as Nature's Hydride Source

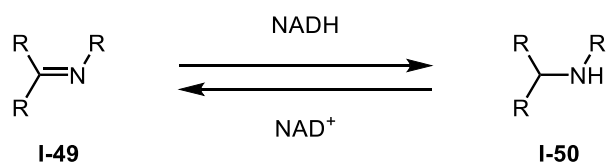
Nicotinamide adenine dinucleotide (NADH) is a cofactor found in biological systems that has inspired the development of small molecules as a natural hydride source. NADH was first discovered by Harden and Young in 1906 when studying alcohol fermentation.²⁹ In 1936, Warburn identified NADH as the hydride transfer source in biological redox reactions.³⁰ In their work, they described the mechanism for hydride transfer as a reversible reaction where NAD⁺ **I-45** oxidizes alcohol **I-47** in the forward direction and NADH **I-46** reduces ketone **I-48** in the reverse (Scheme 1.11).

Scheme 1.11: Mechanism for NADH Hydride Transfer



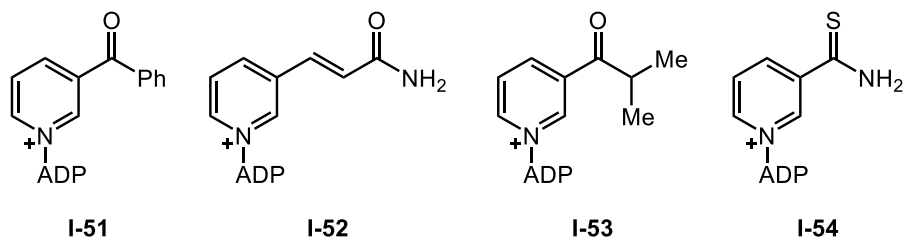
Kaplan and others have shown that NADH is responsible for the catalytic activity of a number of dehydrogenase and reductase enzymes (Scheme 1.12).^{31, 32} Although NADH acts as a stoichiometric reagent in biological reductions, NAD^+ is in turn an oxidant that can easily be reduced.

Scheme 1.12: Enzymatic Dihydrofolate Reductase by NAD^+ and NADH



In the 1950s, researchers began studying the possibility of using other nicotinamide derivatives as a reducing agent. It was shown that NADH can be replaced by other pyridine bases without the loss of the coenzyme function in various biological systems.³³⁻³⁵ Kaplan and co-workers demonstrated nicotinamide variants could provide reactivities rivaling that of NAD^+ , some of which are shown in Figure 1.4.

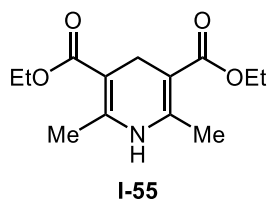
Figure 1.4: Early Examples of NAD^+ Variants



Given its potential as an organic reducing reagent, NADH mimics have been an important target for synthetic development. Without knowing at the time, Hantzsch synthesized a 1,4-

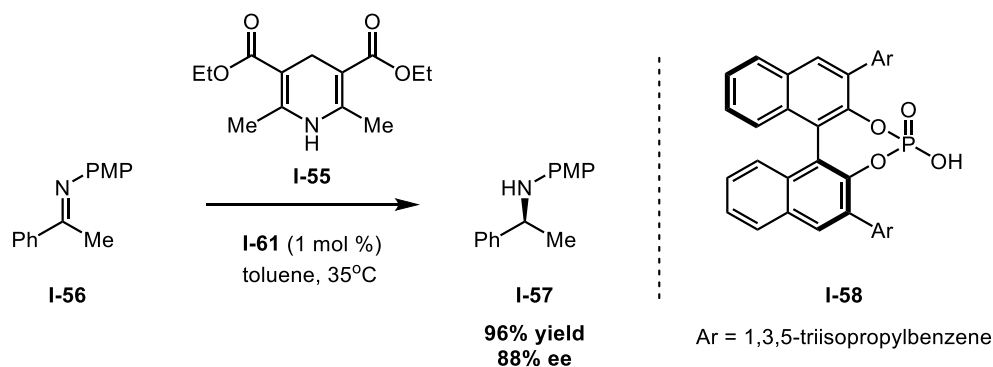
dihydropyridine dicarboxylate (**I-55**) in 1882 that would eventually serve as such a molecule (Figure 1.5).³⁶ Experiments on what is known as the Hantzsch ester continued, but it wasn't until after the discovery of the function of NADH in the 1930s that the Hantzsch ester was used as an organic reducing agent.³⁷⁻³⁹

Figure 1.5: Hantzsch Ester



A recent example of such was reported by the List group in development of an asymmetric transfer hydrogenation catalyzed by a chiral Brønsted acid (Scheme 1.13).⁴⁰ In this work, List showed a highly enantioselective imine reduction where **I-55** served as the hydride source. Before the development of NADH mimics, powerful asymmetric reductions were commonly catalyzed by metals using stoichiometric quantities of metal hydride reagents.⁴⁰

Scheme 1.13: Reduction of Imine via Enantioselective Transfer Hydrogenation Using Hantzsch Ester



1.5 Summary for Chapter 1

The development of cofactor mimics inspired by biological systems has had a dramatic influence on the field of organocatalysis. The idea of using small molecules that mimic cofactors in biological systems is of interest to the Clift group. Specifically, we are interested in developing new cofactor-inspired reactions using quinone catalysts.

Chapter 2

Development of Quinone-Catalyzed Oxidative C–C Bond Cleavage and its Application to Amino Acid Homologation

Portions of this chapter will appear in the following publication:

Haugeberg, B. J.; Phan, J. H.; Liu, X.; O'Connor, T. J.; Clift, M. D. "Homologation of α -Aryl Amino Acids through Quinone-Catalyzed Decarboxylation/Mukaiyama-Mannich Addition." *Manuscript submitted*.

Leon, M. A.; Liu, X.; Phan, J. H.; and Clift, M. D. "Amine Functionalization through Sequential Quinone-Catalyzed Oxidation/Nucleophilic Addition" *Manuscript submitted*.

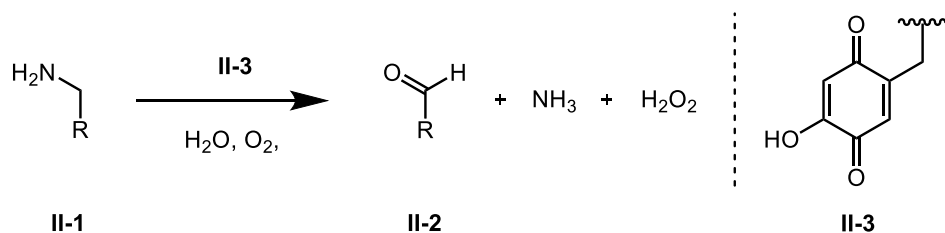
Chapter 2 Quinone Cofactor Mimics

In Chapter 1, we explored the use of cofactor mimics as organocatalysts – a concept that has led to the discovery of many new reactions. This chapter will focus on the development of a new method for amino acid homologation that is catalyzed by a topaquinone cofactor mimic.

2.1 Introduction to Quinone Cofactors and Their Applications in Organocatalytic Reactions

Owing to their ability to oxidize amines in biological systems, quinones have become a reagent of interest in organic synthesis. In the 1990s, Mure and Klinman studied the active site of amine oxidases in detail where they reported copper-containing amine oxidases catalyze the oxidative deamination of primary amines (**II-1**) to their corresponding aldehydes (**II-2**).⁴¹ In their work, they identified a topa-quinone cofactor (TPQ, **II-3**) responsible for promoting the amine oxidation (Scheme 2.1) from experiments using varying classes of bovine serum amine oxidase (BSAO).⁴²

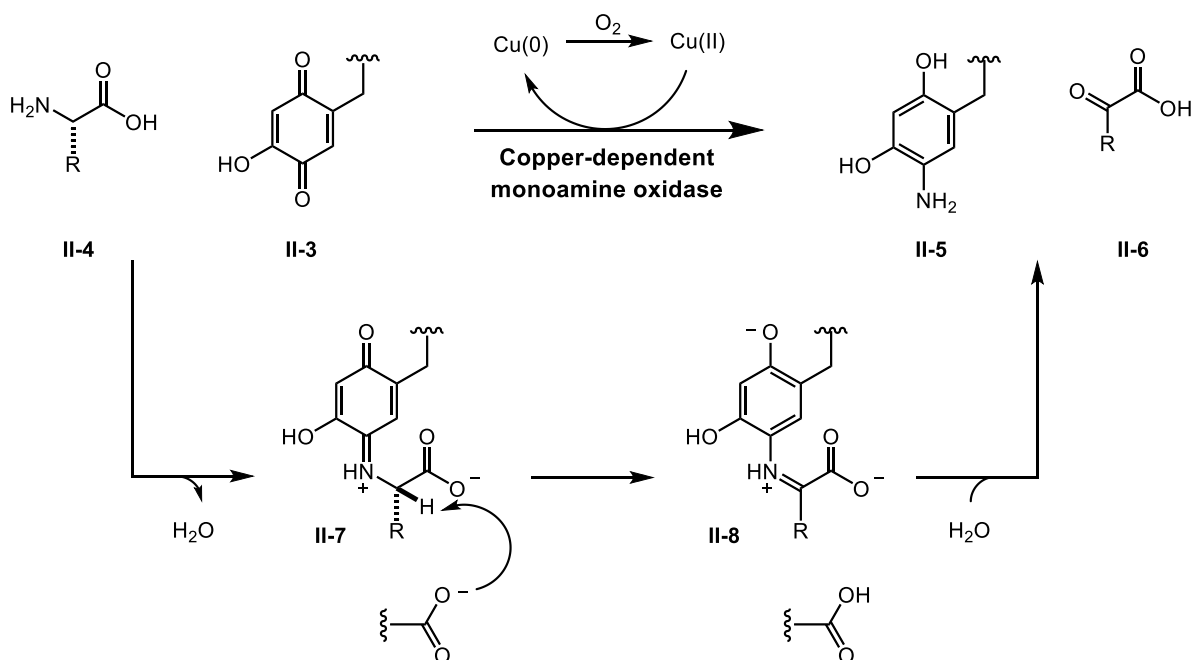
Scheme 2.1: Discovery of TPQ as Cofactor in Active Site of BSAO



Having identified the cofactor responsible for amine oxidation, Mure and Klinman proposed a general mechanism for quinone-containing monoamine oxidases. (Scheme 2.2).⁴³ First, an amino acid substrate would condense to an enzyme-bound topa-quinone to deliver

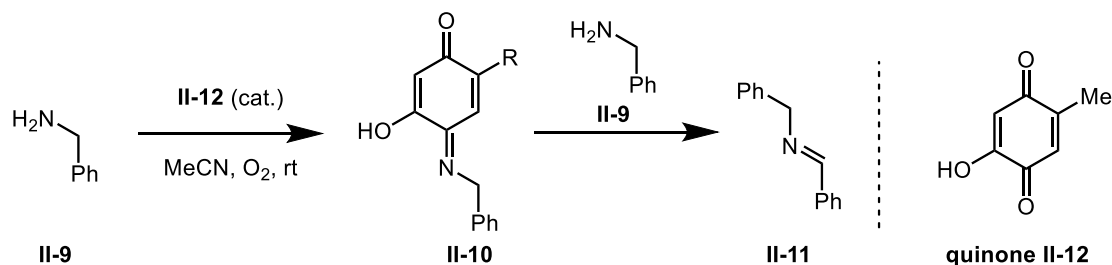
iminoquinone intermediate **II-7**. A subsequent deprotonation event occurs at the hydrogen on the α -carbon to deliver N-aryl imine **II-8**. Then, hydrolysis of imine **II-8** delivers keto-acid **II-6** and a reduced form of the quinone (**II-5**). A copper-promoted oxidation returns the active quinone species **II-3** to complete the catalytic cycle.

Scheme 2.2: Mechanism of Topa-quinone Oxidation of Amino Acid



Following elucidation of the active cofactor species, they conducted a series of experiments examining the ability of TPQ mimics to oxidize amines. During these studies, they developed conditions for the aerobic oxidation of benzylamine (**II-9**) into homo-dimeric imine products (Scheme 2.3, **II-11**) using a series of 2-hydroxy-5-alkyl-1,4-benzoquinones (**II-12**) as cofactor mimics.^{44, 45}

Scheme 2.3: Quinone-Catalyzed Amine Oxidation Developed by Mure and Klinman



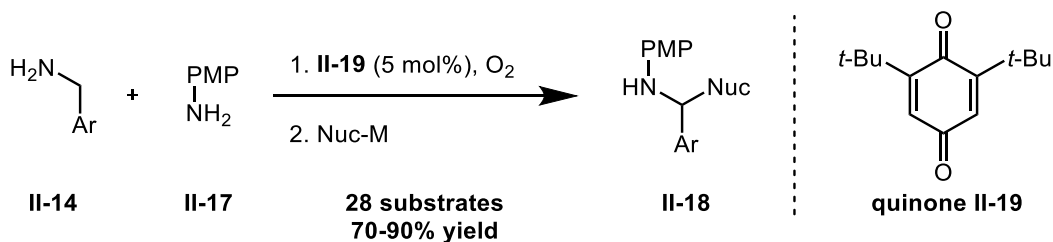
The Stahl group has parlayed Mure and Klinman's discovery of aerobic oxidation of primary benzylic amines (**II-14**) by using a quinone (**II-16**) as a catalyst (Scheme 2.4).⁴⁶ They were able to develop conditions for quinone-catalyzed aerobic cross-coupling of primary benzylic amines to afford secondary imines (**II-15**) using mild reaction conditions. This contribution demonstrates transimination could be promoted selectively by primary amine derivatives (such as aniline based compounds, **II-13**) that are incapable of undergoing quinone-promoted oxidation. The development of this quinone-catalyzed process by Stahl inspired the Clift group to pursue the use of quinone organocatalysts in amine functionalization reactions.

Scheme 2.4: Stahl's Quinone-Catalyzed Amine Oxidation



Initial research in the Clift group focused on exploring the formal quinone-catalyzed α -C–H bond functionalization of primary amines. Methods for α -functionalization of α -C–H bonds in secondary and tertiary amines are well known;⁴⁷⁻⁴⁹ however α -functionalization of primary amines is far less developed. By combining quinone-catalyzed amine oxidation with established imine addition protocols,⁵⁰ the Clift group sought to develop a method for primary amine functionalization. Ultimately the successful development of a new method for formal C–H functionalization using a sequential, one pot quinone-catalyzed amine oxidation/nucleophilic addition process was achieved along with the discovery of a commercially available quinone catalyst for aerobic amine oxidation (Scheme 2.5). These studies set the stage for the discovery of related quinone-catalyzed reactions.

Scheme 2.5: Formal Quinone-Catalyzed Amine Functionalization

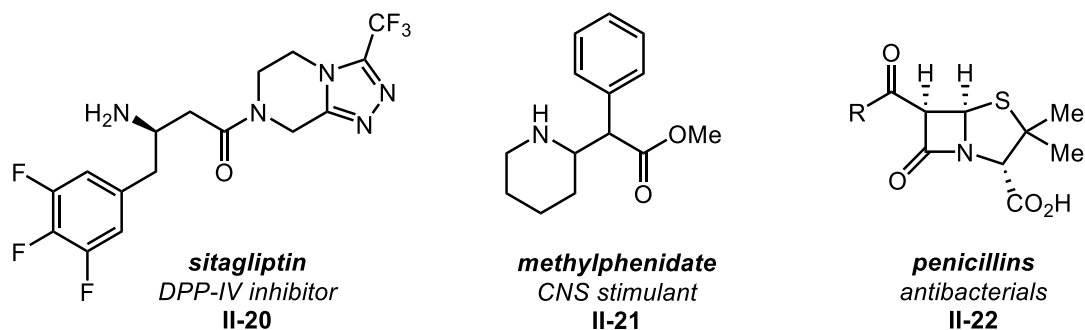


2.2 β -Amino Acid Synthesis via Oxidative-Decarboxylation/Mukaiyama–Mannich Addition

After concluding this work, we began to envision other potential applications for quinone organocatalysis. One potential application is α -amino acid homologation to enable β -amino acid synthesis. β -amino acid derivatives have become valuable synthetic targets owing to their ability to resist protease degradation and stabilize protein structure, and their use as designer β -peptides (showing potential as anti-bacterial⁵¹ and anti-HIV agents⁵²) and an extensive range of FDA-

approved pharmaceutical agents **II-20–II-22** (Figure 2.1). We sought to develop a new method to access these important compounds via quinone-promoted α -amino acid homologation.⁵³⁻⁵⁷

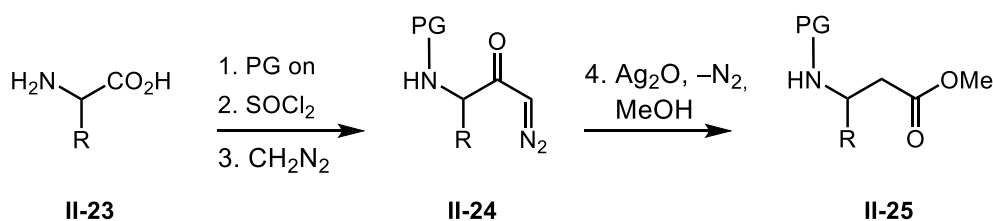
Figure 2.1: Selected β -Amino Acid-Derived Pharmaceuticals



2.2.1 Classical Methods for β -Amino Acid Synthesis

Over the years, a number of methods have been developed to carry out α -amino acid homologation. The Arndt–Eistert homologation is a commonly employed method designed to convert carboxylic acids to a higher carbonyl homologue (Scheme 2.6).^{58, 59}

Scheme 2.6: Arndt-Eistert Homologation

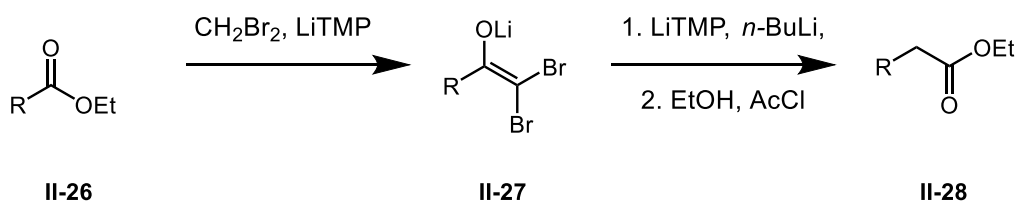


In a multi-step procedure, the described Arndt–Eistert homologation for α -amino acids (**II-23**) begins with protecting the amine, followed by converting the carboxylic acid to an acid chloride. Upon treatment with diazomethane, followed by treatment with a nucleophile and silver

catalyst, the diazoketone (**II-24**) will undergo a Wolff-type rearrangement to give the homologated product (**II-25**). Although it has been widely employed for α -amino acid homologations, this method requires the use of a very dangerous reagent (diazomethane) and an expensive metal catalyst.

The Kowalski ester homologation was specifically designed to avoid the use of diazomethane to provide a safer means for α -amino acid homologation (Scheme 2.7). Kowalski showed esters treated with pre-formed dibromomethylithium, followed by a strong base at low temperature, could afford intermediate α,α -dibromo enolate (**II-27**). Subsequent addition of *n*-butyllithium results in lithium-halogen exchange and rearrangement provides an ynone intermediate (not shown), which upon quenching with the appropriate alcohol, results in production of the homologation product **II-28**.⁶⁰

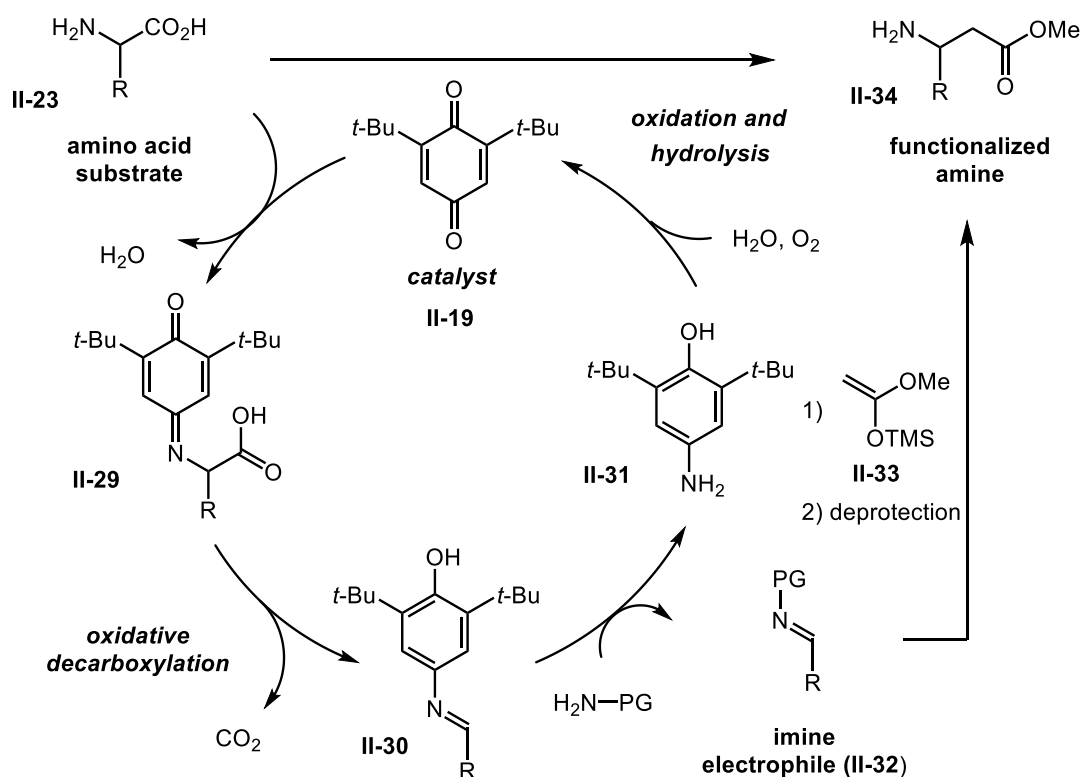
Scheme 2.7: Kowalski Ester Homologation



While these reactions, and their contemporary counterparts⁶¹⁻⁶⁴ have been broadly employed, they typically require multi-step synthetic operations, utilize costly or dangerous reagents, and proceed through highly reactive intermediates. Therefore, developing a new protocol for amino acid homologation that proceeds in fewer steps under mild conditions is desirable. We envisioned a process to proceed by quinone-catalyzed oxidative-decarboxylation.^{65, 66}

Specifically, we envisioned that a quinone-catalyst could enable α -amino acid decarboxylation to provide an imine, which could be trapped in-situ via Mukaiyama–Mannich addition to provide the homologated product (Figure 2.2).

Figure 2.2: Proposed Mechanism for Quinone-Catalyzed Amino Acid Functionalization



We expected that first an amino acid (**II-23**) would condense with the quinone catalyst **II-19**. At this point, instead of deprotonation at the α -position of the amino acid, a base would deprotonate the more acidic carboxylic acid, in turn promoting a decarboxylation of **II-29** to provide the N-aryl imine **II-30**. This species would readily undergo transimination with a stable N-protected amine to afford an N-protected imine product **II-32**. The active catalyst would then be regenerated through auto-oxidation and β -amino esters could be accessed by subjecting imine

II-32 to a Mukaiyama–Mannich addition using silyl ketene acetal **II-33**. Subsequent deprotection would provide the homologation product **II-34**. Our studies began with an examination of the oxidative-decarboxylation, as this step was unprecedented.

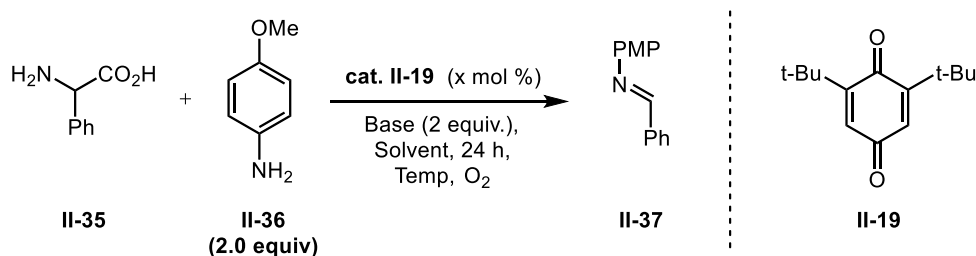
2.3 Development of Oxidative-Decarboxylation: Substrate Scope and Reaction Conditions

We began by examining the potential of phenylglycine to undergo oxidative-decarboxylation in the presence of quinone catalyst **II-19** (Table 2.1). Phenylglycine was chosen as a test substrate for reaction optimization because the expected imine product would be incapable of tautomerization. In initial experiments, the organic solvents tested provided only heterogeneous reaction mixtures, resulting in no observed product formation (entries 1-3, 0%). Using a DMSO solvent also produced a heterogeneous reaction mixture, but provided the first observation of imine formation (entry 4, 39%). Prior to this point, we anticipated that one of the free amines in the reaction mixture would act as a base to promote decarboxylation. In entry 5, triethylamine was added as a base, which provided a slightly better yield (entry 5, 42%). Increasing the reaction temperature in DMSO solvent showed improvement but insufficient conversion (entry 6, 68%,) and using only water as the solvent provided low solubility of other organic reagents (entry 7, 63%).

At this point, biphasic conditions were explored using Acetonitrile:water at 80°C (entry 8, 74%), along with a variety of catalyst loadings and bases (entries 9-13, 75-90%), This led to the discovery of optimal biphasic conditions (entry 14, 91%). At this point, we recognized the presence of water in the reaction mixture may interfere with subsequent Mukaiyama–Mannich additions. Fortunately, using ethanol as a solvent provided a good yield under similar reaction

conditions (entry 15, 70%), and increasing the reaction temperature provided an excellent yield of 92% (entry 16). Entries 16 and 17 suggests solvent polarity is an important factor for promoting quinone-catalyzed oxidative-decarboxylation as an ethanol solvent provides good yields while isopropanol does not (entry 17, 10%).

Table 2.1: Reaction Discovery and Optimization



Entry	Solvent	Temperature	Catalyst Loading	Base	Yield ^a
1	1,4-Dioxane	50°C	5%	-	0%
2	THF	50°C	5%	-	0%
3	CH ₃ CN	50°C	5%	-	0%
4	DMSO	50°C	5%	-	39%
5	DMSO	50°C	5%	Et ₃ N	42%
6	DMSO	80°C	5%	Et ₃ N	68%
7	H ₂ O	80°C	5%	Et ₃ N	63%
8	CH ₃ CN:H ₂ O (1:1)	80°C	5%	Et ₃ N	74%
9	CH ₃ CN:H ₂ O (1:1)	80°C	10%	Et ₃ N	90%
10	CH ₃ CN:H ₂ O (1:1)	80°C	10%	Na ₃ PO ₄	84%
11	CH ₃ CN:H ₂ O (1:1)	80°C	10%	DIPEA	87%
12	CH ₃ CN:H ₂ O (1:1)	80°C	10%	K ₂ PO ₄	75%
13	CH ₃ CN:H ₂ O (1:1)	50°C	5%	Et ₃ N	84%
14	CH₃CN:H₂O (1:1)	50°C	10%	Et₃N	91%
15	EtOH	50°C	10%	Et ₃ N	70%
16	EtOH	70°C	10%	Et₃N	92%
17	<i>i</i> PrOH	70°C	10%	Et ₃ N	10%

^a Determined by ¹H NMR using methyl benzoate as an internal standard

These results prompted a study on the scope of oxidative-decarboxylation using a range of amino acids. With knowledge of the results from the study, we would then begin developing a protocol for β-amino acids synthesis.

2.3.1 Scope of Oxidative-Decarboxylation in Acetonitrile:Water

With both sets of optimized conditions in hand (entries 14 and 16, Table 2.1), the oxidative-decarboxylation was studied on a variety of amino acids that were either purchased from commercial sources or synthesized by a Petasis reaction.⁶⁷ Determining which amino acids the quinone catalyst **II-19** could oxidize was expected to provide information regarding the application of this method to β -amino acid synthesis. The results are summarized in Table 2.2. The imine product provided from oxidative-decarboxylation of phenylglycine was isolated in 85% yield (entry 1). When analyzing para-substituted aryl glycines, electron withdrawing groups provided generally higher yields than did electron donating groups with yields ranging from 85-87% (entries 9-12). The aryl substituents with electron donating substituents at the para position gave notably lower yields (entry 7, 76%, entry 8, 78%). It should be noted that oxidation of aryl glycine to lend imine **II-46** also required increased catalyst loading presumably owing to the strong electron donating ability of the methoxy group. **II-42** was isolated in the highest yield at 95%. Substitution at the ortho-position of the aryl rings showed no steric bias while at the same time mirrored the para- substitution in terms of electronic effects (entry 3, 86% and entry 2, 75%). A vinylogous aryl substituent was also tolerated, providing **II-51** in 69% yield, indicating α -aryl substituents are not required (entry 13). Hetro-aromatic substituents are also suitable reaction partners (entry 5, 80% and entry 6, 58%), following similar trends of other electron rich substituents.

Table 2.2: Isolated Yields for Oxidative-Decarboxylation with Acetonitrile:Water Solvent

II-23			II-38		
			II-19		
entry	product	yield ^a	entry	product	yield ^a
1		II-39 , R = H, 85%	13		II-51 , R = H, 69%
2		II-40 , R = Me, 75%			
3		II-41 , R = Cl, 86%			
4		II-42 , R = F, 95%	14		II-52 , R = H, 0%
5		II-43 , X = S, 80%	15		II-53 , R = OH, 0%
6 ^b		II-44 , X = O, 53%	16		II-54 , R = OH, 0%
7		II-45 , R = Me, 76%	17		
8 ^b		II-46 , R = OMe, 78%	18		
9		II-47 , R = F, 85%			II-55 , R = Me, 0%
10		II-48 , R = Cl, 86%			II-56 , R = Et, 0%
11		II-49 , R = Br, 86%			
12		II-50 , R = CF ₃ , 86%			

^a Isolated yields, ^b 20 mol % catalyst.

One limitation of this protocol is that it fails to oxidize any natural amino acids (entries 14-18, 0% yields). From these results, we presume sp^2 hybridization at the carbon β to the amine is required in decarboxylation promoted by quinone **II-19**. We speculate that substrates with β - sp^2

carbons more readily accept electron density from the C–C bond cleavage event of the decarboxylation. This proposal is supported when analyzing trends in substituted aryl glycines where electron rich substituents lead to reduced yields whereas electron poor substituents lead to higher yields. Another possible explanation for not observing oxidative decarboxylation products of natural amino acids is potential decomposition of the imine products. The products in entries 14-18 could tautomerize under reaction conditions to their corresponding enamines and form Mannich products. It should be noted such products have not been observed. Further discussion on the mechanism for oxidative-decarboxylation can be found in later sections (Section 2.5).

2.3.2 Scope of Oxidative-Decarboxylation in EtOH

Although there is evidence to the contrary, we recognized the presence of water in the reaction mixture may interfere with subsequent Mukaiyama–Mannich additions.^{68, 69} To better prepare for this potential limitation, a similar substrate scope study was conducted using the optimized conditions wherein ethanol was employed as the solvent (Table 2.3).

In these experiments, products of electron donating substituents (**II-40**, 97% and **II-45**, 98%) gave yields that rivaled their electron withdrawing counterparts (entry 3, 97%, entry 8, 98%, entry 9, 98%, entry 10, 99%) and an electron rich hetroaromatic amino acid substrate gave a high yield (**II-43**, 92%). **II-46** was provided in 88% yield, also higher than under the previous conditions with half the catalyst loading, albeit requiring longer reaction time. Unfortunately, natural amino acids remain resistant to oxidation under these conditions as well (entries 11-15).

Table 2.3: NMR Yields for Oxidative-Decarboxylation with EtOH Solvent

II-23			II-38		
entry	product	yield ^a	entry	product	yield ^a
1		II-39 , R = H, 92%	6		II-45 , R = Me, 98%
2		II-40 , R = Me, 97%	7 ^b		II-46 , R = OMe, 88%
3		II-41 , R = Cl, 97%	8		II-47 , R = F, 98%
			9		II-48 , R = Cl, 98%
			10		II-49 , R = Br, 99%
4		II-42 , R = F, 97%	11		II-52 , R = H, 0%
			12		II-53 , R = OH, 0%
5		II-43 , 92 %	13		II-54 , R = OH, 0%
			14		II-55 , R = Me, 0%
			15		II-56 , R = Et, 0%

^a ¹H NMR yields, ^b 48 h reaction time

2.3.3 Study of Amine Reaction Partners Other Than Anisidine

A study to assess the possibility of utilizing other N-protected amines for the transimination event was also conducted (Table 2.4). α -Methylbenzyl amine derivatives provided good yields (entry 1, 91% and entry 2, 97%) in the described process, which was anticipated on the basis of previous results.⁶ The imine products derived from this amine could be synthetically useful in developing subsequent diastereoselective additions if enantiopure α -methylbenzyl amine is used.

Table 2.4: Substrate Scope for Primary Amine Coupling Partners

<div style="display: flex; align-items: center; justify-content: space-around;"> <div style="text-align: center;"> <chem>N[C@@H](Cc1ccccc1)C(=O)O</chem> II-35 </div> <div style="text-align: center;"> $\xrightarrow[\text{2.0 equiv. Et}_3\text{N, 50}^\circ\text{C, 24 h, O}_2]{\text{cat. II-18 (10 mol\%), MeCN:H}_2\text{O, 0.312 M, 2.0 equiv. amine}}$ </div> <div style="text-align: center;"> <chem>RN=Cc1ccccc1</chem> II-64 </div> <div style="border-left: 1px dashed black; width: 10px; height: 100px; margin: 0 10px;"></div> <div style="text-align: center;"> <chem>CC(C)(C)C1=C(C(=O)C(C)=C(C(=O)O1)C(C)(C)C</chem> II-19 </div> </div>			
entry	amine	product	yield ^a
1	<chem>Rc1ccc(cc1)C(C)N</chem>	<chem>Rc1ccc(cc1)C(C)N=Cc2ccccc2</chem>	II-57 , R = H, 91%
2			II-58 , R = F, 97%
3	<chem>Rc1ccccc1CN</chem>	<chem>Rc1ccccc1CN=Cc2ccccc2</chem>	II-59 , R = Me, 75%
4			II-60 , R = OMe, 45%
5 ^b	<chem>Rc1ccc(cc1)C(c2ccc(R)cc2)N</chem>	<chem>Rc1ccc(cc1)C(c2ccc(R)cc2)N=Cc3ccccc3</chem>	II-61 , R = H, 78%
6			II-62 , R = OMe, 72%
7 ^c	<chem>C[C@H](C)(C)N</chem>	<chem>C[C@H](C)(C)N=Cc1ccccc1</chem>	II-63 , 90% ^c

^a yields determined by ¹H NMR using methyl benzoate a standard. ^b 20 mol % catalyst.

^c 6 equiv. amine

Benzylamines could also promote transimidation (entry 3, 75% and entry 4, 45%), but reactions showed significant quantities of homo-coupled imine products, resulting in lower yields. This should not be surprising considering that quinone-catalyzed amine oxidations of such substrates have been reported.⁴ Interestingly, the bulkiness of the ortho-substituent seems to affect

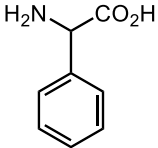
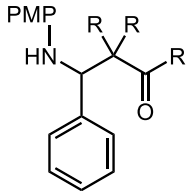
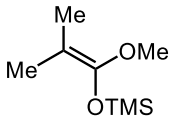
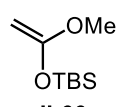
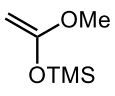
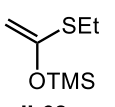
the reaction outcome, indicating bulky groups may hinder condensation of the amine to the quinone catalyst leading to increased efficiency (entries 3 and 4). Benzyhydril amine derivatives were tolerated at increased catalyst loading (entry 5, 78% and entry 6, 72%), forming phenylmethanimines products. An alkyl amine (entry 7, 90%) provided a high yield but required a super stoichiometric equivalence due to amine volatility under the elevated temperature of the reaction conditions. Aside from the results from benzylamine reaction partners, the quinone-catalyzed oxidation proceeds selectively with amino acid decarboxylation over C–H oxidation.

2.4 Development of Conditions for β -amino ester synthesis

With the capability to generate electrophilic imine intermediates via quinone-catalyzed oxidative-decarboxylation of amino acids, we next pursued the development of a new method for β -amino acid synthesis through acid catalyzed Mukaiyama–Mannich addition (Table 2.5). In developing a protocol for a streamlined two-step, one-pot synthesis, we began by testing addition reactions with a known, robust silyl ketene acetal (SKA) nucleophile (**II-65**) using imines generated via quinone-catalyzed oxidative-decarboxylation in acetonitrile:water.^{28,29} We started by testing potential Lewis acid catalysts, but found very limited success (entries 1-4, 0-13%). This may be a result of the excess amine species in the reaction mixture binding with the Lewis acids. Using catalytic tetrafluoroboric acid (HBF₄) provided a promising initial addition result (entry 5, 24%), and super stoichiometric amounts of HBF₄ were able to promote the desired reactivity in good yield (entry 8, 87%). The amount of HBF₄ required to promote addition may be a result of competing acid-base reactions. In a separate analysis, it was observed that the SKA undergoes

proto-desilylation in the presence of HBF₄. Therefore, addition of super stoichiometric amounts of both reagents is required to obtain efficient addition.

Table 2.5: Optimization of Two-Step, 1-Pot β -Amino Ester Synthesis

<div style="display: flex; align-items: center; justify-content: space-around;"> <div style="text-align: center;">  <p>II-36</p> </div> <div style="text-align: center;"> <p>1. cat. II-19 (10 mol%) anisidine (2.0 equiv.) solvent, Et₃N, 50 °C, 24 h, O₂</p> <p>2. SKA (3.0 equiv.) acid (x equiv.) N₂, 0°C</p> </div> <div style="text-align: center;">  <p>II-64</p> </div> <div style="border-left: 1px dashed black; padding-left: 10px;"> <div style="display: flex; flex-direction: column; align-items: center;"> <div style="text-align: center;">  <p>II-65</p> </div> <div style="text-align: center;">  <p>II-66</p> </div> </div> <div style="display: flex; flex-direction: column; align-items: center;"> <div style="text-align: center;">  <p>II-67</p> </div> <div style="text-align: center;">  <p>II-68</p> </div> </div> </div> </div>					
entry	SKA	solvent	Lewis or Brønsted Acid	acid equiv.	yield ^a
1 ^b	II-65	MeCN:H ₂ O	Sc(OTf) ₃	0.2	0 %
2 ^b	II-65	MeCN:H ₂ O	Yb(OTf) ₃	0.2	0 %
3 ^b	II-65	MeCN:H ₂ O	La(OTf) ₃	0.2	0 %
4 ^b	II-65	MeCN:H ₂ O	Zn(OTf) ₂	0.2	13 %
5 ^b	II-65	MeCN:H ₂ O	HBF ₄	0.2	24 %
6 ^b	II-65	MeCN:H ₂ O	HBF ₄	0.5	28 %
7 ^b	II-65	MeCN:H ₂ O	HBF ₄	1.0	38 %
8 ^b	II-65	MeCN:H₂O	HBF₄	2.2	87 %
9 ^b	II-66	MeCN:H ₂ O	HBF ₄	2.2	0 %
10 ^b	II-67	MeCN:H ₂ O	HBF ₄	2.2	0 %
11 ^b	II-68	MeCN:H ₂ O	HBF ₄	2.2	0 %
12 ^c	II-65	EtOH/THF	HBF₄	2.2	89 %
13 ^c	II-66	EtOH/THF	HBF ₄	2.2	0 %
14 ^c	II-68	EtOH/THF	HBF₄	2.2	74 %

^a isolated yields. ^b MeCN:H₂O solvent in both steps. ^c solvent from step 1 was completely removed and replaced.

With the optimized conditions in hand, SKA (**II-66**, **II-67**, and **II-68**) additions that would yield true homologation products were attempted, but each failed to add into the imine intermediate under the optimized conditions (entries 9-11, 0%). Fortunately, replacing acetonitrile:water with EtOH, which could easily be removed under reduced pressure after imine formation solved this problem (entry 12, 89%). By using THF as a solvent for Mukaiyama–Mannich addition, the homologation reaction proceeded smoothly when SKA **II-65** was employed (entry 12, 89%). SKA

II-66 and **II-68** were tested using this protocol, and we found that **II-68** provided the best result (entry 13, 0%, entry 14, 74%).

2.4.1 β -Amino Ester Synthesis Using gem-Dimethyl Silyl Ketene Acetal Nucleophile

With proper conditions in place, the subsequent two-step, one-pot procedure was studied with the gem-dimethyl silyl ketene acetal (**II-65**) using a variety of aryl glycine derivatives. Using phenylglycine as the substrate, the homologated product was isolated in 89% yield (Table 2.6, entry 1).

Table 2.6: Scope Studies Using gem-Dimethyl Silyl Ketene Acetal Nucleophile

	1. II-19 (10 mol%), O ₂ , Et ₃ N, anisidine, EtOH, 70°C		
II-69	2. II-65 HBF ₄ , N ₂ THF, 0°C	II-70	II-19

entry	product	yield ^a	entry	product	yield ^a
1		II-71 , R = H, 89%	5		II-75 , R = Me, 80%
2 ^b		II-72 , R = Me, 15%	6		II-76 , R = OMe, 83%
3		II-73 , R = Cl, 65%	7		II-77 , R = F, 80%
			8		II-78 , R = Cl, 87%
			9		II-79 , R = Br, 85%
4		II-74 , R = F, 94%	10		II-80 , 82%

^a Isolated yields. ^b Determined by ¹H NMR using methyl benzoate as an internal standard.

Although electronic effects did not seem to significantly alter addition yields, steric effects were more prominently noticed. The ortho-substituted aryl imines seemed less susceptible to addition from the relatively bulky nucleophile, as ortho-methyl product **II-72** was determined to only yield 15% by ^1H NMR, while a smaller ortho-chloro group provided product **II-73** in 65% yield (entry 2 and 3).⁷⁰ The meta-substituted product **II-74** was isolated in the best yield at 94% (entry 4).

In terms of para-substituted substrates, electronic factors seem to have minimal influence of reaction efficiency as all electron donating and electron withdrawing substituents tested were isolated in yields at or above 80% (entries 5-9). An electron rich heteroaromatic species **II-80** also was isolated in 82% yield. From these results, a clear steric bias was noticed when comparing ortho- and para- substituted imines of the same substitution. The ortho-methyl product **II-72** was isolated in a much lower yield than its para-substituted counterpart (entries 2 and 5), and this trend was also observed when testing the chlorinated derivatives (entry 3, **II-73**, 65% and entry 8, **II-78**, 87%).

2.4.2 β -Amino Ester Synthesis Using Silyl Ketene (Thio)Acetal Nucleophile

In order to perform a true amino acid homologation, the aryl glycine derivatives were then subjected to nucleophilic addition with a silyl ketene (thio)acetal (Table 2.7). In line with the trends noticed previously, ortho-substituted aryl glycines again show steric effects. Ortho-methyl substituted phenylglycine provided the lowest yield of all substrates (entry 2, 56%) while ortho-chloro gave the highest (entry 3, 95%). This observation may line itself with the smaller nature of

the chlorine atom, experiencing reduced steric hindrance of nucleophilic addition.³⁰ The meta-substituted **II-85** was isolated in 78%.

Table 2.7: Scope Studies using Silyl Ketene (Thio)acetal Nucleophile

entry	product	yield ^a	entry	product	yield ^a
1		II-82 , R = H, 74%	5		II-86 , R = Me, 89%
2		II-83 , R = Me, 56%	6		II-87 , R = OMe, 88%
3		II-84 , R = Cl, 95%	7		II-88 , R = F, 84%
			8		II-89 , R = Cl, 94%
			9		II-90 , R = Br, 72%
4		II-85 , R = F, 78%	10		II-91 , 77%

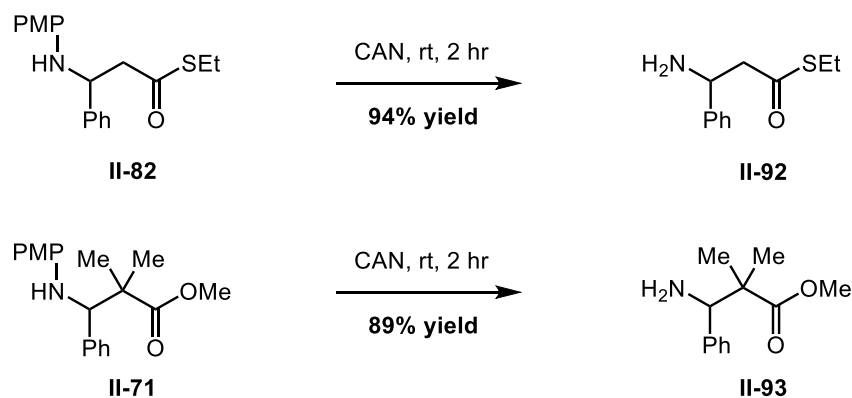
^a Isolated yields.

Electronic effects do not seem to have a strong influence on the addition as indicated by mostly good yields of entries 5-9 (72-94%). Electron rich heteroaromatic species were tolerated by this process (entry 10, 77%). Again, information regarding steric effects can be gleaned by comparing electronically similar ortho- and para- substituted glycine derivatives. Although both ortho- and para-chlorinated substituents provide excellent yields (entry 3, 95%, entry 8, 94%), the ortho- and para-methyl derivatives show significant differences in product formation (entry 2, 56%, entry 5, 89%)

2.4.3 Deprotection of Homologation Products

The described process demonstrates conversion of an α -amino acid into a β -amino acid derivative bearing an N-PMP-protected amine. Although in many synthetic applications, protected amines, as well as esters, are more easily manipulated than unprotected amines and carboxylic acids, an amine deprotection was carried out to provide the free amine (Scheme 2.9). Using cerium ammonium nitrate (CAN) as an oxidant, PMP deprotection was easily achieved in high yields to afford the corresponding products of direct amino acid homologation (**II-92** and **II-93**).⁷¹

Scheme 2.9: Deprotection of Homologation Products



2.5 Mechanistic Studies for Quinone-Catalyzed Oxidative-Decarboxylation

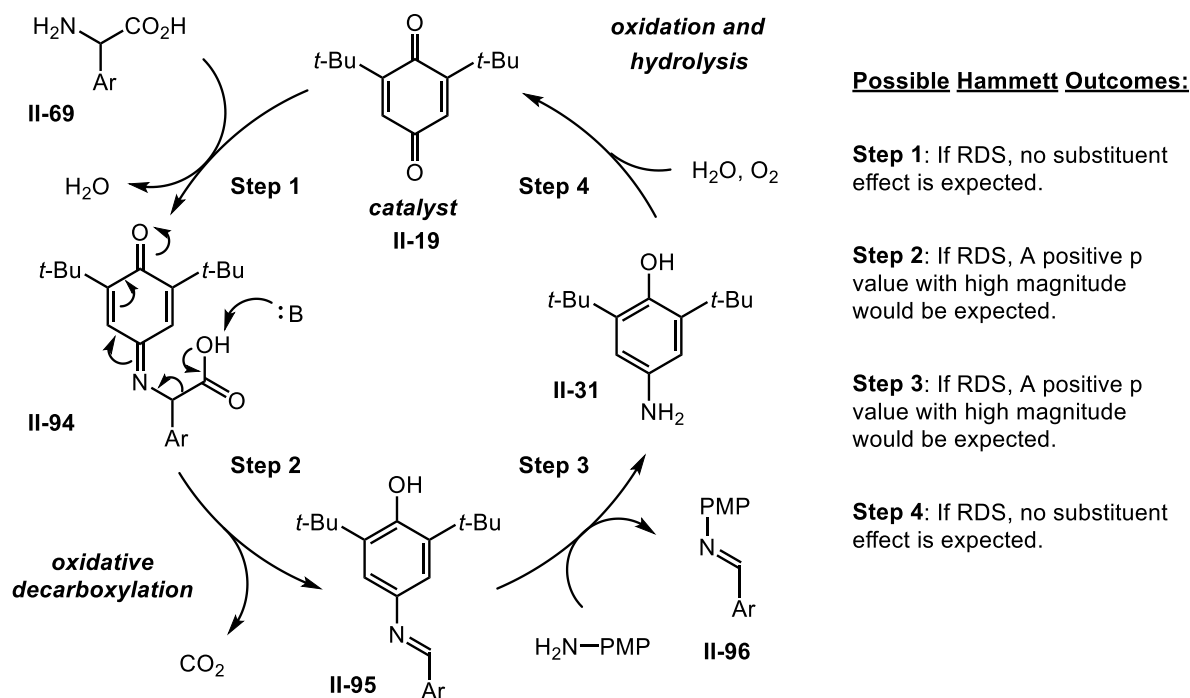
The previously described method for quinone-catalyzed oxidative-decarboxylation has a significant limitation, the inability to oxidize naturally occurring amino acids. Initial speculation leads us to believe this limitation can be overcome through catalyst design. In order to understand the properties that will ultimately provide a functional catalyst, we must determine what hinders the current system from promoting oxidative-decarboxylation of natural amino acids. We expect that experimentally establishing the mechanism of quinone-catalyzed amino acid decarboxylation

will provide the appropriate knowledge to design a catalyst capable of carrying out the desired transformations.

2.5.1 Hammett Analysis on Quinone-Catalyzed Oxidative-Decarboxylation

A Hammett analysis was conducted to provide evidence for the rate-determining step (RDS) of quinone-catalyzed amino acid decarboxylation.⁷² In this set of experiments, a series of commercially available aryl glycine derivatives with varying substituents in the para-position were utilized. In each case, the initial rate of the reaction for a given para-substituent X (expressed as k_X) was assessed using ^1H NMR. These rates (k_X) were compared with the baseline rate of the reaction where $X = \text{H}$ (expressed as k_{H}), and the logarithm of the quotient k_X/k_{H} was plotted as a function of the Hammett parameter σ_{para} .³² A series of expected possible results is discussed in Figure 2.3.

Figure 2.3 Proposed Mechanism and Interpretation of the Hammett Analysis



If step 1 were rate-determining, one would expect a ρ value of 0, as substitution of the aryl amino acid should not dictate its ability to condense with the quinone. A positive ρ value may be an indication that step 2 or step 3 are rate-determining. In step 2, the decarboxylation could shift electron density to the benzylic carbon.⁷³ In step 3, a transimination event would provide a positive ρ value, as a decrease in positive charge would be expected from pyramidalization.⁷⁴

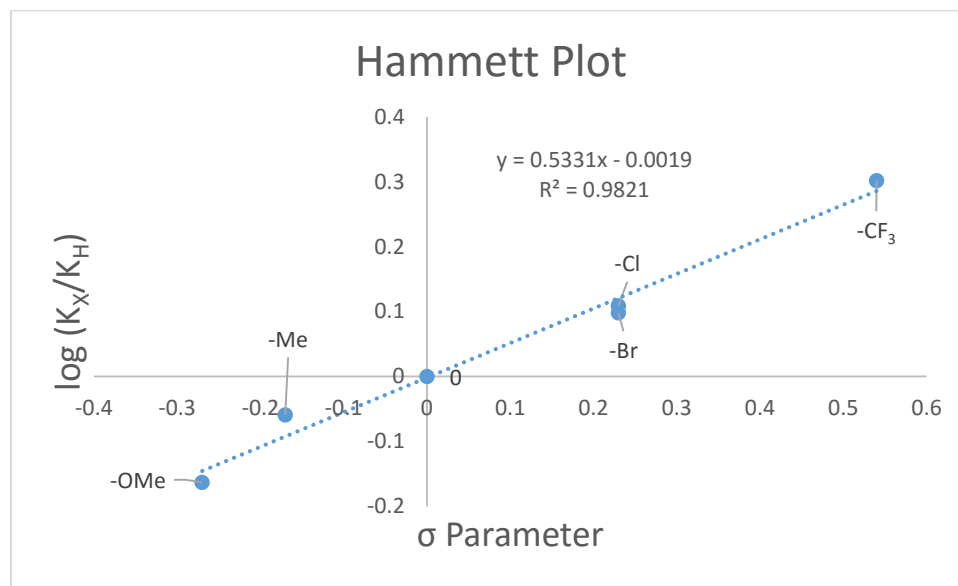
The initial rates for oxidative decarboxylation were determined and the data is shown in Figure 2.4. Using this data to construct a Hammett Plot revealed a ρ value, indicating negative charge density accumulates at the reaction center (Figure 2.5). This observation allows for the elimination of proposed steps 1 and 4 as potential RDS, but leaves us to differentiate between steps 2 and 3 as potential RDS. If step 2 was rate determining, this positive ρ value could indicate a negative charge build up resulting from decarboxylation. If step 3 was rate determining, this positive ρ value could indicate a decrease in positive charge would be expected from pyramidalization of the imine during transamination. For complete mechanistic elucidation, further experimentation is needed.

Figure 2.4: Reaction Rates for Quinone-Catalyzed Oxidative-Decarboxylation

entry	R	rate (mol/(L*h))	entry	R	rate (mol/(L*h))
1	H	0.0220	4	Cl	0.0283
2	Me	0.0192	5	Br	0.0276
3	OMe	0.0151	6	CF ₃	0.0441

1,3,5-trimethoxybenzene as internal NMR standard

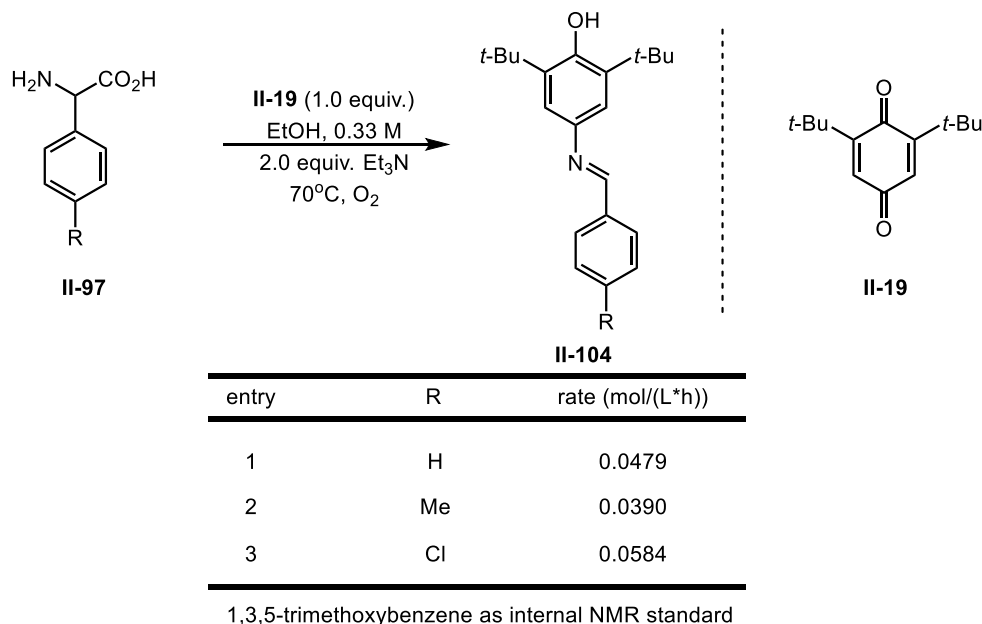
Figure 2.5: Hammett Plot for Quinone-Catalyzed Oxidative-Decarboxylation



2.5.2 Hammett Analysis on Stoichiometric Quinone-Promoted Oxidative-Decarboxylation

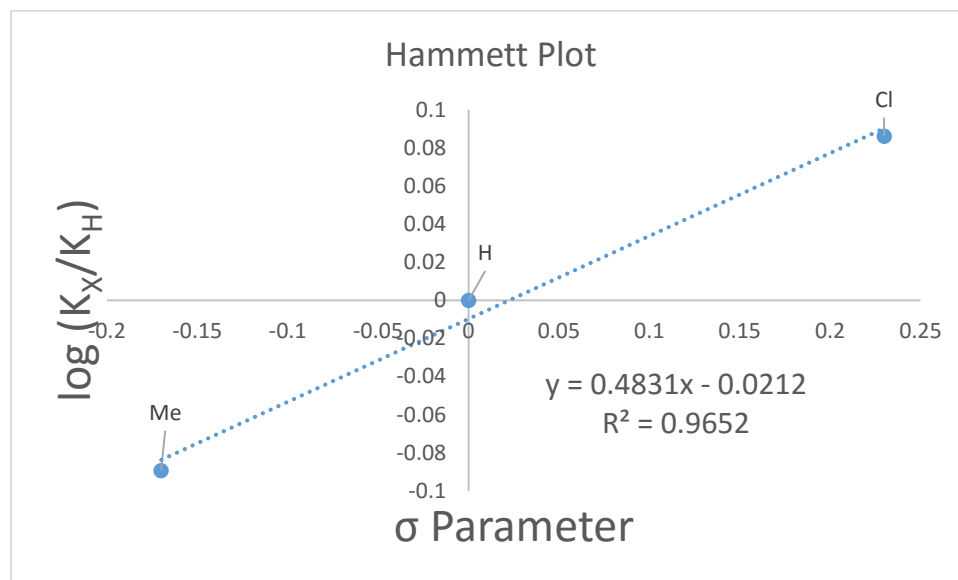
In order to obtain more information on the decarboxylation step in the catalytic cycle, we recorded rate data for the oxidative decarboxylation event by monitoring a stoichiometric quinone-promoted decarboxylation of α -aryl amino acids. This would eliminate the transimination step and allow a more direct analysis of decarboxylation. α -Aryl amino acids were submitted to conditions with 1.0 equiv. of quinone (**II-19**) in the absence of anisidine, and conversion was measured by ¹H NMR by the formation of imine **II-95** and its corresponding aldehyde, a hydrolysis byproduct.

Figure 2.6: Reaction Rates for Stoichiometric Quinone-Promoted Oxidative-Decarboxylation



As expected, the rates for stoichiometric decarboxylation were much faster than the catalytic process. Again, a Hammett plot was constructed and revealed a positive ρ value, indicating negative charge density accumulation occurs at the reaction center (Figure 2.6). It was also observed that the ρ value for both quinone-catalyzed and stoichiometric quinone-promoted oxidative-decarboxylation were very similar ($\rho = 0.5331$ and $\rho = 0.4831$). Although these studies are not conclusive, the results provide evidence to support decarboxylation as the RDS. If this is indeed the case, a more electron deficient catalyst may encourage decarboxylation of natural α -amino acids by drawing electron density from the reaction center.

Figure 2.7: Hammett Plot for Stoichiometric Quinone-Promoted Oxidative-Decarboxylation



2.6 Quinone-Catalyzed Amino Alcohol Deformylation

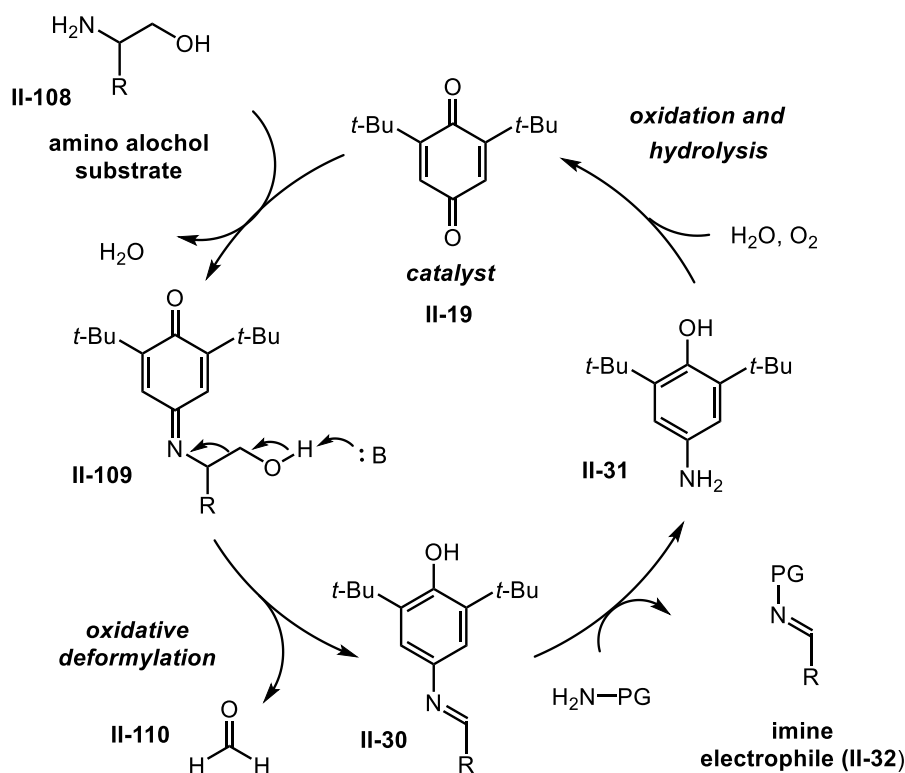
Following the development of quinone-catalyzed oxidative-decarboxylation, we sought to explore the potential of quinone catalysts in related oxidative C–C bond cleavage reactions. One specific idea we decided to test was the oxidative-deformylation of amino alcohols. A deformylation process is comparable to decarboxylation, but is fundamentally distinct in that the oxidative decarboxylation of amino acids requires sp^3 – sp^2 C–C bond cleavage, while amino alcohol deformylation would proceed through sp^3 – sp^3 C–C bond cleavage. It is our interest to develop conditions for quinone-catalyzed amino alcohol deformylation, an unreported transformation.

2.6.1 Development of Quinone-Catalyzed Amino Alcohol Deformylation

We expected deformylation of amino alcohols to proceed through a similar mechanism as that of amino acid decarboxylation (Figure 2.8). First an amino alcohol (**II-108**) would condense

with the quinone catalyst **II-19**. At this point, a base would deprotonate the O–H bond of the amino alcohol, in turn promoting a deformylation of **II-109** to provide the N-aryl imine **II-30**. This species would readily undergo transimination with a stable N-protected amine to give an N-protected imine product **II-32**. The active catalyst would then be regenerated through auto-oxidation. We began our studies by examining the oxidative-deformylation of phenylglycinol.

Figure 2.8: Proposed Mechanism for Quinone-Catalyzed Amino Alcohol Deformylation



2.6.2 Optimization of Quinone-Catalyzed Amino Alcohol Deformylation

Deformylation of amino alcohols to imine products would provide the first example of quinone promoted sp^3 C–C bond cleavage. Initial experiments using phenylglycinol (**II-111**) as the substrate and 2,6-Di-tert-butyl-1,4-benzoquinone (**II-19**) as the catalyst were performed using

conditions initially developed for oxidative-decarboxylation (Table 2.8); these conditions provided **II-64** in 18% yield (entry 1). A subsequent reaction was attempted under identical conditions, but using 2-(tert-butyl)-5-hydroxycyclohexa-2,5-diene-1,4-dione (**II-16**) as the quinone catalyst. After 24 hours the PMP-protected imine **II-64** was formed in 38% yield (entry 2). Following these initial experiments, other solvents were studied at elevated temperatures with varied catalyst loading. Isopropanol seemed to promoted better oxidation with respect to both catalysts (entry 3, 44%, entry 4, 59%), and hydroxy-quinone **II-16** provided a much better yield in ethanol than quinone **II-19** (entry 5, 31%, entry 6, 75%).

Table 2.8: Optimization of Amino Alcohol Deformylation

II-111			II-64	II-19	II-16
Entry	Solvent	Temperature	Catalyst	Base	Yield
1	MeCN:H ₂ O	50°C	II-19	Et ₃ N	18%
2	MeCN:H ₂ O	50°C	II-16	Et ₃ N	38%
3	isopropanol	70°C	II-19	Et ₃ N	44%
4	isopropanol	70°C	II-16	Et ₃ N	59%
5	EtOH	70°C	II-19	Et ₃ N	31%
6	EtOH	70°C	II-16	Et ₃ N	75%
7	MeCN:H ₂ O	50°C	II-19	-	47%
8	isopropanol	70°C	II-19	-	71%
9	EtOH	70°C	II-19	-	73%
10 ^b	EtOH	70°C	II-19	-	99%
11 ^c	EtOH	70°C	II-19	-	85%

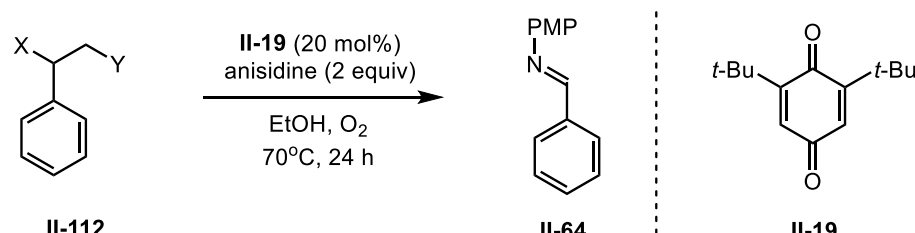
^a Isolated yields, ^b 20 mol % catalyst, ^c 48 h reaction time

To our surprise, when triethylamine was not included as a base, yields increased when comparing entries with otherwise identical conditions (entry 7, 47%, entry 8, 71%, entry 9, 73%). Taking the best result and employing higher catalyst loading delivered the imine product in 99% yield (entry 10). The catalyst loading can be reduced to 10 mol % but the yield drops and an extended reaction time is required (entry 11, 85%). These results demonstrate quinone-catalyzed deformylation of amino alcohols have been realized.

2.6.3 Preliminary Scope Studies for Quinone-Catalyzed Deformylation

With an optimized condition in hand (entry 10, Table 2.9), the oxidative deformylation was studied. We began with an isomer of phenylglycinol, which provided imine **II-64** in 99% yield and complete conversion (entry 2). In thinking this observation could be a result of either C–C bond cleavage promoted by amine condensation to the quinone or by the alcohol, a diol was submitted to the reaction conditions to find no conversion after 24 hours (entry 3, 0%). A series of amino alcohols will be studied in the future to determine a full extent of the substrate scope.

Table 2.9: Preliminary Scope Studies for Deformylation

				
Entry	X	Y	% conversion ^a	% yield ^a
1	NH ₂	OH	99	99
2	OH	NH ₂	99	99
3	OH	OH	0	0

^a ¹H NMR yields

2.7 Summary for Chapter 2

We have developed a new protocol for sequential quinone-catalyzed oxidative-decarboxylation/Mukaiyama–Mannich addition to provide an efficient method for α -amino acid homologation under mild reaction conditions (20 substrates, 15–95% yield). This is the first application of quinone-catalyzed oxidative-decarboxylation. This method is currently limited to aryl amino acids, and studies directed at addressing this limitation are underway. We have also developed a protocol for quinone-catalyzed oxidative-deformylation of amino alcohols. Currently, we have developed conditions for deformylation of phenylglycinol, and plan to continue this project by studying the scope of this reaction using various aryl glycinols and amino ethers.

2.8 General Experimental Section

All reactions were carried out in 8 mL reaction vials with magnetic stirring unless otherwise stated. EtOH was used as purchased from Fisher Chemical (190 Proof). Other reagents were used as delivered from commercial sources. Purification of reaction products was carried out by flash chromatography using Fisher Chemical silica gel (230–400 Mesh, Grade 60). Analytical thin layer chromatography (TLC) was performed on EMD millipore TLC silica gel 60 – F 254: 25 glass plates. Visualization was accomplished with UV light and/or phosphomolybdic acid staining followed by heating. Melting point data were recorded using a Digimelt SRS. Film and KBr pellet infrared spectra were recorded using a Shimadzu FTIR-8400S. ^1H -NMR spectra were recorded on a Bruker Advance 400 (400 MHz) or a Bruker 500 (500 MHz) spectrometer and are reported in ppm using solvent as a reference (residual CHCl_3 at 7.26 ppm). Data are reported as (app =

apparent, s = singlet, d = doublet, t = triplet, q = quartet, m = multiplet, b = broad); integration; coupling constant(s) in Hz. Proton-decoupled ^{13}C -NMR spectra were recorded on a Bruker 500 (125 MHz) and are reported in ppm using solvent as a reference (CDCl_3 at 77.16 ppm). Mass spectra data were obtained on a Micromass Ltd. LCT Premier quadrupole and time-of-flight tandem mass analyzer.

2.9 General Experimental Procedures for Sequential Oxidative–Decarboxylation/Mannich Addition

A: General procedure for glycine derivative decarboxylation/ silyl ketene (thio)acetal addition (II-82-II-90):

To a solution of 2,6-di-tert-butyl-1,4-benzoquinone (11.0 mg, 0.050 mmol, unless otherwise noted) and p-anisidine (123.1 mg, 1.0 mmol) in ethanol (1.6 mL, 0.312 M) with respect to the glycine substrate) was added the glycine derivative (0.50 mmol), followed by purging the reaction vial with a balloon of O_2 . The reaction mixture was allowed to stir under O_2 at 70 °C for 24 h unless otherwise noted. The ethanol was removed by rotary evaporation and the oxidative-decarboxylation product was further pumped for 0.5h with a high-vacuum pump. The remaining solid was dissolved in dry THF (1.6 mL, 0.312 M) and the solution was cooled to 0 °C. To this solution was added tetrafluoroboric acid solution (48 wt. % in H_2O , 90.0 μL , 0.75 mmol) and silyl ketene (thio)acetal (1.5 mmol). The resulting solution was allowed to stir for 1.5h under N_2 at 0

°C. Sodium phosphate buffer (pH = 7, 2 mL) was added followed by saturated aq. NaHCO₃ (0.5 mL). The mixture was transferred to a separatory funnel by aid of Et₂O, shaken vigorously and the organic phase was collected. The aqueous phase was further extracted with Et₂O (3 x 5.0 mL) and the combined organic extracts were dried (Na₂SO₄), filtered and concentrated under reduced pressure. Flash chromatography on TEA neutralized silica gel (10% ethyl acetate in hexanes) provided the desired aryl amine thioesters (**II-82-II-91**).

B: General Procedure for Glycine Derivative Decarboxylation/ Silyl Ketene Acetal Addition (II-71-80):

To a solution of 2,6-di-tert-butyl-1,4-benzoquinone (11.0 mg, 0.050 mmol, unless otherwise noted) and p-anisidine (123.1 mg, 1.0 mmol) in ethanol (1.6 mL, 0.312 M) with respect to the glycine substrate) was added the glycine derivative (0.50 mmol) , followed by purging the reaction vial with a balloon of O₂. The reaction mixture was allowed to stir under O₂ at 70 °C for 24 h unless otherwise noted. The ethanol was removed by rotary evaporation and the oxidative-decarboxylation product was further pumped for 0.5h with a high-vacuum pump. The remaining solid was dissolved in dry THF (1.6 mL, 0.312 M) and the solution was cooled to 0 °C. To this solution was added tetrafluoroboric acid solution (48 wt. % in H₂O, 90.0 µL, 0.75 mmol) and silyl ketene (gem-dimethyl)acetal (1.5 mmol) dropwise over 6 iterations by 15 min intervals. After 1.5 h, the solvent was removed under reduced pressure. Flash chromatography on TEA neutralized silica gel (5%-20% ethyl acetate in hexanes) followed by recrystallization in CHCl₃ and pentane provided the desired aryl amine methyl-esters (**II-71-80**).

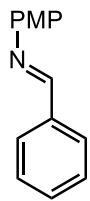
C: General Procedure for Aryl Glycine Decarboxylation (II-39-51):

To a solution of 2,6-di-*tert*-butyl-1,4-benzoquinone (22.0 mg, 0.10 mmol, unless otherwise noted) and p-anisidine (246 mg, 2.0 mmol) in Acetonitrile:water (3.2 mL, 0.312 M with respect to the glycine substrate) was added the glycine derivative (1.00 mmol), followed by purging the reaction vial with a balloon of O₂. The reaction mixture was allowed to stir under O₂ at 50 °C for 24 h unless otherwise noted. The crude reaction mixture was placed in a separatory funnel and the organic layer was extracted in H₂O and CHCl₃ followed by concentration. Flash chromatography on TEA neutralized silica gel (5%-20% ethyl acetate in hexanes) followed by recrystallization (when described) in CHCl₃ and pentane provided the desired imine **II-39-51**).

D: General Procedure for Quinone-Catalyzed Amino Alcohol Deformylation:

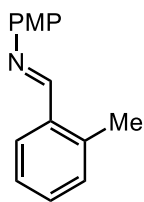
To a solution of 2,6-di-*tert*-butyl-1,4-benzoquinone (22.0 mg, 0.10 mmol, unless otherwise noted) and p-anisidine (123 mg, 1.0 mmol) in EtOH (1.6 mL, 0.312 M with respect to the glycinol substrate) was added the glycine derivative (0.50 mmol), followed purging the reaction vial with a balloon of O₂. The reaction mixture was allowed to stir under O₂ at 70 °C. After 24h, crude reaction mixtures concentrated under reduced pressure and ¹H NMR analysis was conducted.

2.9.1 Characterization Data for II-39-51, II-71-80, and II-82-91



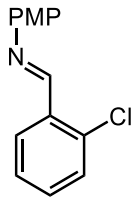
(E)-N-(4-methoxyphenyl)-1-phenylmethanimine (II-39): The reaction was carried out according to the general oxidation procedure (C) using 2-Phenylglycine (151 mg, 1.00 mmol) to provide after purification product **II-39** (178.8 mg, 85%) as an orange crystal.

IR (KBr) 2955, 2837, 1622 cm^{-1} . ^1H NMR (400 MHz, CDCl_3) 8.49 (s, 1H), 7.90 (m, 2H), 7.47 (m, 3H), 7.25 (d, $J = 8.7$ Hz, 2H), 6.94 (d, $J = 8.9$ Hz, 2H), 3.84 (s, 3H). ^{13}C NMR (101 MHz, CDCl_3) 158.2, 158.1, 144.7, 136.3, 130.8, 128.5, 128.4, 122.0, 114.2, 55.3. HMRS (ESI): Exact mass calcd for $\text{C}_{14}\text{H}_{13}\text{NO}$ $[\text{M}+\text{H}]$, 212.1075. Found 212.1056.



(E)-N-(4-methoxyphenyl)-1-(o-tolyl)methanimine (II-40): The reaction was carried out according to the general oxidation procedure (C) using 2-amino-2-(o-tolyl)acetic acid (165.2 mg, 1.00 mmol) to provide after purification product **II-40**

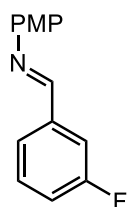
(169.6 mg, 75%) as a white crystal; IR (KBr), 2968, 2841, 1616 cm^{-1} . ^1H NMR (400 MHz, CDCl_3) 8.77 (s, 1H), 8.07 (dd, $J = 7.6, 1.6$ Hz, 1H), 7.32 (m, 3H), 7.22 (d, $J = 8.8$ Hz, 2H), 6.94 (d, $J = 8.9$ Hz, 2H), 3.84 (s, 3H), 2.59 (s, 3H). ^{13}C NMR (101 MHz, CDCl_3) 158.2, 157.2, 145.6, 138.3, 134.4, 131.0, 130.7, 127.6, 126.3, 122.2, 114.4, 55.5, 19.4. HMRS (ESI): Exact mass calcd for $\text{C}_{15}\text{H}_{15}\text{NO}$ $[\text{M}+\text{H}]$, 226.1232. Found 226.1211.



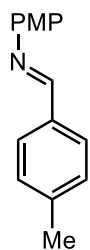
(E)-1-(2-chlorophenyl)-N-(4-methoxyphenyl)methanimine (II-41): The reaction was carried out according to the general oxidation procedure (C) using 2-amino-2-(2-chlorophenyl)acetic acid (185.6 mg, 1.00 mmol) to provide after purification product

II-41 (217.8 mg, 89%) as a white crystal; IR (KBr) 2999, 2837, 1618 cm^{-1} . ^1H NMR (500 MHz,

CDCl₃) 8.94 (s, 1H), 8.23 (dd, J = 7.0, 2.5 Hz, 1H), 7.38 (m, 3H), 7.28 (d, J = 8.9 Hz, 1H), 6.95 (d, J = 8.9 Hz, 2H), 3.84 (s, 3H). ¹³C NMR (126 MHz, CDCl₃) 158.8, 154.9, 144.8, 135.9, 133.6, 131.9, 130.1, 128.5, 127.2, 122.7, 114.5, 55.7. HMRS (ESI): Exact mass calcd for C₁₄H₁₂NOCl [M+H], 246.0686. Found 246.0666.

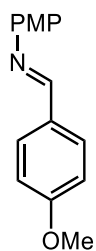


(E)-1-(3-fluorophenyl)-N-(4-methoxyphenyl)methanimine (II-42): The reaction was carried out according to the general oxidation procedure (C) using 2-amino-2- (3-fluorophenyl)acetic acid (169.2 mg, 1.00 mmol) to provide after purification product **II-42** (219.0.0 mg, 95%) as a white crystal; IR (KBr) 3082, 2843, 1622 cm⁻¹. ¹H NMR (500 MHz, CDCl₃) 8.46 (s, 1H), 7.65 (ddd, J = 9.6, 2.7, 1.5 Hz, 1H), 7.61 (dt, J = 7.7, 1.3 Hz, 1H), 7.43 (td, J = 7.9, 5.6 Hz, 1H), 7.25 (d, J = 8.9 Hz, 2H), 7.16 (tdd, J = 8.3, 2.7, 1.0 Hz, 1H), 6.94 (d, J = 8.9 Hz, 2H), 3.84 (s, 3H). ¹³C NMR (101 MHz, CDCl₃) 163.2 (d, J = 246.6 Hz), 158.6, 156.68 (d, J = 3.1 Hz), 144.3, 138.8 (d, J = 7.3 Hz), 130.2 (d, J = 7.9 Hz), 124.7 (d, J = 2.8 Hz), 122.3, 117.9 (d, J = 21.7 Hz), 114.4 (d, J = 22.2 Hz), 114.4, 55.5. HMRS (ESI): Exact mass calcd for C₁₄H₁₂NFO [M+H], 230.0981. Found 230.0958.

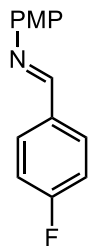


(E)-N-(4-methoxyphenyl)-1-(p-tolyl)methanimine (II-43): The reaction was carried out according to the general oxidation procedure (C) using 2-amino-2-(p-tolyl)acetic acid (165.2 mg, 1.00 mmol) to provide after purification product **II-43** (186. mg, 76%) as a white crystal; IR (KBr) 2912, 2885, 1624 cm⁻¹. ¹H NMR (400 MHz, CDCl₃) 8.44 (s, 1H), 7.78 (d, J = 7.7 Hz, 2H), 7.27 (d, J = 7.9 Hz, 2H), 7.23 (d, J = 8.4 Hz, 2H), 6.93 (d, J = 8.5 Hz,

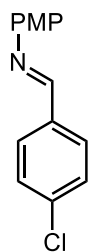
2H), 3.83 (s, 3H), 2.42 (s, 3H). ^{13}C NMR (101 MHz, CDCl_3) 158.6, 158.3, 145.3, 141.6, 134.1, 129.6, 128.7, 122.3, 114.5, 55.7, 21.8. HMRS (ESI): Exact mass calcd for $\text{C}_{15}\text{H}_{15}\text{NO}$ $[\text{M}+\text{H}]$, 226.1232. Found 226.1205.



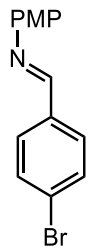
(E)-N,1-bis(4-methoxyphenyl)methanimine (II-44): The reaction was carried out according to the general oxidation procedure (C), using 2-amino-2- (4-methoxyphenyl) acetic acid (181.1, 0.50 mmol) and 20 mol % quinone catalyst to provide after purification product **II-44** (93.5 mg, 78%) as a white crystal; IR (KBr) 2956, 2839, 1622 cm^{-1} . ^1H NMR (500 MHz, CDCl_3) 8.41 (s, 1H), 7.83 (d, $J = 8.8$ Hz, 2H), 7.21 (d, $J = 8.9$ Hz, 1H), 6.98 (d, $J = 8.8$ Hz, 2H), 6.92 (d, $J = 9.0$ Hz, 1H), 3.87 (s, 3H), 3.83 (s, 3H). ^{13}C NMR (126 MHz, CDCl_3) 162.11, 158.07, 158.06, 145.41, 130.38, 129.62, 122.20, 114.47, 114.28, 55.64, 55.56. HMRS (ESI): Exact mass calcd for $\text{C}_{15}\text{H}_{15}\text{NO}_2$ $[\text{M}+\text{H}]$, 242.1181. Found 242.1156.



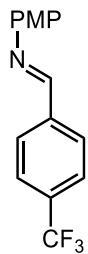
(E)-1-(4-fluorophenyl)-N-(4-methoxyphenyl)methanimine (II-45): The reaction was carried out according to the general oxidation procedure (C) using 2-amino-2-(4-fluorophenyl)acetic acid (169.2 mg, 1.00 mmol) to provide after purification product **II-45** (193.9 mg, 85%) as a white crystal; IR (KBr) 3016, 2879, 1622 cm^{-1} . ^1H NMR (500 MHz, CDCl_3) 8.44 (s, 1H), 7.89 (m, 2H), 7.23 (d, $J = 8.9$ Hz, 2H), 7.15 (m, 2H), 6.94 (d, $J = 8.9$ Hz, 2H), 3.84 (s, 3H). ^{13}C NMR (126 MHz, CDCl_3) 164.6 (d, $J = 251.6$ Hz), 158.4, 156.97, 144.8, 132.9 (d, $J = 3.1$ Hz) 130.6 (d, $J = 8.7$ Hz), 122.3, 116.0 (d, $J = 22.0$ Hz), 114.5, 55.6. HMRS (ESI): Exact mass calcd for $\text{C}_{14}\text{H}_{12}\text{NFO}$ $[\text{M}+\text{H}]$, 230.0981. Found 230.0958.



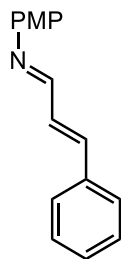
(E)-1-(4-chlorophenyl)-N-(4-methoxyphenyl)methanimine (II-46): The reaction was carried out according to the general oxidation procedure (C) using 2-amino-2-(4-chlorophenyl)acetic acid (185.6 mg, 1.00 mmol) to provide after purification product **II-46** (214.1 mg, 87%) as a white crystal; IR (KBr) 2962, 2839, 1620 cm^{-1} . ^1H NMR (500 MHz, CDCl_3) 8.45 (s, 1H), 7.83 (d, $J = 8.5$ Hz, 2H), 7.44 (d, $J = 8.5$ Hz, 2H), 7.24 (d, $J = 8.9$ Hz, 2H), 6.94 (d, $J = 8.9$ Hz, 2H), 3.84 (s, 3H). ^{13}C NMR (126 MHz, CDCl_3) 158.6, 156.8, 144.6, 137.1, 135.1, 129.8, 129.2, 122.4, 114.6, 55.7. HMRS (ESI): Exact mass calcd for $\text{C}_{14}\text{H}_{12}\text{NOCl}$ [M+H], 246.0686. Found 246.0668.



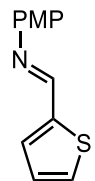
(E)-1-(4-bromophenyl)-N-(4-methoxyphenyl)methanimine (II-47): The reaction was carried out according to the general oxidation procedure (C) using 2-amino-2-(4-bromophenyl)acetic acid (230.1 mg, 1.00 mmol) to provide after purification product **II-47** (248.3 mg, 86%) as a white crystal; IR (KBr) 2960, 2879, 1622 cm^{-1} . ^1H NMR (400 MHz, CDCl_3) 8.43 (s, 1H), 7.76 (d, $J = 8.2$ Hz, 2H), 7.60 (d, $J = 8.2$ Hz, 2H), 7.24 (d, $J = 8.6$ Hz, 2H), 6.94 (d, $J = 8.6$ Hz, 2H), 3.84 (d, $J = 1.0$ Hz, 3H). HMRS (ESI): Exact mass calcd for $\text{C}_{14}\text{H}_{12}\text{NOBr}$ [M+H], 290.0181. Found 292.0194.



(E)-N-(4-methoxyphenyl)-1-(4-(trifluoromethyl)phenyl)methanimine (II-48): The reaction was carried out according to the general oxidation procedure (C) using 4-trifluoromethyl-phenylglycine (219.2 mg, 1.00 mmol) to provide after purification product **II-48** (240.9 mg, 86%) as a white crystal; IR (KBr) 2881, 1622 cm^{-1} . ^1H NMR (500 MHz, CDCl_3) 8.54 (s, 1H), 8.00 (m, 2H), 7.72 (d, $J = 8.0$ Hz, 2H), 7.28 (d, $J = 8.9$ Hz, 2H), 6.95 (d, $J = 8.9$ Hz, 2H), 3.85 (s, 3H). ^{13}C NMR (126 MHz, CDCl_3) 158.9, 156.4, 144.2, 139.7, 132.49 (q, $J = 32.6$ Hz), 128.8, 125.82 (q, $J = 3.8$ Hz), 125.15 (q), 122.54 (d), 114.6, 55.7. HMRS (ESI): Exact mass calcd for $\text{C}_{15}\text{H}_{12}\text{F}_3\text{NO}$ $[\text{M}+\text{H}]$, 280.0949. Found 280.0919.

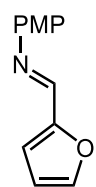


(1E,2E)-N-(4-methoxyphenyl)-3-phenylprop-2-en-1-imine (II-49): The reaction was carried out according to the general oxidation procedure (C) 2-amino-4-phenylbut-3-enoic acid (177.7 mg, 1.00 mmol) to provide after purification product **II-49** (151.2 mg, 69%) as a white crystal; IR (KBr) 2956, 2837, 1629 cm^{-1} . ^1H NMR (400 MHz, CDCl_3) 8.30 (dd, $J = 5.4, 2.9$ Hz, 1H), 7.53 (m, 2H), 7.37 (m, 3H), 7.21 (d, $J = 8.7$ Hz, 2H), 7.12 (m, 2H), 6.92 (d, $J = 8.7$ Hz, 2H), 3.83 (d, $J = 1.0$ Hz, 3H). HMRS (ESI): Exact mass calcd for $\text{C}_{16}\text{H}_{15}\text{NO}$ $[\text{M}+\text{H}]$, 238.1232. Found 238.1207.

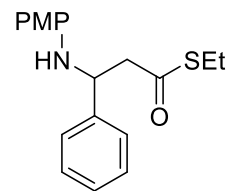


(E)-N-(4-methoxyphenyl)-1-(thiophen-2-yl)methanimine (II-50): The reaction was carried out according to the general oxidation procedure (C) using 2-amino-2-(thiophen-2-yl)acetic acid (157.2 mg, 1.00 mmol) to provide after purification product **II-50** (173.2 mg, 80%) as a white crystal; IR (KBr) 2997, 2833, 1610 cm^{-1} . ^1H NMR (400 MHz, CDCl_3) 8.61

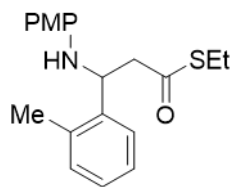
(s, 1H), 7.49 (dd, 2H), 7.25 (d, $J = 8.6$ Hz, 2H), 7.15 (t, $J = 4.3$ Hz, 1H), 6.94 (d, $J = 8.5$ Hz, 2H), 3.85 (d, $J = 1.1$ Hz, 3H). ^{13}C NMR (101 MHz, CDCl_3) 158.4, 151.2, 144.5, 143.3, 131.6, 129.8, 127.8, 122.4, 114.5, 55.6. HMRS (ESI): Exact mass calcd for $\text{C}_{12}\text{H}_{12}\text{NSO}$ $[\text{M}+\text{H}]$, 218.0640. Found 218.0632.



(E)-1-(furan-2-yl)-N-(4-methoxyphenyl) methanimine (II-51): The reaction was carried out according to the general oxidation procedure (C) using 2-amino-2-(furan-2-yl)acetic acid (141.1 mg, 1.00 mmol) and 20 mol % quinone catalyst to provide after purification product **II-51** (106.8 mg, 53%) as a white crystal: IR (KBr) 3093, 2958, 1622 cm^{-1} . ^1H NMR (400 MHz, CDCl_3) 8.30 (s, 1H), 7.59 (s, 1H), 7.26 (d, $J = 8.7$ Hz, 2H), 6.91 – (m, 3H), 6.54 (dt, $J = 3.1, 1.4$ Hz, 1H), 3.82 (s, 3H). ^{13}C NMR (101 MHz, CDCl_3) 158.6, 152.5, 145.9, 145.5, 144.4, 122.4, 115.6, 114.6, 112.2, 55.6. HMRS (ESI): Exact mass calcd for $\text{C}_{12}\text{H}_{12}\text{NO}_2$ $[\text{M}+\text{H}]$, 202.0868. Found 202.0854.

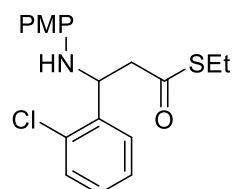


S-ethyl 3-((4-methoxyphenyl)amino)-3-phenylpropanethioate (II-82): The reaction was carried out according to the general procedure (A) using 2-Phenylglycine (75.6 mg, 0.50 mmol) to provide after purification product **II-82** (117.6 mg, 75%) as an orange solid ; which was spectroscopically identical to previous reports



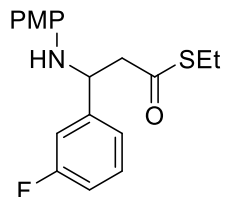
S-ethyl 3-((4-methoxyphenyl)amino)-3-(o-tolyl)propanethioate (II-83):

The reaction was carried out according to the general procedure (A) using 2-amino-2-(o-tolyl)acetic acid (82.6 mg, 0.50 mmol) to provide after purification product **II-83** (92.8 mg, 56%) as an orange oil; IR (film) 3523, 3055, 2962, 1676 cm^{-1} . ^1H NMR (400 MHz, CDCl_3) 7.41 (d, 1H, $J = 5.6$ Hz), 7.21 – 7.11 (m, 3H), 6.68 (d, 2H, $J = 8.3$ Hz), 6.45 (d, 2H, $J = 8.3$ Hz), 4.94 (dd, 1H, $J = 8.4, 5.0$ Hz), 3.69 (s, 3H), 2.87 (m, 4H), 2.45 (s, 3H), 1.21 (t, 3H, $J = 7.4$ Hz). ^{13}C NMR (126 MHz, CDCl_3) 197.7, 152.4, 141.2, 140.0, 134.9, 130.9, 127.4, 126.8, 125.4, 114.90, 114.87, 55.8, 53.1, 50.2, 23.8, 19.3, 14.7; HMRS (ESI): Exact mass calcd for $\text{C}_{19}\text{H}_{24}\text{NO}_2\text{S}$ $[\text{M}+\text{H}]^+$, 330.1528. Found 330.1536.



S-ethyl 3-(2-chlorophenyl)-3-((4-methoxyphenyl)amino)propanethioate (II-84):

The reaction was carried out according to the general procedure (A) using 2-amino-2-(2-chlorophenyl)acetic acid (92.8 mg, 0.50 mmol) while 1 equivalent of silyl ketene (thio)acetal (0.50 mmol) was added and the addition was repeated twice after each 30 min to provide after purification product **II-84** (166.6mg, 95%) as an orange oil. IR (film) 3390, 3062, 2966, 1674 cm^{-1} . ^1H NMR (500 MHz, CDCl_3) 7.45 – 7.41 (m, 1H), 7.40 – 7.37 (m, 1H), 7.22 – 7.14 (m, 2H), 6.72 – 6.63 (m, 2H), 6.47 – 6.38 (m, 2H), 5.13 (dd, 1H, $J = 9.0, 3.7$ Hz), 4.57 (bs, 1H), 3.68 (s, 3H), 3.09 (dd, 1H, $J = 14.6, 3.7$ Hz), 2.98 – 2.67 (m, 3H), 1.21 (t, 3H, $J = 7.5$ Hz). ^{13}C NMR (126 MHz, CDCl_3) 197.7, 152.4, 140.6, 138.9, 132.7, 130.0, 128.7, 127.9, 127.4, 114.9, 114.8, 55.8, 53.6, 49.1, 23.8, 14.7; HMRS (ESI): Exact mass calcd for $\text{C}_{18}\text{H}_{21}\text{NO}_2\text{SCl}$ $[\text{M}+\text{H}]^+$, 350.0982. Found 350.0975.



S-ethyl 3-(3-fluorophenyl)-3-((4-methoxyphenyl)amino)propanethioate

(II-85): The reaction was carried out according to the general procedure (A)

using 2-amino-2-(3-fluorophenyl)acetic acid (84.6 mg, 0.50 mmol) to provide

after purification product **II-85** (130.1mg, 78%) as an orange solid, m.p. 84 °C. IR (KBr pellet)

3402, 3070, 2989, 1672 cm^{-1} . ^1H NMR (400 MHz, CDCl_3) 7.32 – 7.27 (m, 1H), 7.16 (d, 1H, J =

7.7 Hz,), 7.09 (dt, 1H, J = 9.8, 2.1 Hz), 6.93 (app td, 1H), 6.70 (d, 2H, J = 8.7 Hz, 1H), 6.51 (d,

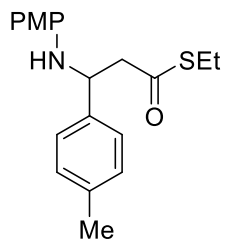
2H, J = 8.3 Hz), 4.74 (t, 1H, J = 6.7 Hz), 3.70 (s, 3H), 2.98 (d, 2H, J = 6.6 Hz), 2.86 (q, 2H, J =

7.4 Hz), 1.21 (t, 3H, J = 7.4 Hz). ^{13}C NMR (126 MHz, CDCl_3) 197.3, 163.3 (d, J = 247.0 Hz),

152.6, 145.2 (d, J = 6.3 Hz), 140.6, 130.4 (d, J = 7.6 Hz), 122.1 (d, J = 2.5 Hz), 115.3, 114.9,

114.5 (d, J = 21.4 Hz), 113.4 (d, J = 22.7 Hz), 56.4, 55.8, 51.5, 23.8, 14.7; HMRS (ESI): Exact

mass calcd for $\text{C}_{18}\text{H}_{21}\text{NO}_2\text{SF}$ $[\text{M}+\text{H}]^+$, 334.1277. Found 334.1281.



S-ethyl 3-((4-methoxyphenyl)amino)-3-(p-tolyl)propanethioate (II-86):

The reaction was carried out according to the general procedure (A) using 2-

amino-2-(p-tolyl)acetic acid (82.6 mg, 0.50 mmol) to provide after purification

product **II-86** (146.2mg, 89%) as a brown solid, m.p. 68 °C. IR (KBr) 3398,

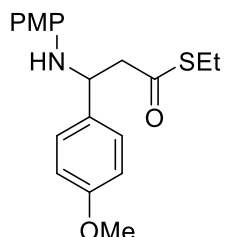
3041, 2904, 1681 cm^{-1} . ^1H NMR (500 MHz, CDCl_3) 7.25 (d, 2H, J = 8.1 Hz), 7.13 (d, 2H, J = 7.8

Hz), 6.69 (d, 2H, J = 9.0 Hz), 6.51 (d, 2H, J = 8.9 Hz), 4.73 (t, 1H, J = 6.8 Hz), 3.69 (s, 3H), 2.98

– 2.92 (m, 2H), 2.86 (q, 2H, J = 7.4 Hz), 2.32 (s, 3H), 1.21 (t, 3H, J = 7.4 Hz). ^{13}C NMR (126

MHz, CDCl_3) 197.6, 152.4, 141.1, 139.3, 137.2, 129.6, 126.3, 115.3, 114.8, 56.5, 55.8, 51.9,

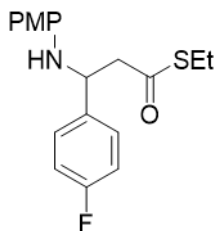
23.7, 21.2, 14.7; HMRS (ESI): Exact mass calcd for C₁₉H₂₄NO₂S [M+H⁺], 330.1528. Found 330.1520.



S-ethyl 3-(4-methoxyphenyl)-3-((4-methoxyphenyl)amino)propanethioate

(II-87): The reaction was carried out according to the general procedure (A) using 2-amino-2-(4-methoxyphenyl)acetic acid (120.6 mg, 0.50 mmol) while the reaction was stirred for 48h in ethanol at 70°C to provide after purification

product **II-87** (151.8mg, 88%) as a lilac solid, m.p. 74 °C. IR (KBr pellet) 3384, 3068, 2929, 1676 cm⁻¹. ¹H NMR (400 MHz, CDCl₃) 7.29 (s, 1H), 6.87 – 6.82 (m, 2H), 6.71 – 6.67 (m, 2H), 6.52 (d, 2H, J = 8.9 Hz), 4.71 (dd, 1H, J = 7.8, 5.7 Hz), 3.78 (s, 3H), 3.69 (s, 3H), 3.00 – 2.91 (m, 2H), 2.89 – 2.81 (q, 2H, J = 7.4 Hz), 1.20 (t, J = 7.4 Hz, 3H). ¹³C NMR (126 MHz, CDCl₃) 197.6, 158.8, 152.4, 140.8, 134.1, 127.4, 115.2, 114.7, 114.1, 56.1, 55.7, 55.3, 51.7, 23.6, 14.6; HMRS (ESI): Exact mass calcd for C₁₉H₂₄NO₃S [M+H⁺], 346.1477. Found 346.1469.

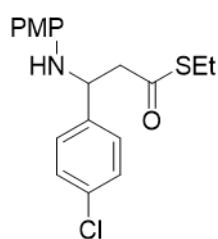


S-ethyl 3-(4-fluorophenyl)-3-((4-methoxyphenyl)amino)propanethioate

(II-88): The reaction was carried out according to the general procedure (A) using 2-amino-2-(4-fluorophenyl)acetic acid (84.6 mg, 0.50 mmol) to provide

after purification product **II-88** (139.8mg, 84%) as an orange solid, m.p. 90 °C. IR (KBr pellet) 3371, 3016, 2983, 1668 cm⁻¹. ¹H NMR (400 MHz, CDCl₃) 7.33 (m, 2H), 7.00 (app t, 2H), 6.69 (d, 2H, J = 8.9 Hz), 6.50 (d, 2H, J = 8.9 Hz), 4.76 – 4.70 (t, 1H, J = 6.7 Hz), 3.70 (s, 3H), 2.97 (m, 2H), 2.85 (q, 2H, J = 7.4 Hz), 1.20 (t, 3H, J = 7.4 Hz). ¹³C NMR (126 MHz, CDCl₃) 197.4, 162.2

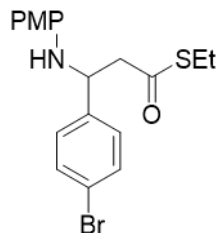
(d, J = 243.8 Hz), 152.6, 140.7, 137.9, 128.1(d, J = 8.8 Hz), 115.8 (d, J = 21.4 Hz), 115.4, 114.8, 56.1, 55.8, 51.7, 23.8, 14.7; HMRS (ESI): Exact mass calcd for C₁₈H₂₁NO₂SF [M+H⁺], 334.1277. Found 334.1281.



S-ethyl 3-(4-chlorophenyl)-3-((4-methoxyphenyl)amino)propanethioate

(II-89): The reaction was carried out according to the general procedure (A) using 2-amino-2-(4-chlorophenyl)acetic acid (92.8 mg, 0.50 mmol) to provide after purification product **II-89** (164.5mg, 94%) as an orange oil. IR (film)

3382, 3060, 2929, 1666 cm⁻¹. ¹H NMR (400 MHz, CDCl₃) 7.33 – 7.27 (m, 4H), 6.69 (d, J = 8.9 Hz, 2H), 6.48 (d, J = 8.8 Hz, 2H), 4.72 (t, 1H, J = 6.7 Hz), 3.69 (s, 3H), 2.98 – 2.92 (m, 2H), 2.86 (q, J = 7.4 Hz, 2H), 1.21 (t, J = 7.4 Hz, 3H). ¹³C NMR (126 MHz, CDCl₃) 197.3, 152.6, 140.9, 140.7, 133.2, 129.1, 127.9, 115.3, 114.8, 56.1, 55.8, 51.6, 23.8, 14.7; HMRS (ESI): Exact mass calcd for C₁₈H₂₁ClNO₂S [M+H⁺], 350.0982. Found 350.0984.

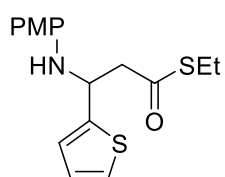


S-ethyl 3-(4-bromophenyl)-3-((4-methoxyphenyl)amino)propanethioate

(II-90): The reaction was carried out according to the general procedure (A) using 2-amino-2-(4-bromophenyl)acetic acid (115.0 mg, 0.50 mmol) to

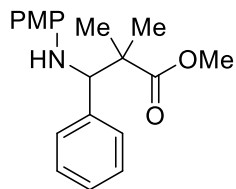
provide after purification product **II-90** (142.0mg, 72%) as a dark orange solid, m.p. 70 °C. IR (KBr pellet) 3392, 3056, 2960, 1679 cm⁻¹. ¹H NMR (500 MHz, CDCl₃) 7.46 – 7.42 (m, 2H), 7.26 – 7.23 (m, 2H), 6.69 (d, 2H, J = 8.9 Hz), 6.48 (d, 2H, J = 8.9 Hz), 4.70 (t, 1H, J = 6.7 Hz), 3.69 (s, 3H), 2.97 – 2.92 (m, 2H), 2.86 (q, 2H, J = 7.5 Hz), 1.21 (t, 3H, J = 7.4 Hz). ¹³C NMR (126

MHz, CDCl₃) 197.3, 152.7, 141.3, 140.5, 132.0, 128.3, 121.4, 115.4, 114.9, 56.3, 55.8, 51.5, 23.8, 14.7; HMRS (ESI): Exact mass calcd for C₁₈H₂₁BrNO₂S [M+H⁺], 394.0476. Found 394.0484



S-ethyl 3-((4-methoxyphenyl)amino)-3-(thiophen-2-yl)propanethioate (II-91):

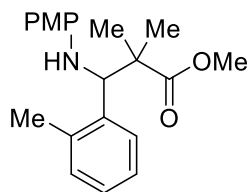
The reaction was carried out according to the general procedure (A) using 2-amino-2-(thiophen-2-yl)acetic acid (78.6 mg, 0.50 mmol) to provide after purification product **II-91** (123.3 mg, 77%) as an orange oil. IR (film) 3369, 3066, 2929, 1666 cm⁻¹. ¹H NMR (500 MHz, CDCl₃) 7.18 (dd, 1H, J = 5.0, 1.2 Hz), 6.98 (app dt, 1H), 6.93 (dd, 1H, J = 5.0, 3.5 Hz), 6.78 – 6.69 (m, 2H), 6.66 – 6.58 (m, 2H), 5.09 (dd, 1H, J = 7.1, 6.0 Hz), 4.19 (bs, 1H), 3.72 (s, 3H), 3.13 (dd, 1H, J = 15.0, 7.4 Hz), 3.07 (dd, 1H, J = 14.9, 5.6 Hz), 2.88 (q, 2H, J = 7.4 Hz), 1.22 (t, 3H, J = 7.4 Hz). ¹³C NMR (126 MHz, CDCl₃) 197.1, 152.9, 147.1, 140.5, 126.9, 124.4, 124.0, 115.8, 114.8, 55.7, 52.8, 51.4, 23.7, 14.7; HMRS (ESI): Exact mass calcd for C₁₆H₂₀NO₂S₂ [M+H⁺], 322.0935. Found 322.0906



methyl 3-((4-methoxyphenyl)amino)-2,2-dimethyl-3-phenylpropanoate (II-71):

The reaction was carried out according to the general oxidation procedure (B) using 2-Phenylglycine (75.6 mg, 0.50 mmol) to provide after purification product **II-71** (140.0. mg, 89%) as a white crystal; m.p. 87.7°C; IR (KBr) 3369, 2955, 1716 cm⁻¹; ¹H NMR (400 MHz, CDCl₃) 7.32 – 7.22 (m, 4H), 7.24 – 7.18 (m, 1H), 6.63 (d, 2H, J = 8.9 Hz), 6.45 (d, 2H J = 8.8 Hz), 4.45 (s, 1H), 3.65 (s, 6H), 1.24 (s, 3H), 1.15 (s, 3H); ¹³C NMR

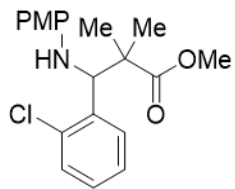
(101 MHz, CDCl₃) 177.3, 152.1, 141.3, 139.5, 128.5, 128.1, 127.5, 114.9, 114.8, 65.4, 55.8, 52.2, 47.3, 24.6, 20.6; HMRS (ESI): Exact mass calcd for C₁₉H₂₃NO₃ [M+H], 314.1756. Found 314.1747.



methyl 3-((4-methoxyphenyl)amino)-2,2-dimethyl-3-(o-tolyl)

propanoate (II-72): The reaction was carried out according to the general oxidation procedure (B) using 2-amino-2-(o-tolyl)acetic acid (82.6 mg, 0.50

mmol) to provide after purification product **II-72**, (15% by NMR) as a white crystal; m.p. 87.4°C; IR (KBr) 3389, 3066, 2831, 1742 cm⁻¹; ¹H NMR (400 MHz, CDCl₃) 7.24 (s, 1H), 7.15 – 7.08 (m, 3H), 6.64 (d, 2H, J = 8.9 Hz), 6.43 (d, 2H J = 8.4 Hz), 4.82 (s, 1H), 3.68 (s, 3H), 3.66 (s, 3H), 2.50 (s, 3H), 1.26 (s, 3H), 1.21 (s, 3H); ¹³C NMR (101 MHz, CDCl₃) 177.5, 152.2, 136.7, 130.6, 130.6, 127.3, 127.2, 126.0, 126.0, 114.9, 114.9, 60.3, 55.8, 52.3, 48.4, 24.7, 20.6, 20.3; HMRS (ESI): Exact mass calcd for C₂₀H₂₅NO₃ [M+H+], 328.1913. Found 328.1922.

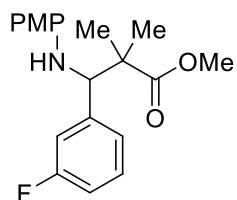


methyl 3-(2-chlorophenyl)-3-((4-methoxyphenyl)amino)-2,2-

dimethylpropanoate (II-73): The reaction was carried out according to the general oxidation procedure (B) using 2-amino-2-(2-chlorophenyl)acetic acid

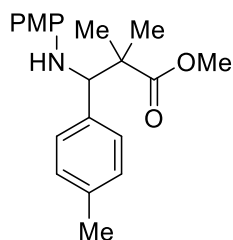
(92.8 mg, 0.50 mmol) to provide after purification product **II-73** (112.3 mg, 65%) as a white crystal; m.p. 107.2 °C; IR (KBr) 3402, 2995, 2833, 1718 cm⁻¹; ¹H NMR (400 MHz, CDCl₃) 7.39 – 7.35 (m, 1H), 7.34 – 7.30 (m, 1H), 7.22 – 7.14 (m, 2H), 6.69 (d, 2H, J = 8.9 Hz), 6.51 (d, 2H, J = 8.9 Hz), 5.12 (s, 1H), 3.71 (s, 3H), 3.69 (s, 3H), 1.39 (s, 3H), 1.24 (s, 3H); ¹³C NMR (101 MHz,

CDCl₃) 177.2, 152.2, 140.9, 137.8, 135.2, 129.6, 128.9, 128.7, 127.0, 114.9, 114.5, 60.1, 55.8, 52.3, 48.0, 25.0, 20.5; HMRS (ESI): Exact mass calcd for C₁₉H₂₂ClNO₃ [M+H], 348.1366. Found 348.1356.



methyl 3-(3-fluorophenyl)-3-((4-methoxyphenyl)amino)-2,2-dimethylpropanoate (II-74): The reaction was carried out according to the general oxidation procedure (B) using 2-amino-2-(3-fluorophenyl)acetic acid

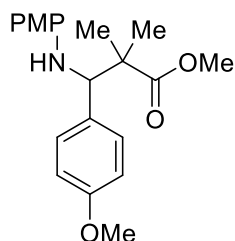
(84.6 mg, 0.50 mmol) to provide after purification product **II-74** (155.0 mg, 94%) as a white crystal; m.p. 118.1 °C; IR (KBr) 3389, 3066, 2901, 1707 cm⁻¹; ¹H NMR (400 MHz, CDCl₃) 7.28 – 7.22 (m, 1H), 7.07 (app dt, 1H), 7.00 (app dt, 1H), 6.93 (app tdd, 1H), 6.66 (d, 2H, J = 8.9 Hz), 6.45 (d, 2H, J = 8.9 Hz), 4.44 (s, 1H), 3.67 (s, 3H), 3.67 (s, 3H), 1.26 (s, 3H), 1.17 (s, 3H); ¹³C NMR (101 MHz, CDCl₃) 177.0, 162.9 (d, J = 245.9 Hz), 152.3, 142.6 (d, J = 5.0 Hz), 141.0, 129.5 (d, J = 8.1 Hz), 124.3 (d, J = 2.9 Hz), 115.3 (d, J = 21.7 Hz), 114.872, 114.870, 114.6 (d, J = 21.2 Hz), 65.1, 55.8, 52.3, 47.2, 24.6, 20.8; HMRS (ESI): Exact mass calcd for C₁₉H₂₂FNO₃ [M+H], 332.1662. Found 332.1651.



methyl 3-((4-methoxyphenyl)amino)-2,2-dimethyl-3-(p-tolyl) propanoate (II-75): The reaction was carried out according to the general oxidation procedure (B) using 2-amino-2-(p-tolyl)acetic acid (82.6 mg, 0.50 mmol) to provide after purification product **II-75** (131.0 mg, 80%) as a white crystal;

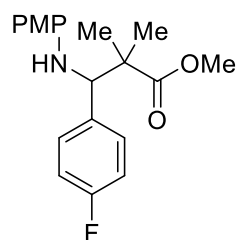
m.p. 111.4 °C; IR (KBr) 3379, 2995, 2825, 1718 cm⁻¹; ¹H NMR (400 MHz, CDCl₃) 7.16 (d, 2H,

$J = 7.9$ Hz), 7.09 (d, 2H, $J = 7.9$ Hz), 6.65 (d, 2H, $J = 8.9$ Hz), 6.47 (d, 2H, $J = 8.9$ Hz), 4.44 (s, 1H), 3.67 (s, 6H), 2.30 (s, 3H), 1.24 (s, 3H), 1.16 (s, 3H); ^{13}C NMR (101 MHz, CDCl_3) 177.3, 152.0, 141.4, 137.1, 136.4, 128.8, 128.4, 114.9, 114.8, 65.1, 55.8, 52.2, 47.3, 24.6, 21.2, 20.6; HMRS (ESI): Exact mass calcd for $\text{C}_{20}\text{H}_{25}\text{NO}_3$ $[\text{M}^+]$, 327.1834. Found 327.1845.



methyl 3-(4-methoxyphenyl)-3-((4-methoxyphenyl)amino)-2,2-dimethylpropanoate (II-76): The reaction was carried out according to the general oxidation procedure (B) using 2-amino-2-(4-methoxyphenyl) acetic acid (120.6 mg, 0.50 mmol) to provide after purification product **II-76** (142.5

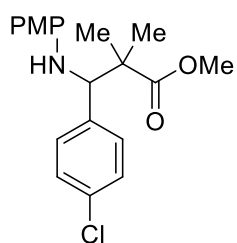
mg, 83%) as a white crystal; m.p. 102.4 °C; IR (KBr) 3416, 2978, 2833, 1724 cm^{-1} ; ^1H NMR (400 MHz, CDCl_3) 7.21 (d, 2H, $J = 8.7$ Hz), 6.84 (d, 2H, $J = 8.7$ Hz), 6.67 (d, 2H, $J = 8.9$ Hz), 6.48 (d, 2H, $J = 8.9$ Hz), 4.43 (s, 1H), 3.79 (s, 3H), 3.69 (s, 3H), 3.68 (s, 3H), 1.26 (s, 3H), 1.18 (s, 3H); ^{13}C NMR (101 MHz, CDCl_3) 177.4, 159.0, 152.0, 141.4, 131.4, 129.5, 114.9, 114.8, 113.5, 64.7, 55.8, 55.3, 52.2, 47.4, 24.6, 20.6; HMRS (ESI): Exact mass calcd for $\text{C}_{20}\text{H}_{25}\text{NO}_4$ $[\text{M}^+]$, 343.1784. Found 343.1781.



methyl 3-(4-fluorophenyl)-3-((4-methoxyphenyl)amino)-2,2-dimethylpropanoate (II-77): The reaction was carried out according to the general oxidation procedure (B) using 2-amino-2-(4-fluorophenyl)acetic acid (84.6 mg, 0.50 mmol) to provide after purification product **II-77** (132.7 mg,

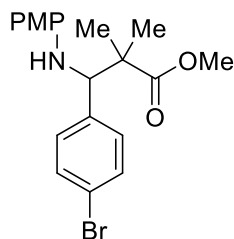
80%) as a white crystal; m.p. 99.1 °C; IR (KBr) 3371, 2983, 1714 cm^{-1} ; ^1H NMR (400 MHz,

CDCl₃) 7.25 (dd, 2H, J = 8.5, 5.4 Hz), 6.98 (app t, 2H), 6.66 (d, 2H, J = 8.8 Hz), 6.44 (d, 2H, J = 8.8 Hz), 4.44 (s, 1H), 3.67 (s, 3H), 3.66 (s, 3H), 1.25 (s, 3H), 1.16 (s, 3H); ¹³C NMR (101 MHz, CDCl₃) 177.1, 163.5, 161.0, 152.2, 141.1, 135.3 (d, J = 3.3 Hz), 129.9 (d, J = 8.0 Hz), 115.1 (d, J = 21.3 Hz), 114.8 (d, J = 2.3 Hz), 64.8, 55.8, 52.3, 47.2, 24.5, 20.7; HMRS (ESI): Exact mass calcd for C₁₉H₂₂FNO₃ [M+H], 332.1662. Found 332.1653.



methyl 3-(4-chlorophenyl)-3-((4-methoxyphenyl)amino)-2,2-dimethylpropanoate (II-78): The reaction was carried out according to the general oxidation procedure (B) using 2-amino-2-(4-chlorophenyl)acetic acid (92.8 mg, 0.50 mmol) to provide after purification product **II-78** (151.7 mg,

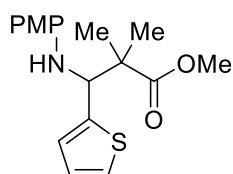
87%) as a white crystal; m.p. 137.0 °C; IR (KBr) 3373, 2953, 2926, 1718 cm⁻¹; ¹H NMR (400 MHz, CDCl₃) 7.30 – 7.20 (m, 4H), 6.66 (d, 2H, J = 8.9 Hz), 6.44 (d, 2H, J = 8.9 Hz), 4.43 (s, 1H), 3.68 (s, 3H), 3.67 (s, 3H), 1.26 (s, 3H), 1.16 (s, 3H); ¹³C NMR (101 MHz, CDCl₃) 177.0, 152.3, 141.0, 138.2, 133.3, 129.8, 128.4, 114.9, 114.9, 64.9, 55.8, 52.3, 47.1, 24.5, 20.7; HMRS (ESI): Exact mass calcd for C₁₉H₂₂ClNO₃ [M+], 347.1288. Found 347.1223.



methyl 3-(4-bromophenyl)-3-((4-methoxyphenyl)amino)-2,2-dimethylpropanoate (II-79): The reaction was carried out according to the general oxidation procedure (B) using 2-amino-2-(4-bromophenyl)acetic acid (115.0 mg, 0.50 mmol) to provide after purification product **II-79** (166.0. mg,

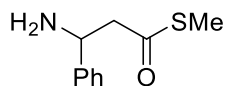
85%) as a white crystal; m.p. 144.3 °C; IR (KBr) 3379, 2978, 2825, 1716 cm⁻¹; ¹H NMR (400

MHz, CDCl₃) 7.44 (d, 2H, J = 8.5 Hz), 7.19 (d, 2H, J = 8.4 Hz), 6.68 (d, 2H, J = 8.9 Hz), 6.45 (d, 2H, J = 9.0 Hz), 4.43 (s, 1H), 3.70 (s, 3H), 3.69 (s, 3H), 1.27 (s, 3H), 1.18 (s, 3H); ¹³C NMR (101 MHz, CDCl₃) 177.0, 152.2, 140.9, 138.8, 131.3, 130.2, 121.5, 114.9, 114.9, 65.0, 55.8, 52.3, 47.1, 24.6, 20.7; HMRS (ESI): Exact mass calcd for C₁₉H₂₂BrNO₃ [M⁺], 391.0783. Found 391.0787.



methyl 3-((4-methoxyphenyl)amino)-2,2-dimethyl-3-(thiophen-2-yl)propanoate (II-80): The reaction was carried out according to the general oxidation procedure (B) using 2-amino-2-(thiophen-2-yl)acetic acid (78.6 mg,

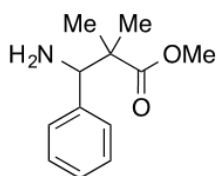
0.50 mmol) to provide after purification product **II-80** (131.0. mg, 82%) as a white crystal; m.p. 85.9 °C; IR (KBr) 3356, 3109, 2910, 1716 cm⁻¹; ¹H NMR (400 MHz, CDCl₃) 7.18 – 7.14 (m, 1H), 6.94 – 6.90 (m, 2H), 6.70 (d, 2H, J = 8.9 Hz), 6.56 (d, 2H, J = 8.9 Hz), 4.77 (s, 1H), 3.69 (s, 6H), 1.31 (s, 3H), 1.28 (s, 3H); ¹³C NMR (101 MHz, CDCl₃) 177.0, 152.6, 144.5, 141.1, 126.6, 126.1, 124.5, 115.3, 114.8, 61.9, 55.8, 52.3, 47.6, 24.1, 21.3; HMRS (ESI): Exact mass calcd for C₁₇H₂₁SNO₃ [M⁺], 319.1242. Found 319.1252.



S-ethyl 3-((4-methoxyphenyl)amino)-3-phenylpropanethioate (II-92) : II-82 (0.5 mmol) was dissolved in CH₃CN (11 mL) and an aqueous solution of

CAN (1.37g, 2.5 mmol in 8mL water) was added dropwise. The reaction mixture was stirred for 2 h. NaHCO₃ was added until pH 6 was reached. Sodium sulfite was then added until the mixture became brown. The product was extracted with EtOAc (3 x 10 mL). The combined organic layers

were dried over sodium sulfate, evaporated and the obtained free amine **II-92** was provided (98.6 mg, 94%) as a brown oil. IR (film) 3413, 3388, 3037, 2927, 1673 cm^{-1} . ^1H NMR (400 MHz, D_2O) 7.55 – 7.43 (m, 5H), 4.85 (t, $J = 7.3$ Hz, 1H), 3.42 (d, $J = 7.3$ Hz, 2H), 2.86 (q, $J = 7.5$ Hz, 2H), 1.15 (t, $J = 7.4$ Hz, 3H). ^{13}C NMR (126 MHz, D_2O) 199.6, 134.6, 129.6, 129.3, 127.0, 51.8, 46.2, 23.4, 13.5; HMRS (ESI): Exact mass calcd for $\text{C}_{11}\text{H}_{16}\text{NOS}$ $[\text{M}+\text{H}]^+$, 210.0953. Found 210.0954.



methyl 3-amino-2,2-dimethyl-3-phenylpropanoate (II-93): **II-71** (0.5

mmol) was dissolved in CH_3CN (11 mL) and an aqueous solution of CAN (1.37g, 2.5 mmol in 8mL water) was added dropwise. The reaction mixture

was stirred for 2 h. NaHCO_3 was added until pH 6 was reached. Sodium sulfite was then added until the mixture became brown. The product was extracted with EtOAc (3 x 10 mL). The combined organic layers were dried over sodium sulfate, evaporated and the obtained free amine **II-93** was provided (92.6 mg, 89%) as a brown solid; which was spectroscopically identical to previous reports.⁷¹

2.11 Experimental Section for Hammett Experiments

A: General Procedure for Mechanism Experiments on Quinone-Catalyzed Decarboxylation:

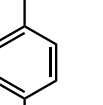
To a solution of 2,6-di-*tert*-butyl-1,4-benzoquinone (22.0 mg, 0.10 mmol, unless otherwise noted) and p-anisidine (246 mg, 2.0 mmol) in EtOH (3.2 mL, 0.312 M with respect to the aryl glycine substrate) was added the glycine derivative (1.00 mmol), followed by addition of 1,3,5-trimethoxybenzene (0.50 mmol) as an internal NMR standard and purging the reaction vial with a

balloon of O₂. The reaction mixture was allowed to stir under O₂ at 70 °C. Aliquots were drawn from the reaction mixture every hour for ¹H NMR analysis and concentrated under reduced pressure. % yield was measured by product formation against the NMR standard and converted from % yield to concentration ([]) in mol/L.

B: General Procedure for Mechanism Experiments on Stoichiometric Quinone-Promoted Decarboxylation:

To a solution of 2,6-di-*tert*-butyl-1,4-benzoquinone (110.0 mg, 0.5 mmol, unless otherwise noted) and p-anisidine (123.0 mg, 1.0 mmol) in EtOH (1.6 mL, 0.312 M with respect to the glycine derivative substrate) was added the glycine derivative (0.50 mmol), followed by addition of 1,3,5-trimethoxybenzene (0.50 mmol) as an internal NMR standard and purging the reaction vial with a balloon of O₂. The reaction mixture was allowed to stir under O₂ at 70 °C. Aliquots were drawn from the reaction mixture every hour for ¹H NMR analysis and concentrated under reduced pressure. % yield was measured by product formation against the NMR standard and converted from % yield to concentration ([]) in mol/L.

Rate Data for Quinone-Catalyzed Decarboxylation of Phenylglycine:



II-35

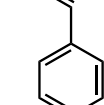
II-19 (10 mol%)

EtOH, 0.312 M

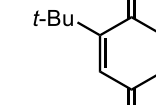
2.0 equiv. anisidine

2.0 equiv. Et₃N

70°C, 24 h, O₂



II-37



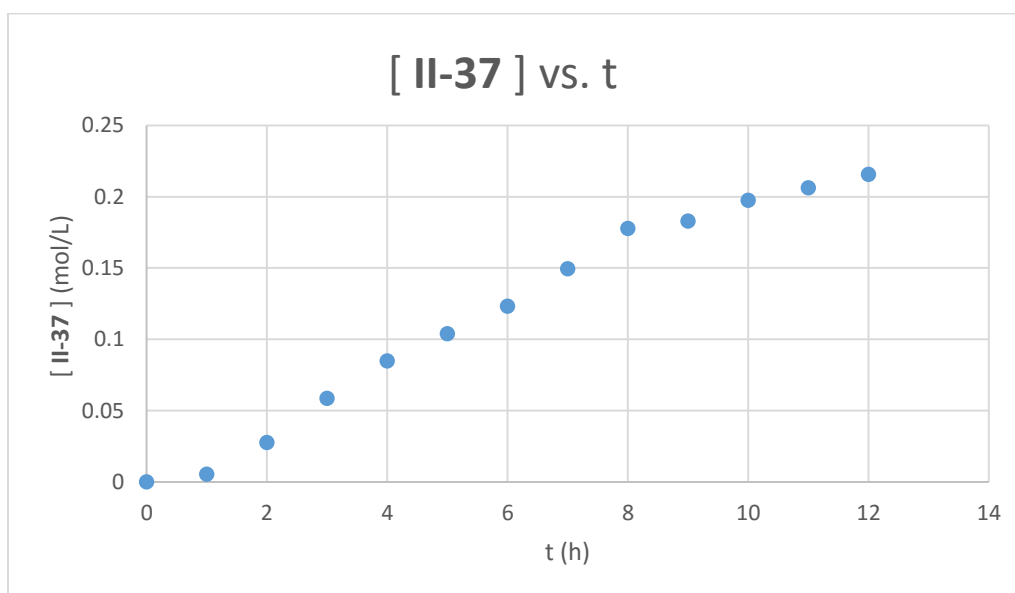
II-19

hour	% yield II-37 ^a	[II-37] ^b	hour	% yield II-37 ^a	[II-37] ^b
0	0	0.00	7	48	0.15
1	2	0.01	8	57	0.18
2	9	0.03	9	59	0.18
3	19	0.06	10	63	0.20
4	27	0.08	11	66	0.21
5	33	0.10	12	69	0.22
6	39	0.12			

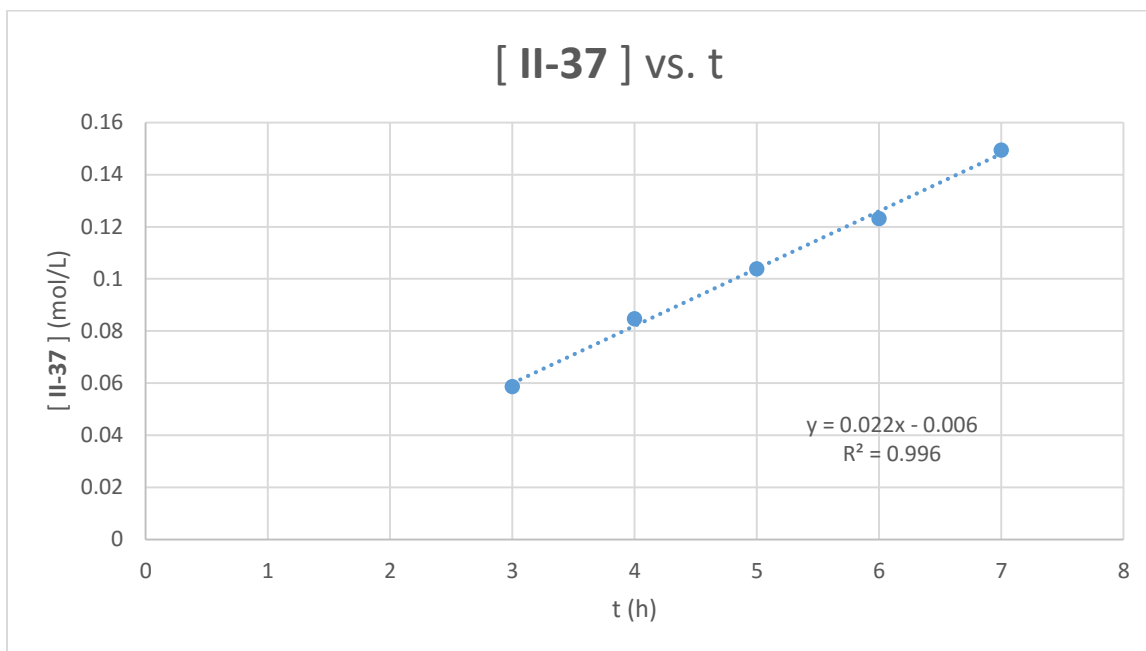
^a value determined by ¹H NMR with 1,3,5-trimethoxybenzene as internal NMR standard

^b calculated by conversion to product

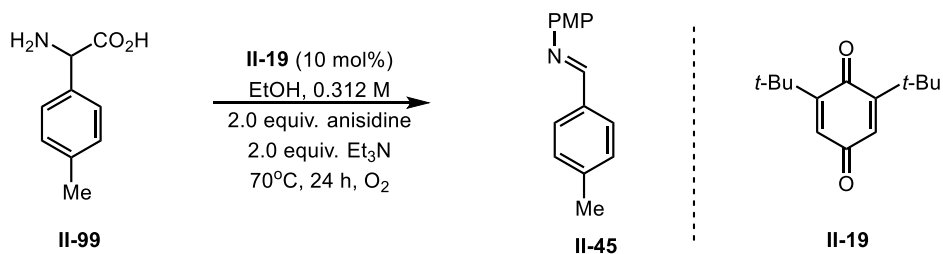
Rate Data Plot for Quinone-Catalyzed Decarboxylation of Phenylglycine:



Rate Data Plot for Linear Portion of Quinone-Catalyzed Decarboxylation:



Rate Data for Quinone-Catalyzed Decarboxylation of 2-amino-2-(p-tolyl)acetic acid:

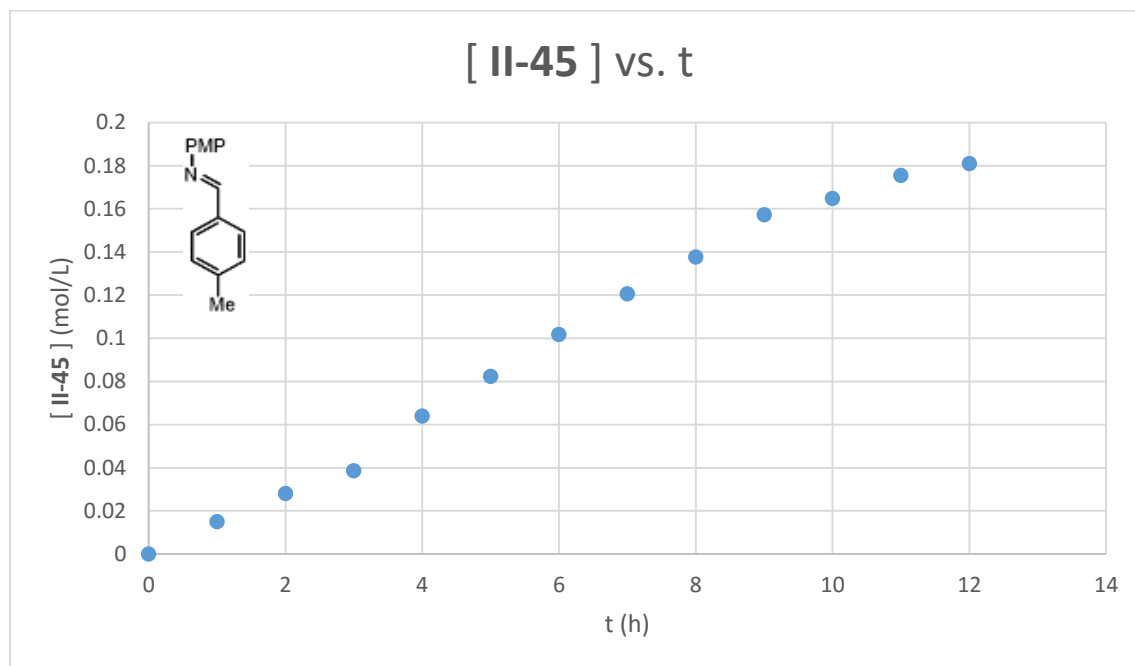


hour	% yield II-45 ^a	[II-45] ^b	hour	% yield II-45 ^a	[II-45] ^b
0	0	0.00	7	39	0.12
1	5	0.02	8	44	0.14
2	9	0.03	9	50	0.16
3	12	0.04	10	53	0.16
4	20	0.06	11	56	0.18
5	26	0.08	12	58	0.18
6	33	0.10			

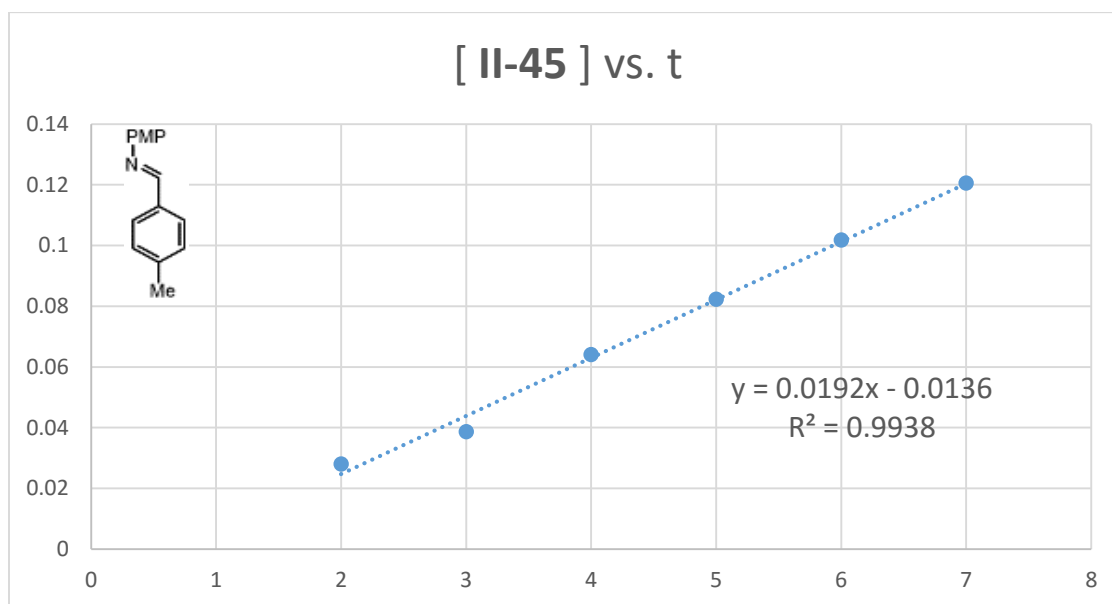
^a value determined by ¹H NMR with 1,3,5-trimethoxybenzene as internal NMR standard

^b calculated by conversion to product

Rate Data Plot for Quinone-Catalyzed Decarboxylation of 2-amino-2-(p-tolyl)acetic acid:



Rate Data Plot for Linear Portion of Quinone-Catalyzed Decarboxylation of 2-amino-2-(p-tolyl)acetic acid:

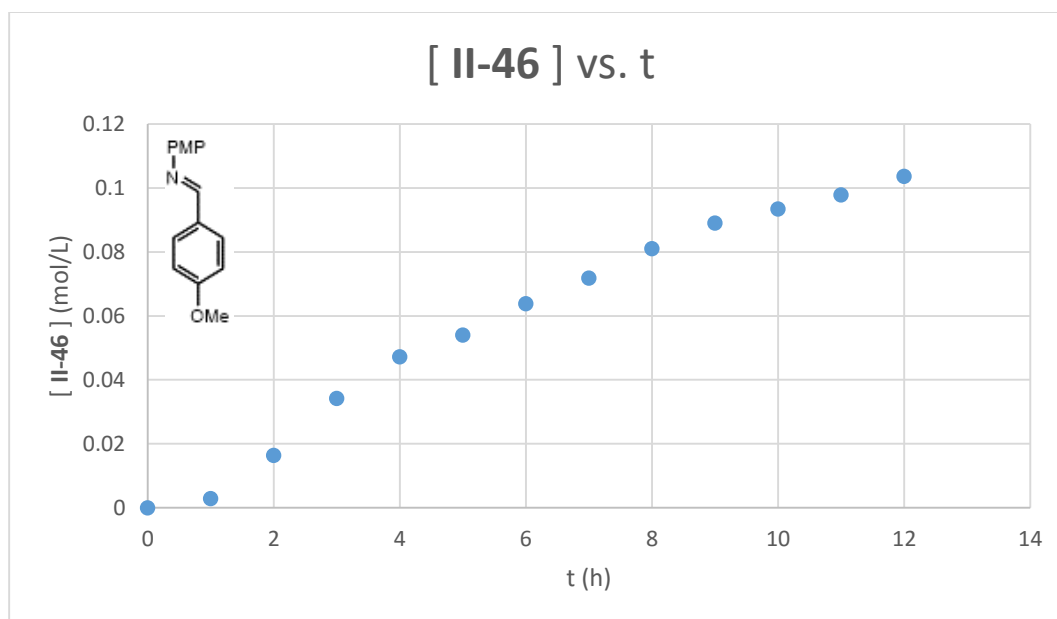


Rate Data for Quinone-Catalyzed Decarboxylation of 2-amino-2-(4-methoxyphenyl)acetic acid:

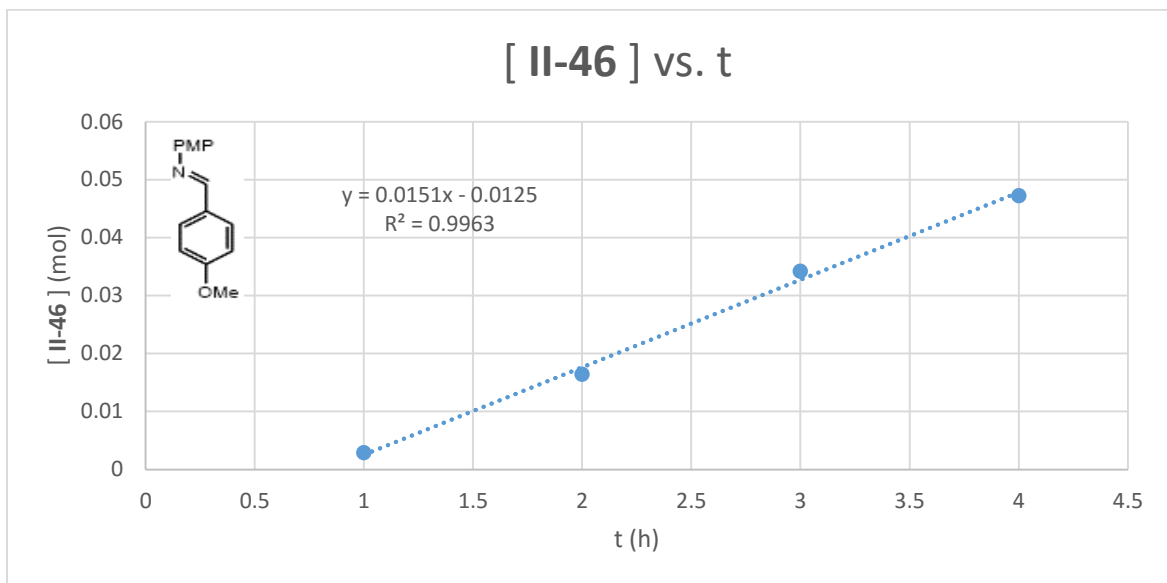
hour	% yield II-46 ^a	[II-46] ^b	hour	% yield II-46 ^a	[II-46] ^b
0	0	0.00	7	23	0.07
1	1	0.00	8	26	0.08
2	5	0.02	9	29	0.09
3	11	0.03	10	30	0.09
4	15	0.05	11	31	0.10
5	17	0.05	12	33	0.10
6	20	0.06			

^a value determined by ¹H NMR with 1,3,5-trimethoxybenzene as internal NMR standard
^b calculated by conversion to product

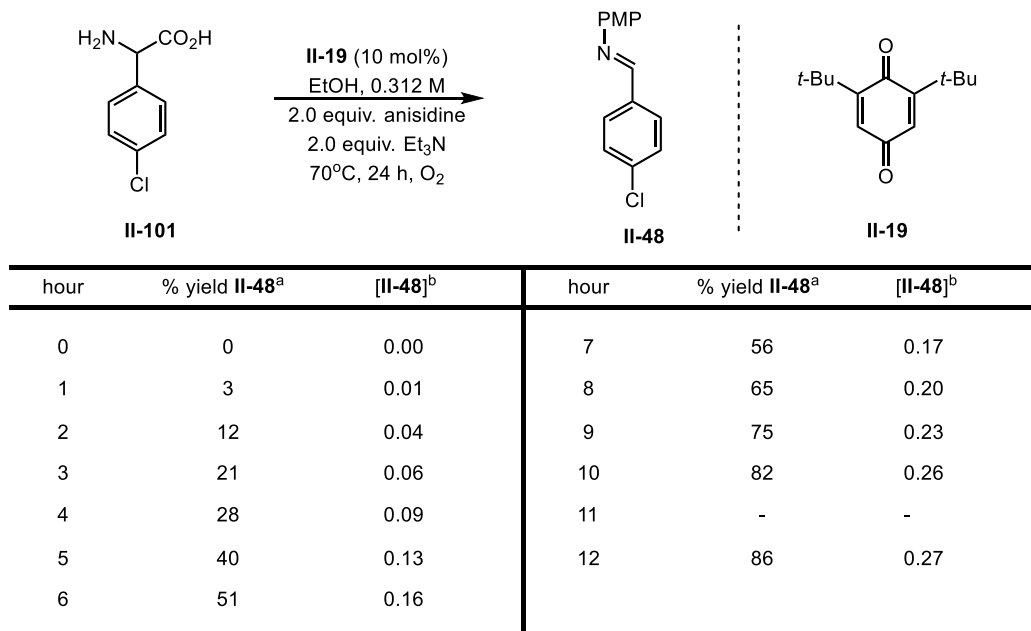
Rate Data Plot for Quinone-Catalyzed Decarboxylation of 2-amino-2-(4-methoxyphenyl)acetic acid:



Rate Data Plot for Linear Portion of Quinone-Catalyzed Decarboxylation of 2-amino-2-(4-methoxyphenyl) acetic acid:



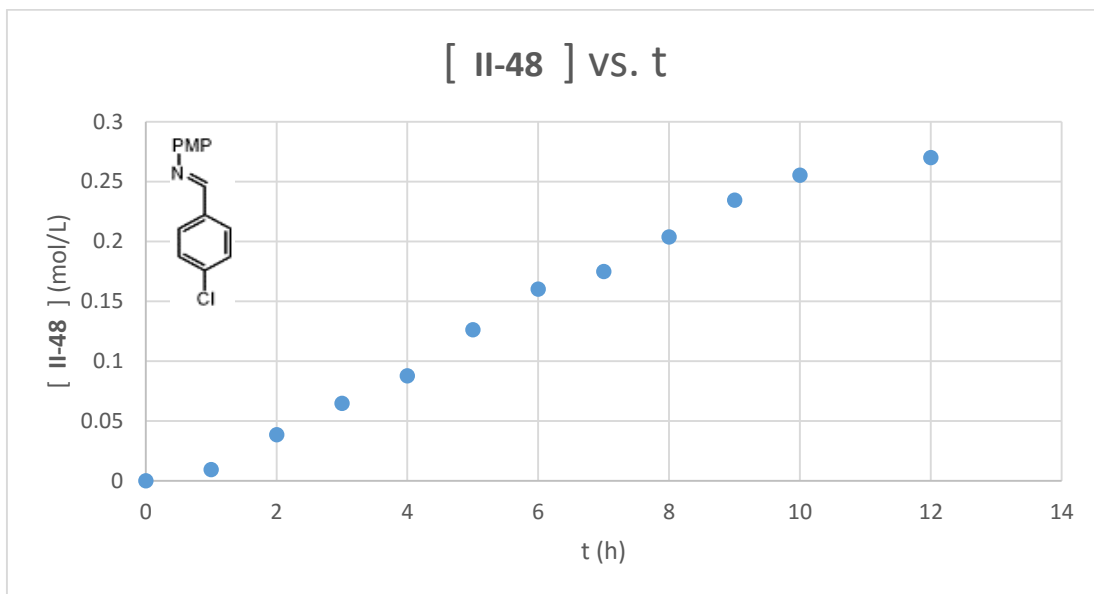
Rate Data for Quinone-Catalyzed Decarboxylation of 2-amino-2-(4-chlorophenyl)acetic acid:



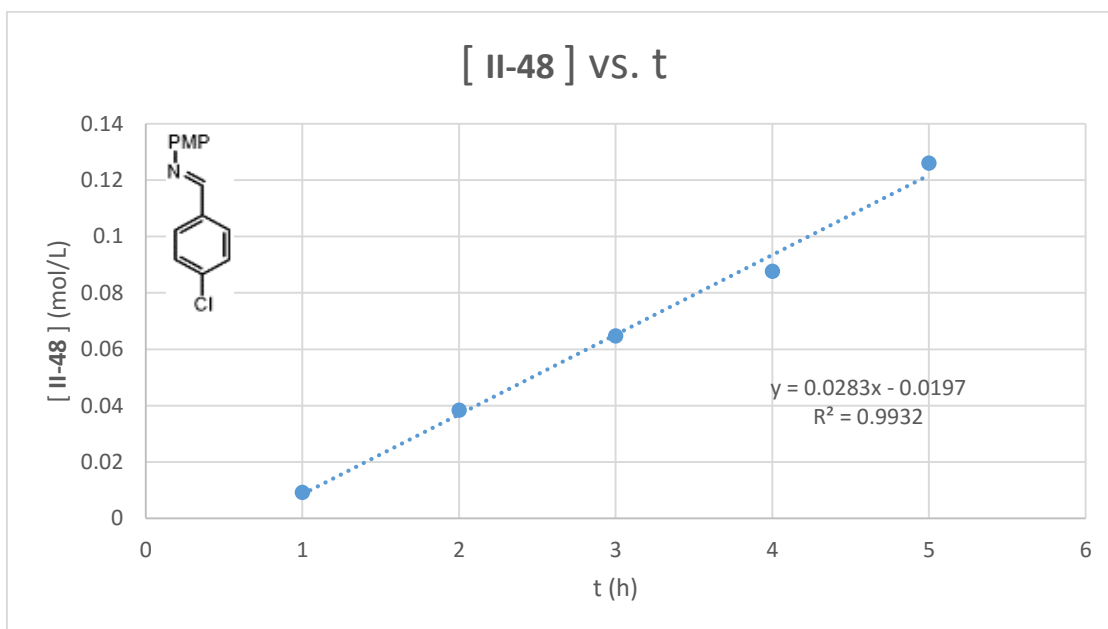
^a value determined by ¹H NMR with 1,3,5-trimethoxybenzene as internal NMR standard

^b calculated by conversion to product

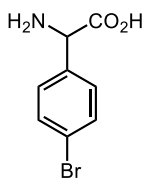
Rate Data Plot for Quinone-Catalyzed Decarboxylation 2-amino-2-(4-chlorophenyl)acetic acid:



Rate Data Plot for Linear Portion of Quinone-Catalyzed Decarboxylation 2-amino-2-(4-chlorophenyl)acetic acid:

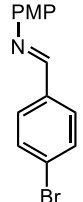


Rate Data for Quinone-Catalyzed Decarboxylation of 2-amino-2-(4-bromophenyl)acetic acid:

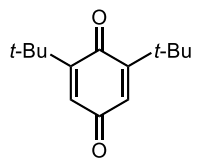


II-102

$\xrightarrow[\substack{\text{EtOH, 0.312 M} \\ \text{2.0 equiv. anisidine} \\ \text{2.0 equiv. Et}_3\text{N} \\ \text{70}^\circ\text{C, 24 h, O}_2}]{\text{II-19 (10 mol\%)}}$



II-49

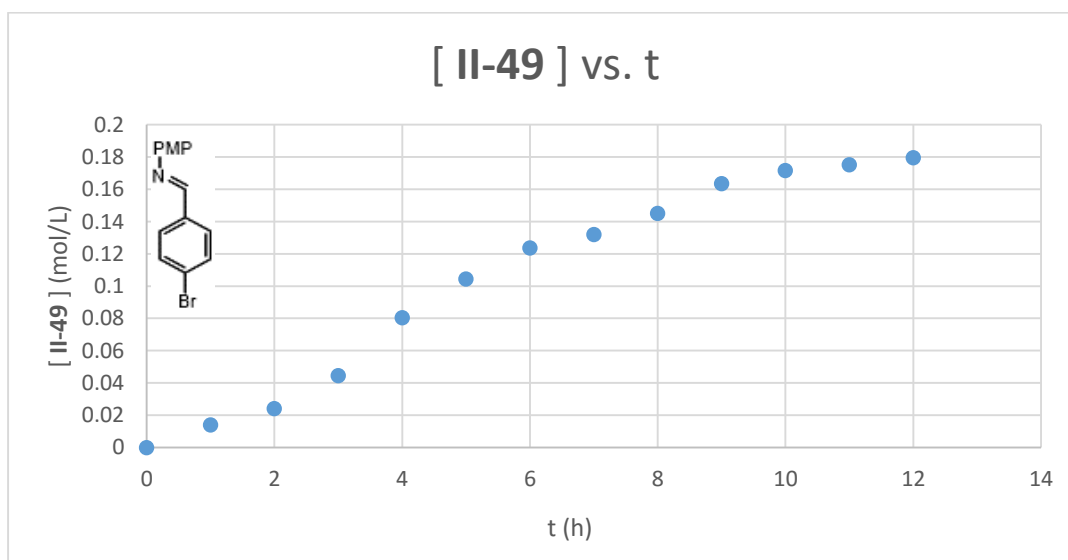


II-19

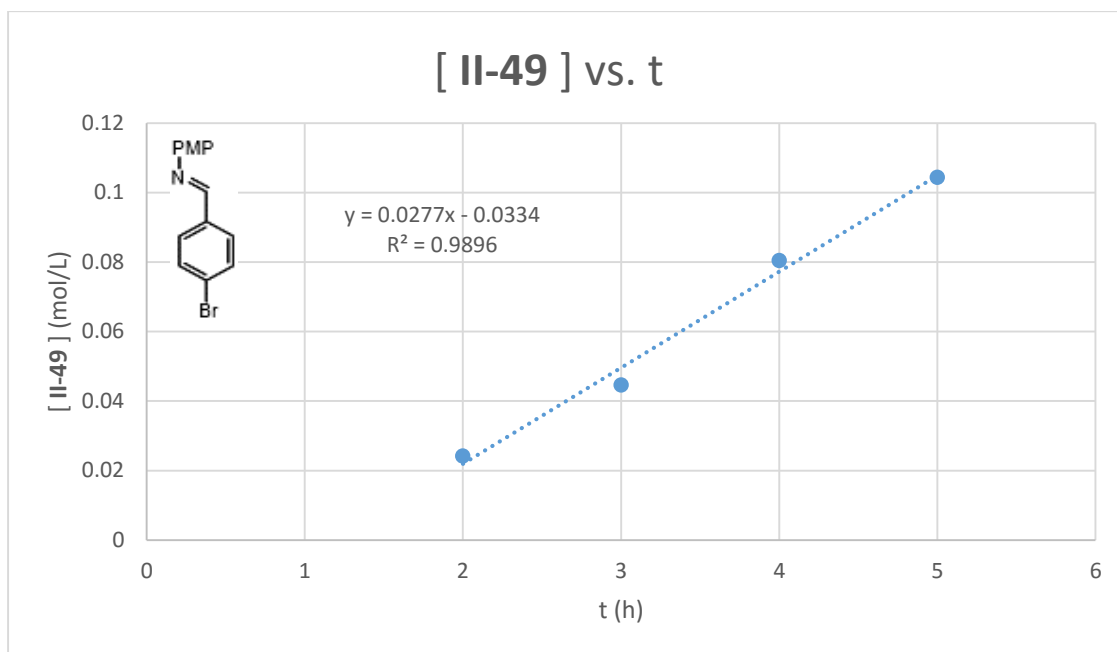
hour	% yield II-49 ^a	[II-49] ^b	hour	% yield II-49 ^a	[II-49] ^b
0	0	0.00	7	42	0.13
1	5	0.01	8	46	0.15
2	8	0.02	9	52	0.16
3	14	0.04	10	55	0.17
4	26	0.08	11	56	0.18
5	33	0.10	12	58	0.18
6	40	0.12			

^a value determined by ¹H NMR with 1,3,5-trimethoxybenzene as internal NMR standard
^b calculated by conversion to product

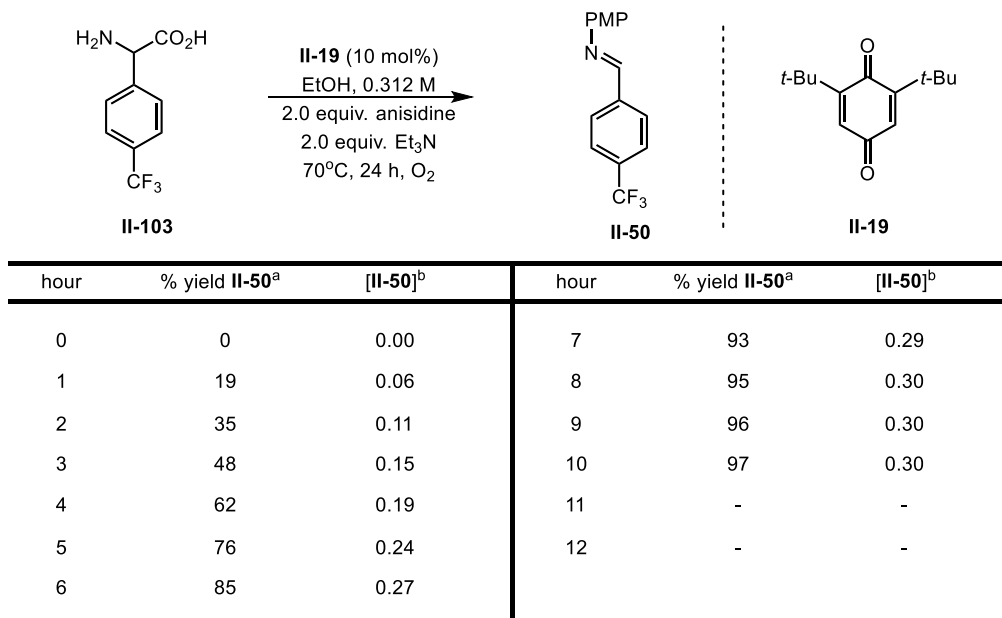
Rate Data Plot for Quinone-Catalyzed Decarboxylation 2-amino-2-(4-bromophenyl)acetic acid:



Rate Data Plot for Linear Portion of Quinone-Catalyzed Decarboxylation 2-amino-2-(4-bromophenyl)acetic acid:



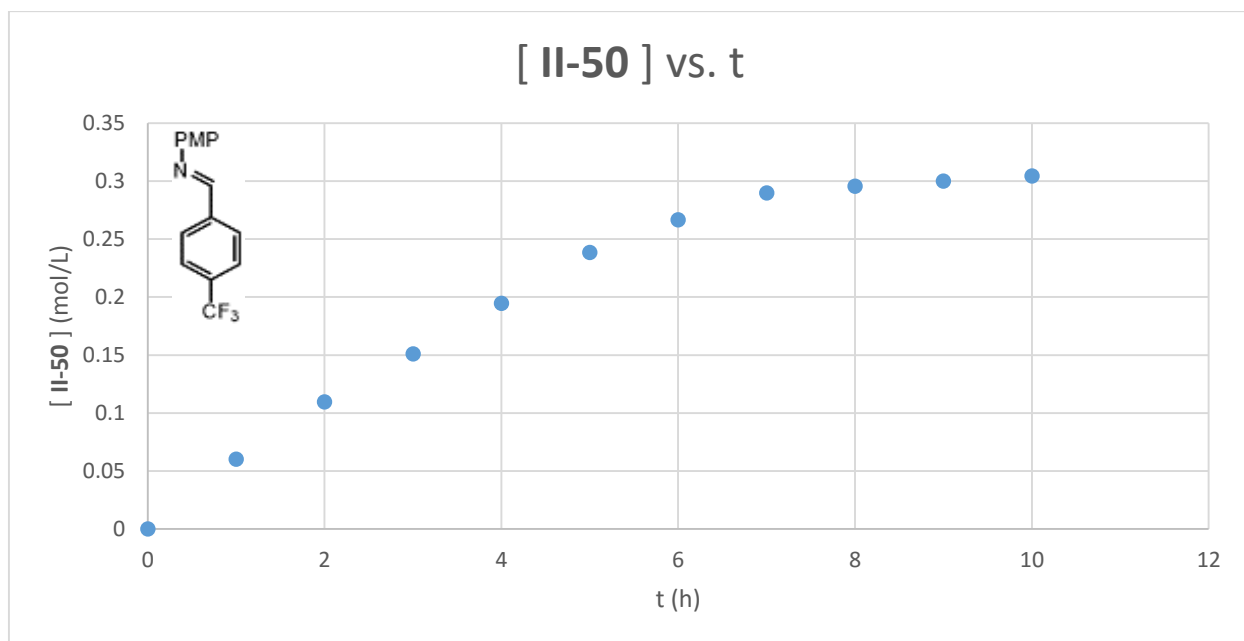
Rate Data for Quinone-Catalyzed Decarboxylation of 2-amino-2-(4-(trifluoromethyl)phenyl)acetic acid:



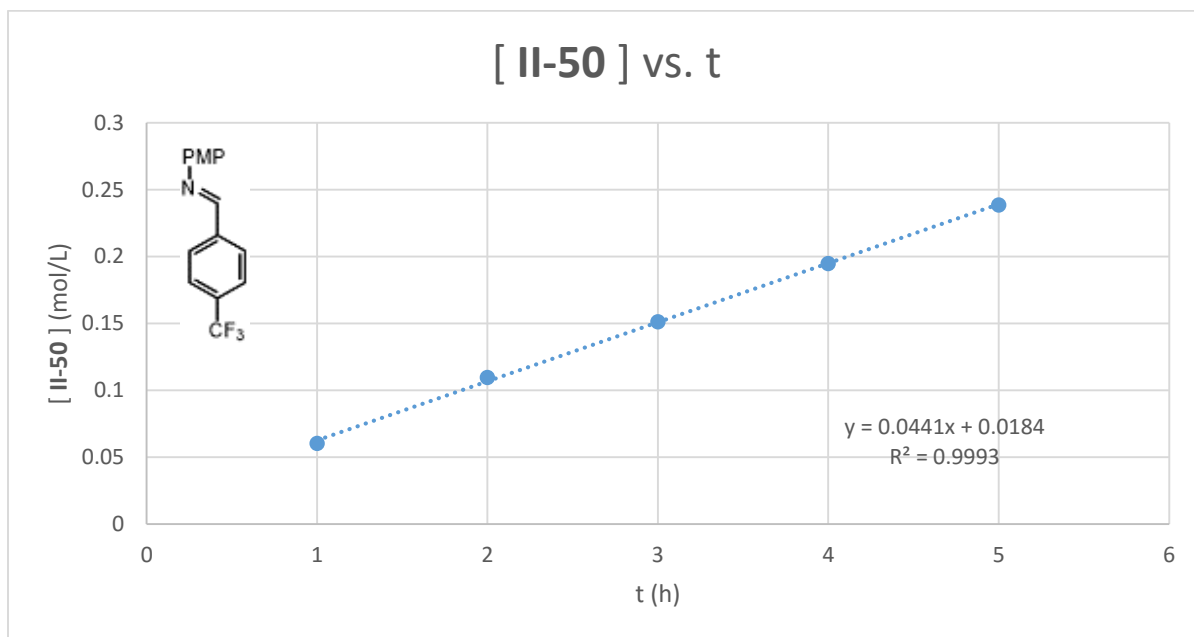
^a value determined by ¹H NMR with 1,3,5-trimethoxybenzene as internal NMR standard

^b calculated by conversion to product

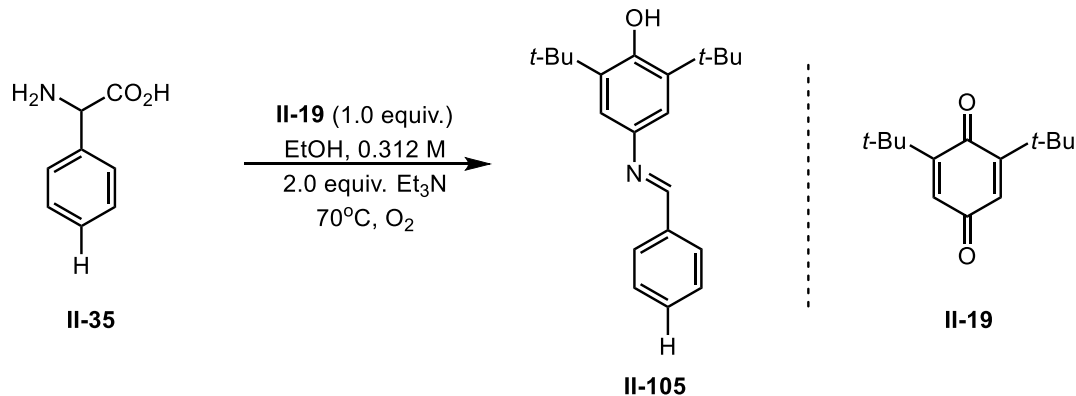
Rate Data Plot for Quinone-Catalyzed Decarboxylation 2-amino-2-(4-(trifluoromethyl) phenyl) acetic acid:



Rate Data Plot for Linear Portion of Quinone-Catalyzed Decarboxylation 2-amino-2-(4-(trifluoromethyl) phenyl) acetic acid:



Rate Data for Stoichiometric Quinone-Promoted Decarboxylation of Phenylglycine:

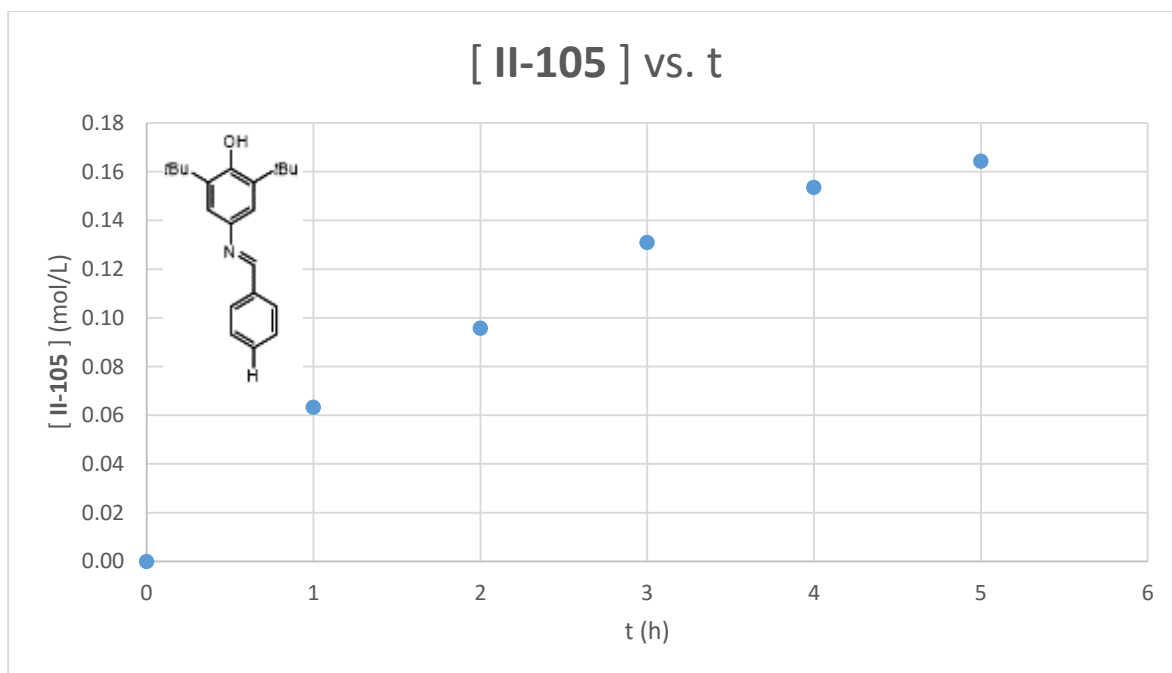


hour	% yield II-105 ^a	[II-105] ^b	hour	% yield II-105 ^a	[II-105] ^b
0	0	0.00	3	42	0.13
1	20	0.06	4	49	0.15
2	31	0.10	5	53	0.16

^a value determined by ¹H NMR with 1,3,5-trimethoxybenzene as internal NMR standard

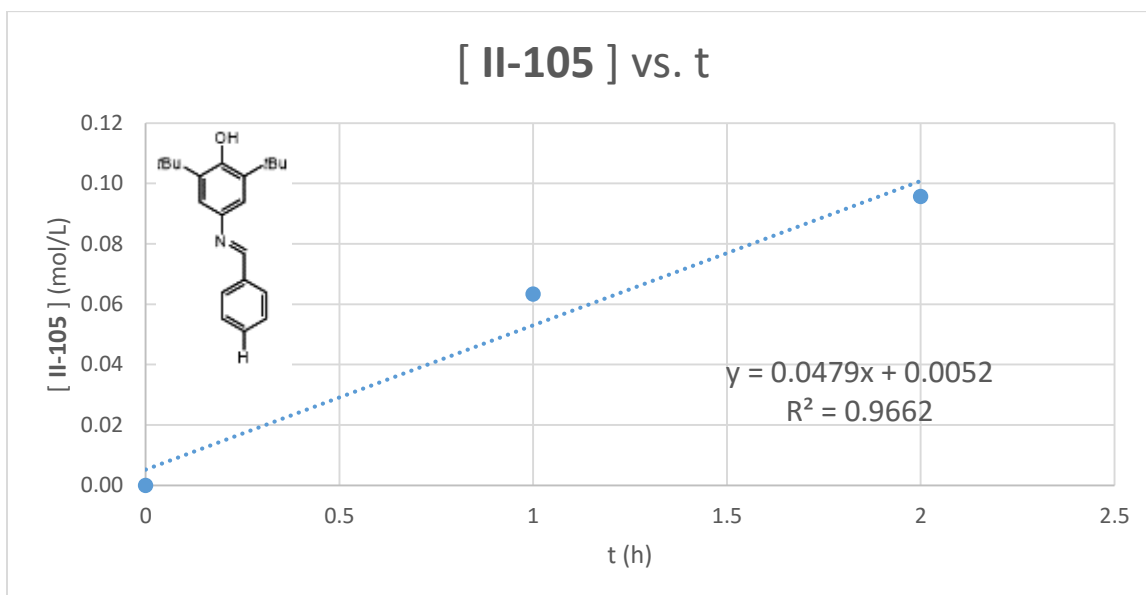
^b calculated by conversion to product

Rate Data Plot for Stoichiometric Quinone-Promoted Decarboxylation Phenylglycine:

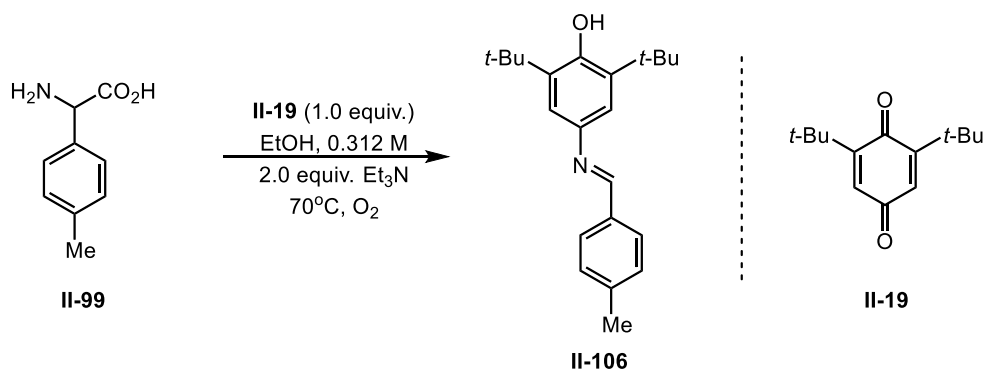


Rate Data Plot for Linear Portion of Stoichiometric Quinone-Promoted Decarboxylation

Phenylglycine:



Rate Data for Stoichiometric Quinone-Promoted Decarboxylation of 2-amino-2-(p-tolyl)acetic acid:

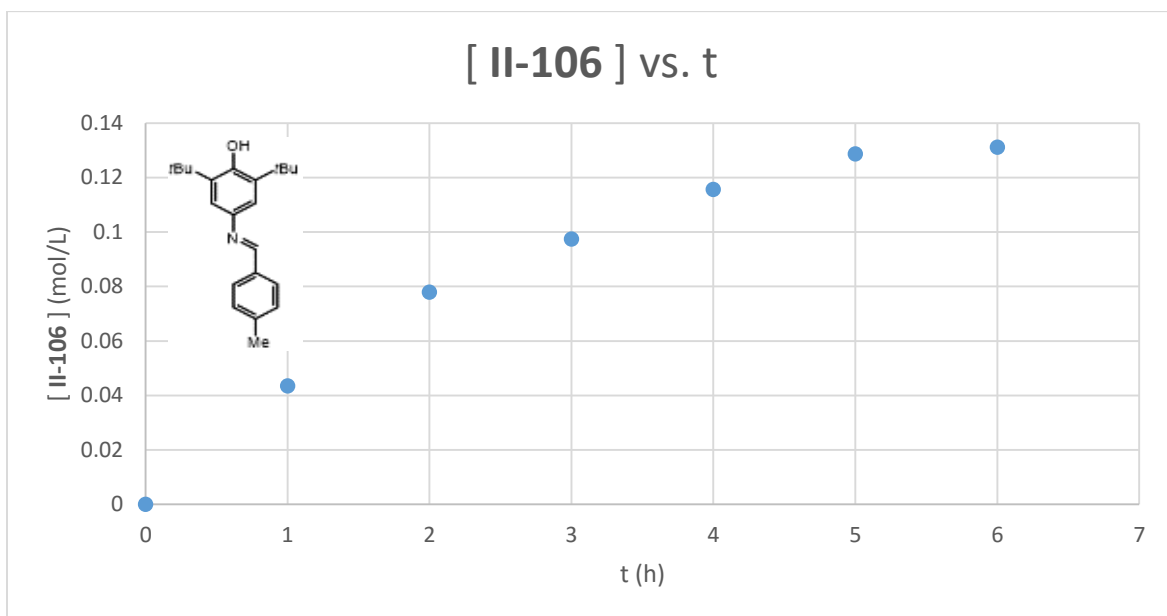


hour	% yield II-106 ^a	[II-106] ^b	hour	% yield II-106 ^a	[II-106] ^b
0	0	0.00	4	37	0.12
1	14	0.04	5	41	0.13
2	25	0.08	6	42	0.13
3	31	0.10			

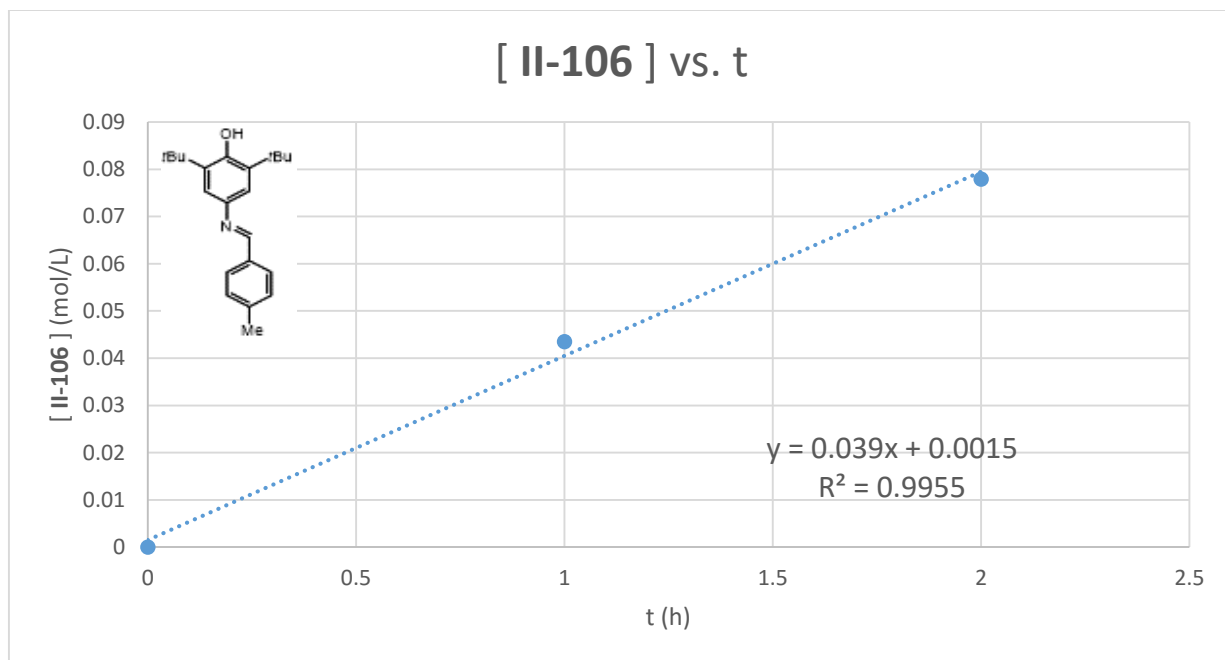
^a value determined by ^1H NMR with 1,3,5-trimethoxybenzene as internal NMR standard

^b calculated by conversion to product

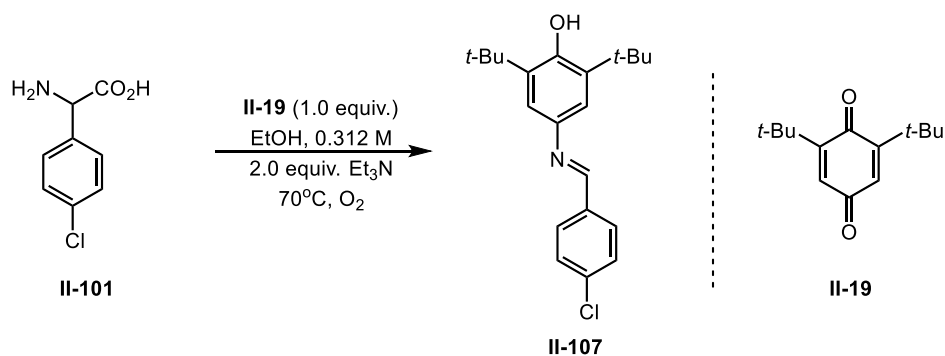
Rate Data Plot for Stoichiometric Quinone-Promoted Decarboxylation of 2-amino-2-(p-tolyl)acetic acid:



Rate Data Plot for Linear Portion of Stoichiometric Quinone-Promoted Decarboxylation of 2-amino-2-(p-tolyl)acetic acid:



Rate Data for Stoichiometric Quinone-Promoted Decarboxylation of 2-amino-2-(4-chlorophenyl)acetic acid:

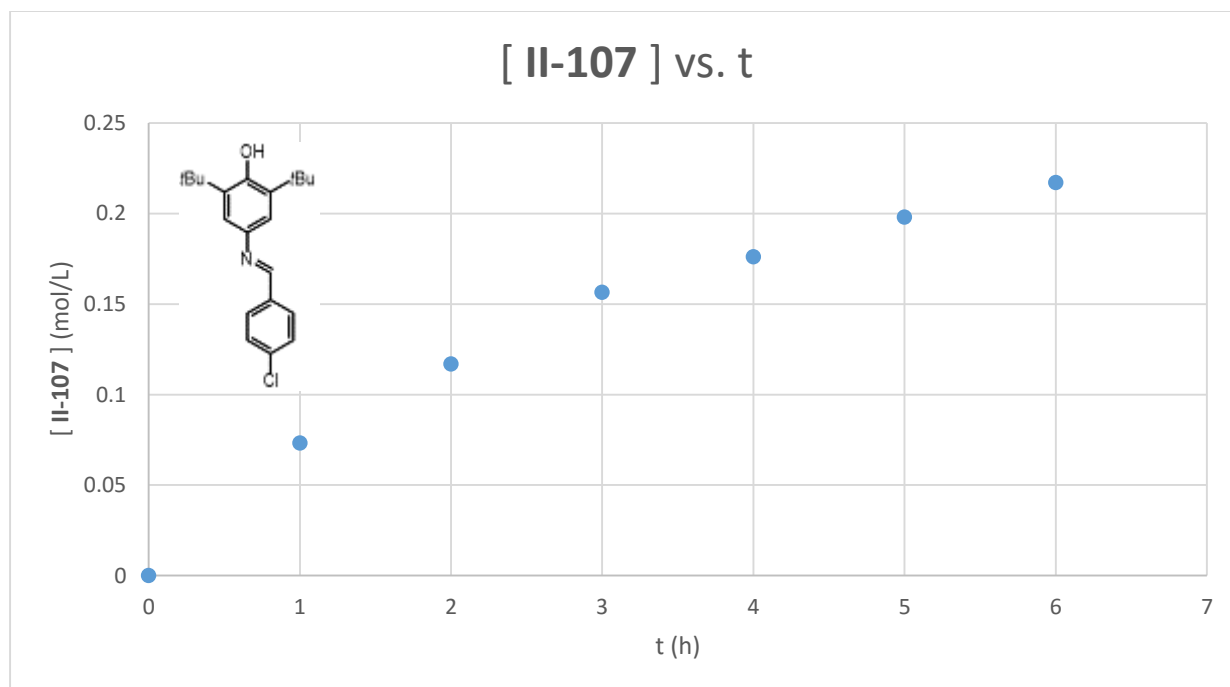


hour	% yield II-107 ^a	[II-107] ^b	hour	% yield II-107 ^a	[II-107] ^b
0	0	0.00	4	56	0.18
1	23	0.07	5	63	0.20
2	37	0.12	6	69	0.22
3	50	0.16			

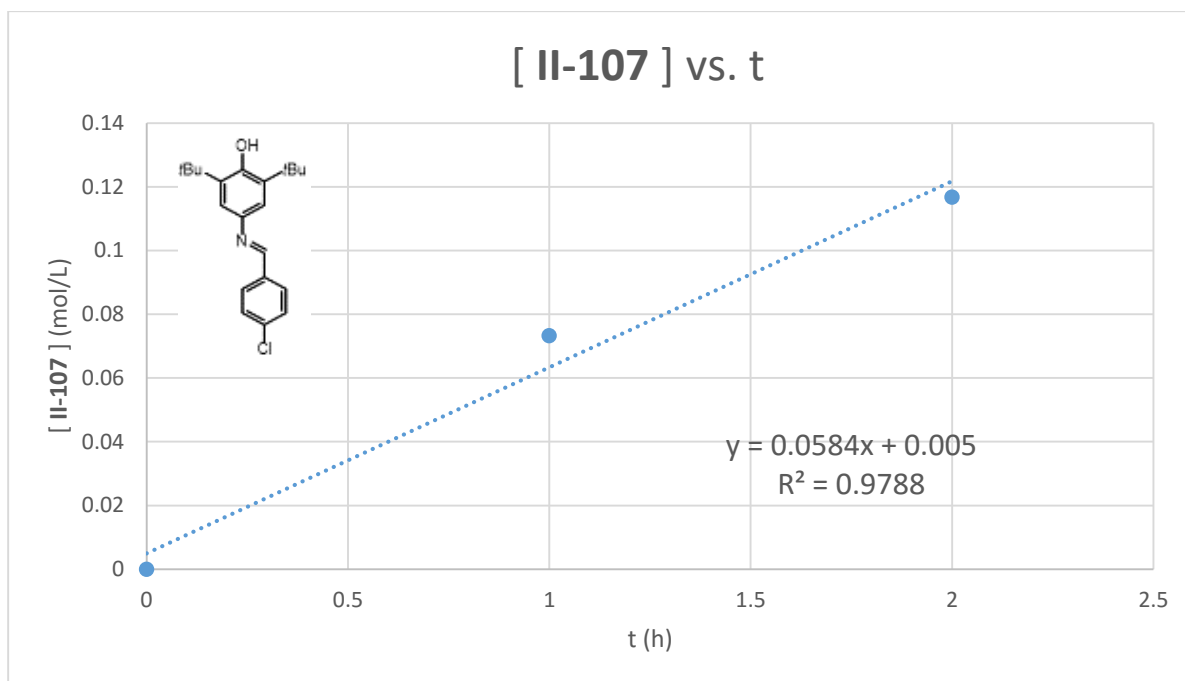
^a value determined by ¹H NMR with 1,3,5-trimethoxybenzene as internal NMR standard

^b calculated by conversion to product

Rate Data Plot for Stoichiometric Quinone-Promoted Decarboxylation of 2-amino-2-(4-chlorophenyl)acetic acid:



Rate Data Plot for Linear Portion of Stoichiometric Quinone-Promoted Decarboxylation of 2-amino-2-(4-chlorophenyl)acetic acid:



2.10 Chapter 1 and 2 References

1. MacMillan, D. W., The advent and development of organocatalysis. *Nature* **2008**, *455*, 304-8.
2. Li, C. J.; Trost, B. M., Green chemistry for chemical synthesis. *Proceedings of the National Academy of Sciences of the United States of America* **2008**, *105*, 13197-202.
3. Hajos, Z. G.; Parrish, D. R., Asymmetric synthesis of bicyclic intermediates of natural product chemistry. *The Journal of Organic Chemistry* **1974**, *39*, 1615-1621.
4. Seayad, J.; List, B., Asymmetric organocatalysis. *Organic & biomolecular chemistry* **2005**, *3*, 719-24.
5. Bertelsen, S.; Jorgensen, K. A., Organocatalysis-after the gold rush. *Chemical Society Reviews* **2009**, *38*, 2178-2189.
6. Ahrendt, K. A.; Borths, C. J.; MacMillan, D. W. C., New Strategies for Organic Catalysis: The First Highly Enantioselective Organocatalytic Diels–Alder Reaction. *Journal of the American Chemical Society* **2000**, *122*, 4243-4244.
7. Mukherjee, S.; Yang, J. W.; Hoffmann, S.; List, B., Asymmetric enamine catalysis. *Chemical reviews* **2007**, *107*, 5471-569.
8. Rutter, W. J., Evolution of Aldolase. *Federation proceedings* **1964**, *23*, 1248-57.
9. Stryer, L., *Biochemistry, 4th ed.* Freedman and Company 1995.
10. Jansen, B. C. P. D., W.F., On the isolation of antiberiberi vitamin. *Koninklijke Nederlandse Akademie van Wetenschappen*. **1926**, *29*, 1390.
11. Williams, R. R.; Cline, J. K., Synthesis of Vitamin B1. *Journal of the American Chemical Society* **1936**, *58*, 1504-1505.

12. Kluger, R.; Tittmann, K., Thiamin Diphosphate Catalysis: Enzymic and Nonenzymic Covalent Intermediates. *Chemical reviews* **2008**, *108*, 1797-1833.
13. Mizuhara, S.; Handler, P., Mechanism of Thiamine-catalyzed Reactions. *Journal of the American Chemical Society* **1954**, *76*, 571-573.
14. Wohler, F. L., J. , Untersuchungen über das Radikal der Benzoesäure. *Annales pharmaceutiques françaises* **1832**, *3*, 249-282.
15. Lapworth, A., Reactions involving the addition of hydrogen cyanide to carbon compounds. *Journal of the Chemical Society, Transactions* **1903**, *83*, 995-1005.
16. Breslow, R., On the Mechanism of Thiamine Action. IV.1 Evidence from Studies on Model Systems. *Journal of the American Chemical Society* **1958**, *80*, 3719-3726.
17. Enders, D.; Balensiefer, T., Nucleophilic Carbenes in Asymmetric Organocatalysis. *Accounts of Chemical Research* **2004**, *37*, 534-541.
18. Stetter, H., Die katalysierte Addition von Aldehyden an aktivierte Doppelbindungen – Ein neues Syntheseprinzip. *Angewandte Chemie* **1976**, *88*, 695-704.
19. Enders, D.; Breuer, K.; Runsink, J.; Teles, J. H., The First Asymmetric Intramolecular Stetter Reaction. Preliminary Communication. *Helvetica Chimica Acta* **1996**, *79*, 1899-1902.
20. Gyorgy, P., Vitamin B2 and the Pellagra-like Dermatitis in Rats. *Nature* **1934**, *133*, 498.
21. Eliot, A. C.; Kirsch, J. F., Pyridoxal phosphate enzymes: mechanistic, structural, and evolutionary considerations. *Annual review of biochemistry* **2004**, *73*, 383-415.
22. Voet, D. V., J. , *Biochemistry*. Wiley: New York, 1995
23. Hayashi, H., Pyridoxal enzymes: mechanistic diversity and uniformity. *Journal of biochemistry* **1995**, *118*, 463-73.

24. John, R. A., Pyridoxal phosphate-dependent enzymes. *Biochimica et biophysica acta* **1995**, *1248*, 81-96.
25. Maley, J. R.; Bruice, T. C., Catalytic reactions involving azomethines. X. Transamination of 1-methyl-4-formylpyridinium iodide. *Journal of American Chemical Society* **1968**, *90*, 2843-7.
26. Tabushi, I.; Kuroda, Y.; Yamada, M., Racemization of phenylglycine catalyzed by pyridoxal. Catalytic effect of phosphate ion. *Tetrahedron Letters* **1987**, *28*, 5695-5698.
27. Felten, A. E.; Zhu, G.; Aron, Z. D., Simplifying Pyridoxal: Practical Methods for Amino Acid Dynamic Kinetic Resolution. *Organic Letters* **2010**, *12*, 1916-1919.
28. Toney, M. D., Controlling reaction specificity in pyridoxal phosphate enzymes. *Biochimica et Biophysica Acta (BBA) - Proteins and Proteomics* **2011**, *1814*, 1407-1418.
29. Harden, A. Y., W. J. , The alcoholic ferment of yeast-juice. *Proceedings of the Royal Society B: Biological Sciences* **1906**, *78*, 369.
30. Warburg, O. C., W. , Pyridin, der wasserstoffübertragende bestandteil von gärungsfermenten. *Biochemistry. Z* **1936**, *287*, 291.
31. Anderson, B. M.; Kaplan, N. O., Enzymatic studies with analogues of diphosphopyridine nucleotide. *The Journal of biological chemistry* **1959**, *234*, 1226-32.
32. Garrett, R. H. G., C. M. , *Biochemistry*. Saunders College Publishing 1995.
33. Kaplan, N. O.; Ciotti, M. M., The 3-Acetylpyridine Analogue of DPN1. *Journal of the American Chemical Society* **1954**, *76*, 1713-1714.
34. Kaplan, N. O.; Ciotti, M. M., Chemistry and Properties of the 3-Acetylpyridine Analogue of diphosphopyridine nucleotide. *Journal of Biological Chemistry* **1956**, *221*, 823-832.

35. Kaplan, N. O.; Ciotti, M. M.; Stolzenbach, F. E., Reaction of Pyridine Nucleotide Analogues with Dehydrogenases. *Journal of Biological Chemistry* **1956**, *221*, 833-844.
36. Hantzsch, A., Ueber die Synthese pyridinartiger Verbindungen aus Acetessigäther und Aldehydammoniak. *Justus Liebigs Annalen der Chemie* **1882**, *215*, 1-82.
37. Dondoni, A.; Massi, A., Asymmetric organocatalysis: from infancy to adolescence. *Angewandte Chemie (International ed. in English)* **2008**, *47*, 4638-60.
38. Eisner, U.; Kuthan, J., Chemistry of dihydropyridines. *Chemical reviews* **1972**, *72*, 1-42.
39. Kuthan, J.; Kurfurst, A., Development in dihydropyridine chemistry. *Industrial & Engineering Chemistry Product Research and Development* **1982**, *21*, 191-261.
40. Hoffmann, S.; Seayad, A. M.; List, B., A Powerful Brønsted Acid Catalyst for the Organocatalytic Asymmetric Transfer Hydrogenation of Imines. *Angewandte Chemie International Edition* **2005**, *44*, 7424-7427.
41. Mure, M.; Klinman, J. P., Synthesis and spectroscopic characterization of model compounds for the active site cofactor in copper amine oxidases. *Journal of the American Chemical Society* **1993**, *115*, 7117-7127.
42. Klinman, J. P., New Quinocofactors in Eukaryotes. *Journal of Biological Chemistry* **1996**, *271*, 27189-27192.
43. Mure, M., Tyrosine-Derived Quinone Cofactors. *Accounts of Chemical Research* **2004**, *37*, 131-139.
44. Mure, M.; Klinman, J. P., Model Studies of Topaquinone-Dependent Amine Oxidases. 1. Oxidation of Benzylamine by Topaquinone Analogs. *Journal of the American Chemical Society* **1995**, *117*, 8698-8706.

45. Mure, M.; Klinman, J. P., Model Studies of Topaquinone-Dependent Amine Oxidases. 2. Characterization of Reaction Intermediates and Mechanism. *Journal of the American Chemical Society* **1995**, *117*, 8707-8718.
46. Wendlandt, A. E.; Stahl, S. S., Chemoselective Organocatalytic Aerobic Oxidation of Primary Amines to Secondary Imines. *Organic Letters* **2012**, *14*, 2850-2853.
47. Wendlandt, A. E.; Stahl, S. S., Modular o-Quinone Catalyst System for Dehydrogenation of Tetrahydroquinolines under Ambient Conditions. *Journal of the American Chemical Society* **2014**, *136*, 11910-11913.
48. Burger, E. C.; Tunge, J. A., Synthesis of Homoallylic Amines via the Palladium-Catalyzed Decarboxylative Coupling of Amino Acid Derivatives. *J. Am. Chem. Soc.* **2006**, *128*, 10002-10003.
49. Noble, A.; MacMillan, D. W. C., Photoredox α -Vinylolation of α -Amino Acids and N-Aryl Amines. *Journal of the American Chemical Society* **2014**, *136*, 11602-11605.
50. Kobayashi, S.; Mori, Y.; Fossey, J. S.; Salter, M. M., Catalytic Enantioselective Formation of C-C Bonds by Addition to Imines and Hydrazones: A Ten-Year Update. *Chemical reviews* **2011**, *111*, 2626-2704.
51. Cheng, R. P.; Gellman, S. H.; DeGrado, W. F., β -Peptides: From Structure to Function. *Chemical reviews* **2001**, *101*, 3219-3232.
52. Stephens, O. M.; Kim, S.; Welch, B. D.; Hodsdon, M. E.; Kay, M. S.; Schepartz, A., Inhibiting HIV Fusion with a β -Peptide Foldamer. *Journal of the American Chemical Society* **2005**, *127*, 13126-13127.

53. Sleebs, B. E.; Van Nguyen, T. T.; Hughes, A. B., Recent advances in stereoselective synthesis and application of β -amino acids. *Organic Preparations and Procedures International* **2009**, *41*, 429-478.
54. Bandala, Y.; Juaristi, E. In *Recent developments in the synthesis of β -amino acids* 2009 Wiley-VCH Verlag GmbH & Co. KGaA; pp 291-365.
55. Weiner, B.; Szymanski, W.; Janssen, D. B.; Minnaard, A. J.; Feringa, B. L., Recent advances in the catalytic asymmetric synthesis of [small beta]-amino acids. *Chemical Society Reviews* **2010**, *39*, 1656-1691.
56. Chhibha, V.; Bode, M.; Mathiba, K.; Brady, D. In *Enzymatic stereoselective synthesis of β -amino acids* 2014 Wiley-VCH Verlag GmbH & Co. KGaA; pp 297-313.
57. Juaristi, E. S., V. A. , *Enantioselective Synthesis of β -Aminoacids*, 2nd ed. Wiley-Interscience: New York, 2005
58. Arndt, F.; Eistert, B., Ein Verfahren zur Überführung von Carbonsäuren in ihre höheren Homologen bzw. deren Derivate. *Berichte der deutschen chemischen Gesellschaft (A and B Series)* **1935**, *68*, 200-208.
59. Ellmerer-Mueller, E. P.; Broessner, D.; Maslouh, N.; Tako, A., Synthesis of N-[(9H-fluoren-9-yl)methoxy]carbonyl}-protected (Fmoc) β -amino acids (homo- α -amino acids) by direct homologation. *Helv. Chim. Acta* **1998**, *81*, 59-65.
60. Kowalski, C. J.; Haque, M. S.; Fields, K. W. Ester homologation via α -bromo α -keto dianion rearrangement. *Journal of the American Chemical Society* **1985**, *107*, 1429-30.
61. Guichard, G.; Abele, S.; Seebach, D., Preparation of N-Fmoc-protected β 2- and β 3-amino acids and their use as building blocks for the solid-phase synthesis of β -peptides. *Helvetica Chimica Acta* **1998**, *81*, 187-206.

62. Yang, H.; Foster, K.; Stephenson, C. R. J.; Brown, W.; Roberts, E., Asymmetric Wolff Rearrangement Reactions with α -Alkylated- α -diazoketones: Stereoselective Synthesis of α -Substituted- β -amino Acid Derivatives. *Organic Letters* **2000**, *2*, 2177-2179.
63. Koch, K.; Podlech, J., Exceptionally simple homologation of protected α - to β -amino acids in the presence of silica gel. *Synthetic Communications* **2005**, *35*, 2789-2794.
64. Pinho, V. D.; Gutmann, B.; Kappe, C. O., Continuous flow synthesis of β -amino acids from α -amino acids via Arndt-Eistert homologation. *Royal Society of Chemistry Advances* **2014**, *4*, 37419-37422.
65. Vander Zwan, M. C.; Hartner, F. W.; Reamer, R. A.; Tull, R., A new reaction of amino acids: conversion to benzoxazoles. *Journal Organic Chemistry* **1978**, *43*, 509-11.
66. Vinsova, J.; Horak, V.; Buchta, V.; Kaustova, J., Highly lipophilic benzoxazoles with potential antibacterial activity. *Molecules* **2005**, *10*, 783-793.
67. Petasis, N. A.; Zavialov, I. A., A New and Practical Synthesis of α -Amino Acids from Alkenyl Boronic Acids. *Journal of the American Chemical Society* **1997**, *119*, 445-446.
68. Iimura, S.; Nobutou, D.; Manabe, K.; Kobayashi, S., Mannich-type reactions in water using a hydrophobic polymer-supported sulfonic acid catalyst. *Chemical Communications* **2003**, 1644-1645.
69. Hamada, T.; Manabe, K.; Kobayashi, S., Enantio- and Diastereoselective, Stereospecific Mannich-Type Reactions in Water. *Journal of the American Chemical Society* **2004**, *126*, 7768-7769.
70. Eliel, E. L. W. S. H. M., L. N. , *Stereochemistry of Organic Compounds*. Wiley: New York, 1994.

71. Onodera, G.; Toeda, T.; Toda, N.-n.; Shibagishi, D.; Takeuchi, R., Cationic iridium complex is a new and efficient Lewis acid catalyst for aldol and Mannich reactions. *Tetrahedron* **2010**, *66*, 9021-9031.
72. Hansch, C. L., A.; Taft, R. W. , A Survey of Hammett Substituent Constants and Resonance and Field Parameters. *Chemical reviews* **1991**, *91*, 165.
73. Straub, T. S.; Bender, M. L., Cycloamyloses as enzyme models. Decarboxylation of benzoylactic acids. *Journal of the American Chemical Society* **1972**, *94*, 8881-8888.
74. Ciaccia, M.; Pilati, S.; Cacciapaglia, R.; Mandolini, L.; Di Stefano, S., Effective catalysis of imine metathesis by means of fast transiminations between aromatic-aromatic or aromatic-aliphatic amines. *Organic & Biomolecular Chemistry* **2014**, *12*, 3282-3287.

¹H and ¹³C-NMR Spectra:

